EFFECT OF RENIN-ANGIOTENSIN SYSTEM BLOCKADE ON CARDIAC REMODELING IN HEART FAILURE AFTER MYOCARDIAL INFARCTION

BY

XIAOBING GUO

A Dissertation Submitted to
The Faculty of Graduate Studies

In Partial Fulfillment of Requirements for the Degree of

DOCTOR OF PHILOSOPHY

Institute of Cardiovascular Sciences
Department of Physiology, Faculty of Medicine
University of Manitoba
Winnipeg, Manitoba

© August 2004

THE UNIVERSITY OF MANITOBA

FACULTY OF GRADUATE STUDIES
*****
COPYRIGHT PERMISSION

EFFECT OF RENIN-ANGIOTENSIN SYSTEM BLOCKADE ON CARDIAC REMODELING IN HEART FAILURE AFTER MYOCARDIAL INFARCTION

BY

XIAOBING GUO

A Thesis/Practicum submitted to the Faculty of Graduate Studies of
The University of Manitoba

in partial fulfillment of the requirement of the degree

of

Doctor of Philosophy

XIAOBING GUO © 2004

Permission has been granted to the Library of the University of Manitoba to lend or sell copies of this thesis/practicum, to the National Library of Canada to microfilm this thesis and to lend or sell copies of the film, and to University Microfilms Inc. to publish an abstract of this thesis/practicum.

This reproduction or copy of this thesis has been made available by authority of the copyright owner solely for the purpose of private study and research, and may only be reproduced and copied as permitted by copyright laws or with express written authorization from the copyright owner.

ACKNOWLEDGEMENTS

I would like to express my appreciation to all the people who have assisted me in accomplishing my Ph.D. program. First, it is my great pleasure to extend my deepest gratitude to my advisor **Dr. Naranjan S. Dhalla**, for his warm heart, fabulous perception, countless care and incredible patience. Without his thoughtful guidance, it would have been impossible for me to face all these challenges during my training. His sharp knowledge and help have kept me on the right track towards my goal.

I would also like to acknowledge my advisory committee, whose critical comments as well as encouragement have greatly helped me to fulfill my task. Dr. Pawan K. Singal has continuously supported me through the past seven years of my graduate study. Dr. Ian M. C. Dixon always "*fixes the problem*" for me immediately. Special thanks are extended to Dr. Paramjit S. Tappia for his help with my project and the editing of my thesis. In addition, it is he, who opened the window of advanced education at the University for me, and has showed me the amazing nature of nutrition science.

I would also like to express my gratitude towards all members of the Experimental Cardiology Laboratory. Every achievement in my work could not have been accomplished without their efforts. Their everlasting solid support and sincere friendship have kept me enjoying science and life. I would also wish to thank all the members in our Institute, who never let me lose hope. It is also time to acknowledge and thank the marvellous academic training given in the Department of Physiology. I appreciate the sustained help of the University of Manitoba and friends in Winnipeg.

I want to thank Manitoba Health Research Council and the University of Manitoba, for the financial assistance. Also I want to thank all the persons who offered

me the academic assistance from as far away as USA and Europe. Also, I would like to thank all the friends and families in China, who have encouraged me to achieve my goal.

I dedicate my thesis to my parents and parents-in-law for their unlimited love. I am highly indebted to them, to my sister, to my brother-in-law and sister-in-law, whose enormous supports and sacrifices are always my sources of strength and power. Finally, I am thankful to my wife, **Dr. Jingwei Wang**, who deserves the best words in the world. She always brings me the love, wisdom, encouragement and energy, and always brings the honour, pleasure, harmony and comfort to the family. All of the best wishes and love are given to my lovely son, **Jiabo**, and my adorable daughter, **Amy**. Their understanding and patience are crucial for my research work. During the most challenging period of my life, I have been granted with confidence, happiness and pride, from their astonishing endurance, talent and collaboration.

ABSTRACT

Congestive heart failure (CHF) is one of the major challenges affecting society. Specifically, myocardial infarction (MI) is the major cause of CHF in the Western world. Cardiac remodeling occurs post MI and contributes to the establishment of CHF, and modification of cardiac remodeling is important in both prevention and treatment of cardiac dysfunction post MI. Activation of the renin-angiotensin system (RAS) is critical in the cardiac remodeling process following MI. Also, the blockade of RAS has shown significant therapeutic effects in research and clinical practice. By employing a rat model of coronary artery ligation, the current project focuses on the mechanism of the beneficial effects of RAS blockade in the failing heart post MI. The angiotensin converting enzyme (ACE) inhibitor (enalapril) and angiotensin II type 1 receptor (AT_1R) antagonist (losartan) were utilized to explore the therapeutic potential of RAS blockade on the heart at the subcellular and molecular levels.

To investigate the mechanisms underlying the depressed sarcolemmal (SL) Na^+-K^+-ATPase activity in the failing heart, different isoforms of Na^+-K^+-ATPase protein contents and gene expression were examined in the left ventricle (LV) at 8 weeks following MI. In addition, these parameters were also studied after 5 weeks of treatment with RAS blockade by enalapril (10 mg/kg/day) and/or losartan (20 mg/kg/day) starting at 3 weeks after the coronary ligation. An infarcted heart features the formation of a scar and significant cardiac hypertrophy as is evident from the increased heart weight and heart weight/body weight ratio. CHF was also evident from increased lung wet weight/dry weight ratio (index for pulmonary edema) and the impaired heart function associated with depressed LV pressure development (+dP/dt) and pressure decay (-dP/dt)

as well as elevation in LV end-diastolic pressure (LVEDP). In the isolated SL preparations, we found that the protein contents for Na^+-K^+-ATPase isoforms underwent significant changes corresponding to similar alterations in gene expression in CHF. These changes were associated with the depressed Na^+-K^+-ATPase activity in the failing heart. The protein contents and the mRNA expression for Na^+-K^+-ATPase α_2 isoform were decreased, whereas the protein content and mRNA level for Na^+-K^+-ATPase α_3 isoform were greatly increased. On the other hand, no changes were observed in the protein contents or mRNA levels for Na^+-K^+-ATPase α_1 and β_1 isoforms. The higher enzyme activity of Na^+-K^+-ATPase α_2 isoform in comparison to the Na^+-K^+-ATPase α_3 isoform may explain the reason for the depressed Na^+-K^+-ATPase activity in the failing heart post MI. The changes in the corresponding mRNA of Na^+-K^+-ATPase isoforms may contribute to the remodeling of different Na^+-K^+-ATPase isoform proteins. The treatment of infarcted animals with enalapril, losartan and combination of enalapril and losartan significantly attenuated lung congestion, cardiac hypertrophy and improved the heart function. The blockade of RAS also partially prevented the remodeling of Na^+-K^+-ATPase isoforms, attenuating the depression in α_2 isoform and the increase in α_3 isoform, at both the protein and mRNA levels. However, the combination therapy with enalapril and losartan did not produce the expected additive effects.

Impaired Ca^{2+}-transport is another important factor that contributes to the pathogenesis of heart failure. To examine the remodeling of SL Ca^{2+}-regulatory proteins in the failing heart post MI, a second series of experiments were conducted in the hemodynamically assessed infarcted animals with or without drug treatment. Three proteins including SL Na^+-Ca^{2+}-exchanger (NCX), Ca^{2+}-pump and Ca^{2+}-channel were

examined in the isolated SL preparations. At 8 weeks post MI, the protein content for NCX was increased in the viable LV ($P < 0.05$). Similar increase in NCX mRNA was identified by Northern blot analysis. These changes were associated with significant cardiac hypertrophy and heart dysfunction. The protein content for SL Ca^{2+}-pump (PMCA1) was markedly increased in the failing heart; this was associated with a significant elevation in the corresponding mRNA expression as determined by RT-PCR. A decrease in the SL Ca^{2+}-channel α_1 subunit and an increase in the SL Ca^{2+}-channel β subunit without any change in the α_2 subunit were evident in the failing heart as compared to sham control. The remodeling of SL NCX, PMCA1 and Ca^{2+}-channel as well as heart dysfunction were partially prevented by blockade of RAS with enalapril and losartan. These results suggest that the beneficial effects of RAS blockade in CHF may be due to partial prevention of SL remodeling with respect to Ca^{2+} transport.

Although, the right ventricle (RV) is as important as the LV in pumping the blood, less information is available regarding gene expression in the RV, especially in the failing heart post MI. In these experiments, both LV and RV were utilized for the isolation of total RNA, in order to investigate if similar remodeling occurs in cardiac gene expression in the LV and RV of the same failing heart. Most of the SL, sarcoplasmic reticular (SR) and myofibrillar proteins were equally expressed in both ventricles of the heart. However, higher expression of PMCA1 and the lower expression of β-myosin heavy chain (β-MHC) as well as β-actin were observed in the RV in comparison to the LV. Following MI, a reduction in PLB and α-myosin heavy chain (α-MHC) gene expression, and an increase in NCX and β-MHC occurred in both the RV and the LV. On the other hand, the depressions in Na^+-K^+-ATPase α_2 subunit, RYR, and SERCA2, were only significant in

the LV. The difference in the remodeling process between the LV (showing hypertrophy and heart failure) and RV (showing hypertrophy) may partially be due to the differential changes in cardiac gene expression between the two ventricles. However, alterations in gene expression in both the RV and the LV as well as hypertrophy and heart dysfunction were partially prevented by treatment of animals showing CHF with enalapril and losartan. These results further support the concept that improvement in cardiac performance in CHF by the blockade of RAS may be associated with partial prevention of SL, SR and myofibril remodeling in the heart.

TABLE OF CONTENTS

ACKNOWLEDGEMENTS I

ABSTRACT III

TABLE OF CONTENTS VII

LIST OF FIGURES X

LIST OF TABLES XIII

LIST OF ABBREVIATIONS XIV

I. LITERATURE REVIEW 1

1. Introduction 1
2. Cardiac Remodeling after MI 2
3. Ca^{2+} Homeostasis in Heart Failure 6
4. SL Na^{+}-K^{+}-ATPase in Heart Failure 10
5. SL Ca^{2+}-Channel in Heart Failure 12
6. SL NCX and Ca^{2+}-pump in Heart Failure 14
7. SR Ca^{2+}-Channel in Heart Failure 16
8. SERCA in Heart Failure 17
9. PLB and CQS in Heart Failure 20
10. MHC and MLC in Heart Failure 21
11. RAS in Cardiovascular System 23
12. Activation of RAS in MI 28
13. Blockade of RAS in MI 31
14. RAS Blockade and Subcelluar Remodeling 47

15. Summary 47

II. STATEMENT OF THE PROBLEM AND HYPOTHESES TO BE TESTED 50

III. MATERIALS AND METHODS 54

1. Experimental Model 54
2. Treatment with Enalapril and Losartan 55
3. EKG Measurement and Analysis 55
4. Hemodynamic Studies 56
5. General Assessment and Tissue Preparation 57
6. Isolation of Cardiac SL Membrane 58
7. Measurement of Na^+-K^+-ATPase Activity 59
8. Analysis of SL Protein Content 59
9. RNA Isolation 62
10. Northern Blot Analysis 63
11. Semi-quantitative PCR 66
12. Data Analysis 67

IV. RESULTS 68

1. SL Na^+-K^+-ATPase Remodeling in Failing Rat Heart 68
2. SL Ca^{2+}-regulatory Proteins Expression in Failing Rat Heart 78
3. Changes in Left and Right Ventricular Gene Expression in Heart Failure 87

V. DISCUSSION 102

1. SL Na^+-K^+-ATPase Remodeling in Failing Rat Heart 102

2. SL Ca^{2+}-regulatory Proteins Expression in Failing Rat Heart 105

3. Changes in Left and Right Ventricular Gene Expression in Heart Failure..... 108

VII. SUMMARY AND CONCLUSIONS 112

VIII. REFERENCES 114

LIST OF FIGURES

Figure 1. Calcium induced calcium release 7

Figure 2. Renin-angiotensin system in cardiovascular system 25

Figure 3. Blockade of renin-angiotensin system 32

Figure 4. Histological alterations at 8 weeks after coronary artery ligation in rats 69

Figure 5. Changes in cardiac sarcolemmal Na^+-K^+-ATPase and Mg^{2+}-ATPase activities of the left ventricles 72

Figure 6. Typical immunoblots and protein contents of cardiac sarcolemmal Na^+-K^+-ATPase different α isoforms 74

Figure 7. Typical immunoblots and protein contents of cardiac sarcolemmal Na^+-K^+-ATPase different β isoforms 75

Figure 8. Typical Northern blots of cardiac sarcolemmal Na^+-K^+-ATPase different isoforms 76

Figure 9. mRNA abundance for cardiac sarcolemmal Na^+-K^+-ATPase different isoforms 77

Figure 10. Typical immunoblots and protein contents of cardiac sarcolemmal Na^+-Ca^{2+}-exchanger in the left ventricles 81

Figure 11. Typical Northern blots and mRNA abundance of cardiac sarcolemmal Na^+-Ca^{2+}-exchanger in the left ventricles 82

Figure 12. Typical immunoblots and protein contents of cardiac sarcolemmal Ca^{2+}-pump in the left ventricles 83

Figure 13. Typical RT-PCR and mRNA abundance of cardiac sarcolemmal Ca^{2+}-pump in the left ventricles 85

Figure 14. Typical immunoblots and protein contents of cardiac sarcolemmal Ca^{2+}-channel different subunits in the left ventricles 86

Figure 15. Typical Northern blots of cardiac sarcolemmal Na^{+}-Ca^{2+}-exchanger, Na^{+}-K^{+}-ATPase different isoforms in the viable tissue of both left and right ventricles 90

Figure 16. mRNA abundance for cardiac sarcolemmal Na^{+}-K^{+}-ATPase different subunits in the viable tissue of both left and right ventricles 91

Figure 17. Typical RT-PCR and mRNA abundance of cardiac sarcolemmal Ca^{2+}-pump in the viable tissue of both left and right ventricles 92

Figure 18. Typical Northern blots of cardiac myofibrillar proteins and sarcoplasmic reticular proteins in the viable tissue of both left and right ventricles..... 94

Figure 19. mRNA abundance for cardiac α-myosin heavy chain, β-myosin heavy chain, myosin light chain, and β-actin in the viable tissue of both left and right ventricles 95

Figure 20. mRNA abundance for cardiac ryanodine receptor, sarco-endoplasmic reticulum Ca^{2+}-ATPase, phospholamban and calsequestrin in the viable tissue of both left and right ventricles..... 96

Figure 21. Comparison of mRNA abundance for cardiac sarcolemmal Na^{+}-Ca^{2+}-exchanger, Na^{+}-K^{+}-ATPase different isoforms, and Ca^{2+}-pump in the viable tissue of both left and right ventricles..... 98

Figure 22. Comparison of mRNA abundance for cardiac α-myosin heavy chain, β-myosin heavy chain, myosin light chain, and β-actin in the viable tissue of both left and right ventricles 99

Figure 23. Comparison of mRNA abundance for cardiac ryanodine receptor, sarco-endoplasmic reticulum Ca^{2+}-ATPase, phospholamban and calsequestrin in the viable tissue of both left and right ventricles 100

LIST OF TABLES

Table 1. Alterations in Cardiac Gene Expression Following MI 5

Table 2. Alterations in SL and SR Proteins Gene Expression Following MI 8

Table 3. Alterations of Myofibrillar Proteins Gene Expression Following MI 9

Table 4. Possible beneficial effects of RAS blockade after MI 33

Table 5. Clinical trials for ACE inhibitors in heart failure 36

Table 6. ACE inhibitors in MI model 38

Table 7. Clinical trials for AT_1R antagonists in MI 43

Table 8. AT_1R antagonists in MI model 44

Table 9. General characteristics and hemodynamic parameters in myocardial infarcted rats 70

Table 10. Modification of Na^+-K^+-ATPase isoforms in myocardial infarcted rats ... 73

Table 11. General characteristics and hemodynamic parameters of myocardial infarcted rats 79

Table 12. General characteristics and hemodynamic parameters of myocardial infarcted rats 88

LIST OF ABBREVIATIONS

$+dP/dt_{(max)}$	(the maximum) rate of pressure development
$-dP/dt_{(max)}$	(the maximum) rate of pressure decay
α-MHC	α-myosin heavy chain
β-MHC	β-myosin heavy chain
ACE	angiotensin converting enzyme
ACE2	ACE-related carboxypeptidase
ADEPT	Addition of the AT_1 receptor antagonist eprosartan to ACE inhibitor therapy in chronic heart failure trial
AIRE:	Acute Infarction Ramipril Efficacy Study
Ang I	angiotensin I
Ang II	angiotensin II
ANP	atrial natriuretic peptid
AR	angiotensin II receptor
AT_1R	angiotensin II type 1 receptor
$AT_{1a}R$	angiotensin II type 1 a subtype receptor
$AT_{1b}R$	angiotensin II type 1 b subtype receptor
AT_2R	angiotensin II type 2 receptor
BP	blood pressure
$[Ca^{2+}]_I$	the intracellular concentration of free Ca^{2+}
CATS	Captopril and Thrombolysis Study
CHF	congestive heart failure
CICR	calcium induced calcium release

CO	cardiac output
COM	combined enalapril and losartan treated infarcted rats
CONSENSUS	Cooperative New Scandinavian Enalapril Survival Study
CONSENSUS I	Cooperative New Scandinavian Enalapril Survival Study I
CQS	calsequestrin
CVP	central venous pressures
DAG	diacylglycerol
DHPS	dihydropyridiens
DS	Dahl salt-senstive (rat)
ECC	excitation-contraction coupling
EDTA	ethylenediaminetetraacetate
EGTA	ethylene glycol-bis(β-aminothyl ether)-N,N,N'-Tetra-acetic acid
EKG	electrocardiography
ELITE	Evaluation of Losartan in the Elderly Study
ENP	enalapril treated infarcted rat
FAMIS	Fosinopril in Acute Myocardial Infarction Study
G-proteins	guanine nucleotide-binding proteins
GAPDH	glyceraldehydes-3-phosphate dehydrogenase
GISSI-3	the Third Gruppo Italiano per lo Studio della Soprav vivenza nel Infarto Miocardico
H + E	hematoxylin and eosin stain
HOCI	hypochlorous acid
HOPE	Heart Outcomes Prevention Evaluation

HRP	horseradish peroxidase
$I_{Na/Ca}$	Na^+-Ca^{2+}-exchanger current
IP_3	phosphatidylinositol 1,4,5-triphosphate
ISIS-4	Fourth International Study of Infarct Survival
kDa	kilo-dalton
LOS	losartan treated infarcted rat
LV	left ventricle
LVEDP	left ventricle end-diastolic pressure
LVSP	left ventricular systolic pressure
MAP	mean arterial blood pressure
MDA	malondialdehyde
MF	myofibril
MHC	myosin heavy chain
MI	myocardial infarction
MLC	myosin light chain
MLCK	myosin light chain kinase
MOPS	3-[N-morpholino]-propanesulfonic acid
NCX	Na^+-Ca^{2+}-exchanger
ND	not detected
OPTIMAAL	Optimal Therapy in Myocardial Infarction with the Angiotensin II Antagonist Losartan study
PIP_2	phosphatidylinosital 4,5-bisphosphate
PKA	protein kinase A
PKC	protein kinase C

PKG	cGMP-dependent protein kinase
PLB	phospholamban
PLC	phospholipase C
PMCA	Ca^{2+}-pump of the plasma membrane
PVDF	polyvinylidene difluoride
RAS	renin-angiotensin system
RT	reverse transcription
RV	right ventricle
RYR	ryanodine receptor
SAVE	Survival and Ventricular Enlargement (Trial)
SERCA	sarco-endoplasmic reticulum Ca^{2+}-ATPase
SDS	sodium dodecyl sulfate
SDS-PAGE	sodium dodecyl sulfate polyacrylamide gel electrophoresis
SHR	spontaneously hypertensive rats
SMILE	Survival of Myocardial Infarction Long-Term Evaluation
SOLVD	Studies of Left Ventricular Dysfunction
SL	sarcolemma
SNS	sympathetic nervous system
SR	sarcoplasmic reticulum
SVR	systemic vascular resistance
TBS	Tris-buffered saline
TBS-T	Tris-buffered saline with 0.1% Tween-20
TCA	trichloroacetic acid
TGF-β	transforming growth factor-β

TRACE	Trandolapril Cardiac Evaluation
TRICH	Masson's trichrome stain
VEGF	vascular endothelial growth factor
wt	weight

I. LITERATURE REVIEW

1. Introduction

Congestive heart failure (CHF) has high mortality and morbidity rates [1] and is regarded as a major challenge affecting both the health care system and the society. In the United States alone, more than 550,000 new cases are identified annually, while over 5 million patients are suffering from CHF and 250,000 deaths occur each year [2]. On the other hand, current health care system and emphasis on quality life style have greatly improved and elongated human life. For example, more patients are surviving from acute myocardial infarction (MI) [3,4]. Nonetheless, prevalence of CHF has also increased, especially in the patients who have survived an acute MI [5]. In patients with MI, successful reperfusion therapy within 2 hours is associated with the greatest degree of myocardial salvage [6,7]. The majority of patients, however, miss this opportunity and this results in the loss of myocardium in the infarcted area. To compensate for the damage inflicted upon the heart, the sympathetic nervous system (SNS), renin-angiotensin system (RAS) and various other neurohumoral mechanisms are activated [8]. Under the influence of these neurohormones thus released, the infarcted heart undergoes cardiac remodeling, resulting in CHF. In addition to the initial insult during acute MI, the cardiac remodeling has an important impact on the ultimate outcome of the patient and thus its therapy is important [9,10]. It is well known that the remodeling process following acute MI is considerably more complex than that in any other pathophysiological condition of hemodynamic overload, however, the way it affects the function of the ventricle and the prognosis of survival are poorly understood [11].

2. Cardiac Remodeling after MI

One important prognostic predictor for MI patients is the degree of ventricular dysfunction [12]. Left ventricular (LV) remodeling after MI refers to the alterations in the topography of both the infarcted and non-infarcted regions of the ventricle and it starts immediately after MI and progresses to the chronic stage of heart failure [9]. The important factors in the genesis of CHF post-MI include reduced myocyte mass (replaced by scar tissue) and nonmyocyte factors, such as increased wall stress, altered LV geometry, and changes in the myocardial interstitium [13].

Within hours of acute MI, necrosis, edema and inflammation are localized to the infarcted area, which are followed by a long-term period of fibroblast proliferation and collagen deposition. This is referred to as scar formation, which is completed within weeks to months depending on the species, and for rats, the period of scar healing is about 3 weeks [9,14,15]. Usually, vessel growth, predominantly in the area adjacent to the scar, results in basal normalization within 7 days, and complete normalization of coronary vasodilatory capacity occurs within 35 days post MI [16]. A discrete thin scar is formed within 7 to 19 days after MI, and further LV enlargement occurs as a result of continuous alterations in the residual myocardium [17]. At the end-stage of heart failure in human, remodeling of the LV following MI is commonly associated with interstitial fibrosis in the noninfarcted hypertrophic myocardium, which is remote from the scar area [18-23]. Of course, there are different opinions regarding whether remodeling post MI in humans is associated with interstitial fibrosis of non-infarcted myocardium [24].

Cardiac growth is another important issue following MI and, in fact, it occurs as a combination of both concentric and eccentric types of cardiac hypertrophy [25].

Hypertrophy in individual cardiomyocyte is significant [25,26]; these become longer by 18% at 1 week [27], 10% at 3 weeks [28], and 131% at 6 weeks post-MI [29] in comparison to sham control. Left ventricular weight (wt)/body wt ratio increases 45% at 6 weeks post MI [29]. It is interesting to note that the cardiomyocytes isolated from right ventricle (RV) following MI, expanded longitudinally by 23% and transversely by 24% [27]. However, when the changes in cardiac dilatation and geometry reach a critical point [30], the remodeling of heart itself may contribute to progression of CHF [31]. In both LV and RV, the elevations in filling pressures are associated with the hypertrophy of that ventricle [32]. This suggests that the cardiac hypertrophy process occurs in both ventricles of the heart. Progressively developing heart failure is associated with cardiac remodeling following MI. Time course of the hemodynamic changes in rats with healed severe MI shows that at 4 weeks after MI, peak LV blood pressure (BP), LV maximum pressure development ($+dP/dt_{max}$), mean arterial blood pressure (MAP), and heart rate are significantly reduced and maintained for a long time, in addition to the increase in the LV end-diastolic pressure (LVEDP) [33]. Cardiac output (CO) and systemic vascular resistance (SVR) are progressively reduced, as well as lung and heart weights are significantly increased; these changes are associated with the reduction in lung dry wt/wet wt ratio, and the reduction of blood flow to stomach, small intestine, and kidney [33].

Generally, the increased lung wet and dry wt [29] or the increase of lung wet wt/dry wt ratio [34] as well as increased LVEDP, depression in both $+dP/dt$ and pressure decay ($-dP/dt$) in infarcted rats are regarded as evidence for the presence of CHF [29,34-37]. It is not common for fluid retention such as pleural effusion and ascites at early weeks to be seen in this model [38], while there is presence of significant ascites at 16 weeks [34]. On the other hand, the subsequent changes in the intracellular signal

transduction pathway initiate alterations of cardiac gene expression which are phenotypic changes [8] and are a part of the cardiac remodeling process. Following MI, immediate early genes [29], contractile proteins [39], Ca^{2+}-regulating proteins [40], and signal transduction pathway proteins [41,42], as well as the component of RAS [43] are significantly altered (Table 1).

In view of the importance of Ca^{2+} in cardiac contractile function and intracellular signal transduction, the cardiac remodeling in Ca^{2+}-regulatory proteins has attracted a great deal of interest. In addition, the activation of the SNS and RAS is known to produce an enhancement in loading conditions in the failing ventricle and may accelerate the progression of cardiac remodeling. RAS affects not only the structural remodeling of the LV, but also the myocyte function in MI. The release of neurohormones especially due to the activation of RAS in CHF not only exacerbates the hemodynamic abnormalities but their continuous release also initiates a series of self-reinforcing events, which lead to LV dysfunction and CHF [44] including hypertrophy. Therefore, cardiac remodeling is characterized by expansion of the infarcted myocardium, compensatory hypertrophy of the viable myocardium, progressive dilation of the LV chamber, neurohormonal changes and heart failure [11]. CHF is regarded as a complicated syndrome, initiates with the myocardial damage with subsequent neurohumoral and cytokine activation. Nonetheless, a complex series of changes in both myocyte and non-myocyte elements following MI, is referred to as the ventricular remodeling process and/or phenotype alteration, associated with the presence of disturbed ventricular function and progressive development to CHF [8,45].

Table 1. Alterations in Cardiac Gene Expression Following MI

Gene	LV	RV	Notes
c-myc	↑	ND	rat cardiomyocytesl to 3 weeks after MI [29]
c-fos	–	ND	rat cardiomyocytes[29]
ANP	↑	ND	Isolated rat LV cardiomyocytes 1-6 weeks after MI [29]
	↑	ND	LV viable tissue 12 weeks after MI [46]
	↑	↑	ANP mRNA increased at 4 and 12 weeks after MI in rats [47]
VEGF	↑	ND	rat cardiomyocytes 1 to 3 weeks after MI [29]
TGF-β_1	–	ND	rat cardiomyocytes 1 to 3 weeks after MI [29]
TGF-β_3	–	ND	rat cardiomyocytes 1 to 3 weeks after MI [29]
Angiotensinogen	↑	–	5 and 25 weeks infarcted rat [42]
ACE	↑	ND	LV viable tissue 12 weeks after MI [46]
AT_1R	↑	ND	LV viable tissue 12 weeks after MI [46]
Prepro-ET-1	↑	ND	LV viable tissue 12 weeks after MI [46]
$AT_{1a}R$	↑	ND	4 weeks infarcted rat [43]
$AT_{1b}R$	–	ND	4 weeks infarcted rat [43]
Collagen I	↑	↑	Collagen I mRNA increased at 4 and 12 weeks after MI in rats [47]
Collagen III	↑	↑	Collagen III mRNA increased at 4 and 12 weeks after MI in rats [47]

ACE: angiotensin converting enzyme; ANP: atrial natriuretic peptid; $AT_{1a}R$: angiotensin II type 1 a subtype receptor; $AT_{1b}R$: angiotensin II type 1 b subtype receptor; AT_1R: angiotensin II type 1 receptor LV: left ventricle; ND: not detected; RV: right ventricle; TGF-β: transforming growth factor-β; VEGF: vascular endothelial growth factor; ↑: increase; ↓: decrease; –: no change.

3. Ca^{2+} Homeostasis in Heart Failure

Ca^{2+} homeostasis is a part of excitation-contraction coupling (ECC) where cardiomyocyte contraction and relaxation are mainly regulated by changes in the intracellular concentration of free Ca^{2+} ($[Ca^{2+}]_i$) [48-50]. Different studies with the failing heart have shown that the magnitude of contraction is directly dependent upon the $[Ca^{2+}]_i$ [27,51,52]. At 3 weeks post MI, the maximal systolic pressure in the isolated heart, and the maximal extent of cell shortening in the isolated cardiomyocyte are significantly reduced. These depression are associated with the reduction in peak $[Ca^{2+}]_i$ [28]. This decreased systolic $[Ca^{2+}]_i$ in the LV is associated with depressed LV function, including the elevation of LVEDP and depression of $\pm dP/dt$ [27]. It has been shown that this reduction in $[Ca^{2+}]_i$ is not normalized by isoproterenol treatment [53]. In contrast, diastolic $[Ca^{2+}]_i$ in infarcted heart is higher than [53] or equal to [54] that in the sham operated animals. In the failing human heart, the capacity to restore a low resting Ca^{2+} level during diastole is diminished [55-57]. This increased diastolic $[Ca^{2+}]_i$ in LV is associated with depressed LV relaxation. However, the RV function was preserved but the RV diastolic $[Ca^{2+}]_i$ is elevated [27]. Nonetheless, it is clear that impaired cardiac Ca^{2+} homeostasis and altered ECC is of significant relevance for the pathophysiology of myocardial dysfunction and consequent CHF, but the identification of the cellular and subcellular mechanisms in failing heart is complicated, including differences in experimental animal models and disease progression [45,56]. Cardiac remodeling occurs at different steps of the ECC, and multiple sites and genes are involved, including sarcolemma (SL) and sarcoplasmic reticulum (SR) and myofibrillar components (Fig.1 and Table 2 and 3).

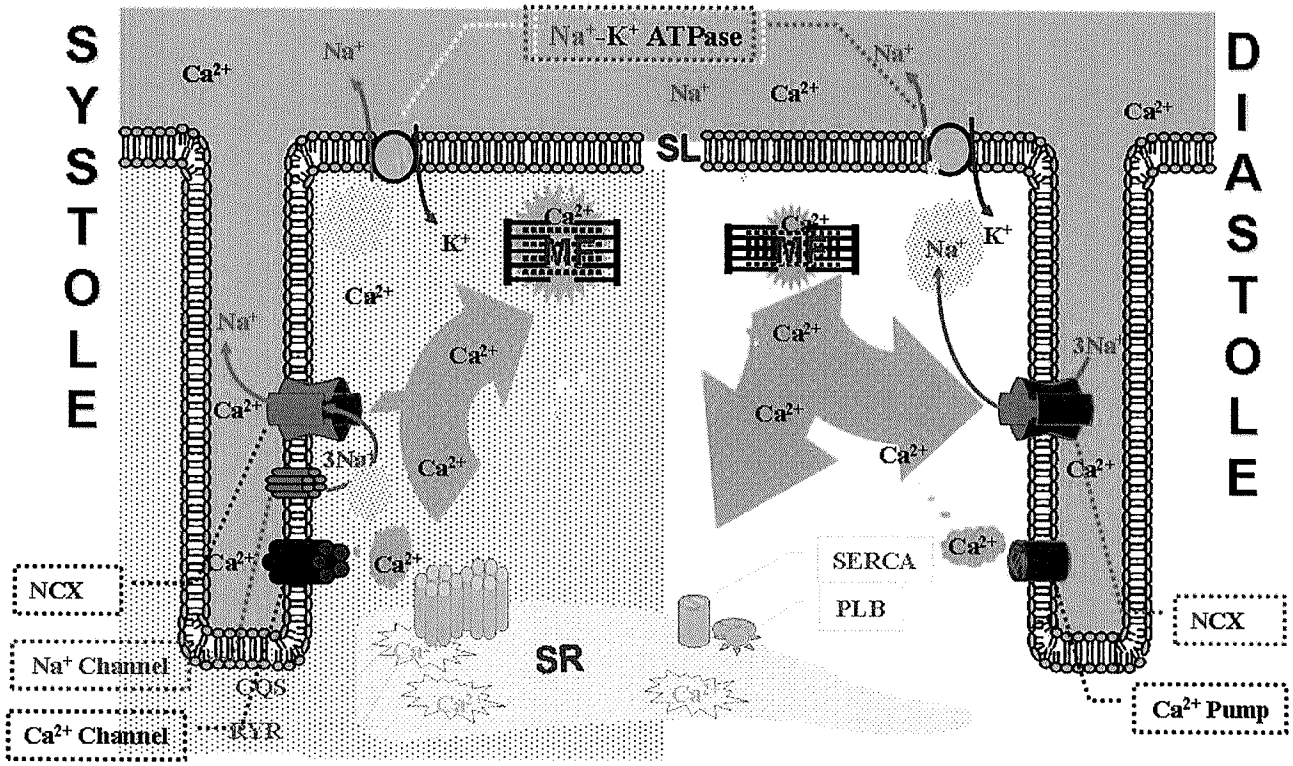

Figure 1. Calcium induced calcium release. CQS: calsequestrin; MF: myofibril; NCX: Na^+-Ca^{2+}-exchanger; PLB: phospholamban; RYR: ryanodine receptor; SERCA: sarco-endoplasmic reticulum Ca^{2+}-ATPase; SL: sarcolemma; SR: sarcoplasmic reticulum.

Table 2. Alterations in SL and SR Proteins Gene Expression Following MI

Gene	LV	RV	Notes
NCX	↑	ND	Human heart failure sample [58,59]
	↑	↑	Protein contents of NCX in failing human myocytes from dilated cardiomyopathic and ischemic cardiomyopathic heart [60].
	↑/–	↑/–	mRNA level of NCX in failing rat heart was decreased at 4 weeks after MI, but not at 12 weeks [47].
SL Ca^{2+}-pump	ND	ND	
Ca^{2+}-channel	ND	ND	
RYR	↓	ND	8 weeks infarcted rat [40]
	↓	ND	LV viable tissue 12 weeks after MI [46]
SERCA2	–	ND	rat cardiomyocytes 6 weeks after MI [29]
	↓	ND	8 weeks infarcted rat [40,61]
	↓	ND	LV viable tissue 12 weeks after MI [46]
	↓	ND	4 weeks infarcted rat [43,62]
	-	↓	mRNA level of SERCA2 in failing rat heart RV was decreased at 12 weeks after MI, but not at 4 weeks; no changes of SERCA2 in LV [47].
	↓	↓	Protein contents of SERCA2a in failing human myocytes from dilated cardiomyopathic and ischemic cardiomyopathic heart [60].
PLB	–	ND	rat cardiomyocytes 6 weeks after MI [29]
	↓	ND	8 weeks infarcted rat [40,61]
CQS	–	ND	8 weeks infarcted rat [40]

CQS: calsequestrin; LV: left ventricle; MI: myocardial infarction; NCX: Na^{+}-Ca^{2+}-exchanger; RV: right ventricle; RYR: ryanodine receptor; PLB: phospholamban; SERCA: sarco-endoplasmic reticulum Ca^{2+}-ATPase; ↑: increase; ↓: decrease; –: no change; ND: not available.

Table 3. Alterations in Myofibrillar Proteins Gene Expression Following MI

Gene	LV	RV	Notes
α-MHC	–	ND	rat cardiomyocytes 6 weeks after MI [29]
	↓	↓	rat viable tissue at 8 weeks post MI [39]
	↓/–	↓/–	α-MHC mRNA decreased at 4 weeks after MI in rats, but not at 12 weeks [47]
β-MHC	↑	ND	rat cardiomyocytes 1 to 6 weeks after MI[29]
	↑/–	↑/–	β-MHC mRNA increased at 4 weeks after MI in rats, but not at 12 weeks [47].
	↑	↑	rat viable tissue at 8 weeks post MI [39]
MLC	–	–	rat viable tissue at 8 weeks after MI [39].
α-actin (cardiac)	–	–	α-actin (cardiac) did not change at 4 and 12 weeks after MI in rat [47]
α-actin (skeleton)	–	ND	rat cardiomyocytes 6 weeks after MI [29]
	↑	↑	α-actin (skeleton) increased at 4 and 12 weeks after MI in rat [47]

LV: left ventricle; MHC: myosin heavy chain; MI: myocardial infarction; MLC: myosin light chain; ND: not detected; RV: right ventricle; ↑: increase; ↓: decrease; –: no change.

4. SL Na^+-K^+-ATPase in Heart Failure

Na^+-K^+-ATPase is ubiquitously expressed in all animal cells and serves as the principal active regulator of intracellular ion homeostasis, especially it is responsible for generating and maintaining transmembrane ionic gradients [63,64]. Na^+-K^+-ATPase maintains the cross membrane Na^+ gradient, which is the trigger and power for Na^+-Ca^{2+}-exchanger (NCX). It belongs to a large family of P-type (phosphor-intermediate type) ATPase; generally, P-type ATPases are inhibited by vanadate. Although the precise molecular structure and 3 dimensional organization of Na^+-K^+-ATPase in the plasma membrane is not elucidated, the complete genome of Na^+-K^+-ATPase is clear in some species (not human and rat) [64]. It is well known that Na^+-K^+-ATPase is composed of three polypeptide subunits (α, β, and γ) embedded in the plasma membrane, forming a heterodimeric protomer (α-β)$_2$ [65] and undergoing conformational changes as part of their reaction cycle [63]. Na^+-K^+-ATPase α subunit is regarded as a catalytic subunit with a molecular wt of 100-112 kilo-dalton (kDa), containing the binding sites for Na^+, K^+, ATP and cardiac glycosides. Multiple genes encode the Na^+-K^+-ATPase α subunit and four different α subunits (α_1, α_2, α_3, and α_4) have been identified at both the genetic and protein levels [64]. Among them, α_1 subunit is regarded as the "housekeeping" isoform, due to its abundance and ubiquitous cellular distribution in majority of the tissues [63], and it (especially α_1-β_1) is essential for life of all mammalian cells [64], except for reticulocytes. Immunohistochemistry and confocal microscopy studies have identified that Na^+-K^+-ATPase α_1 subunit was readily labelled along the entire ventricular SL and intercalated disks and, to a lesser extent, in the transverse tubules [66]. The α_2 isoform is expressed most abundantly in cardiac muscle, skeletal muscle, adipose tissue and glial

cells in the brain [63], and it is identified as a regulator of Ca^{2+} in the mouse heart; heterozygous α_2 hearts are hypercontractile as a result of increased Ca^{2+} transients during the contractile cycle [67]. It should be pointed out that the expression in α_2 isoform is lower in the human heart compared to α_1 and α_3 isoforms [63]. *Jewell and Lingrel* [68] have compared the substrate dependence properties of the rat Na^+-K^+-ATPase and have identified that the affinity of the α_3 subunit is two to three times lower than the α_1 and α_2 isoforms. The α_3 isoform is detected in high concentration in neurons of the central nervous system and cardiac muscle [63]. The α_4 has also been identified at the transcriptional level in mammalian testis [69], it has been shown to be important for the flagellar motor and the mobility of spermatozoa [64].

The Na^+-K^+-ATPase β subunit is referred to as the "regulatory" subunit and is required for the biogenesis and activity of the Na^+-K^+-ATPase complex. The molecular wt of the β subunit ranges from 35 to 55 kDa, depending on the attached *N*-linked sugars [63]. There are three Na^+-K^+-ATPase β isoforms (β_1, β_2, and β_3); however, the β_1 isoform is ubiquitously expressed in all tissues [63] and it is the predominate one in the human heart [63]. Some investigators have reported that the β_3 isoform was not detected in rat heart by Northern blot [63], but it is detected by RT-PCR in human's heart [70]. It should also be mentioned that Na^+-K^+-ATPase γ subunit is a transmembrane protein, with two isoforms [64] and molecular wt ranging 6.5 ~10 kDa [63] but its function is not clear.

In view of the essential role of Na^+-K^+-ATPase in the different aspect of cell life, the alteration of cell specific Na^+-K^+-ATPase isoform as well as their function, are much more important [64] in both pathophysiological and pharmacological studies. In the hypothyroid hearts, cardiac Na^+-K^+-ATPase activities are reduced, while they are

increased in the hyperthyroid heart [71]. In the kidney, Na^+-K^+-ATPase α subunit has been identified and is associated with steroid and thyroid hormones for long term regulation, and with angtiotensin II (Ang II), endothelin, parathyroid hormone and dopamine for the short term regulation [64]. In addition, Na^+-K^+-ATPase α_1 subunit can be phosphorylated by protein kinase A (PKA) and protein kinase C (PKC) in both *in vitro* and in intact cells, both inactivation and activation of Na^+-K^+-ATPase have been reported [64]. Previous experiments have shown that incubation of SL vesicles from normal porcine hearts with hypochlorous acid (HOCI) reduced the Na^+-K^+-ATPase activity in a concentration- and time- dependent manner; this change is associated with the reduction of Na^+-K^+-ATPase β_1-subunit [72]. Similarly, xanthine plus xanthine oxidase increase the malondialdehyde (MDA) content and reduced the Na^+-K^+-ATPase activity in isolated SL vesicles [73]. In the MI induced failing heart, our laboratory has reported a reduction in the Na^+-K^+-ATPase activity; this was associated with the depression in LV contractile function [74,75]. Treatment with L-carnitine [75] is found to partially attenuate the reduction of Na^+-K^+-ATPase activity in this model. It is interesting to know that when Na^+-K^+-ATPase is inhibited by strophanthidin, the $[Na^+]_i$ is increased and associated with the increased $[Ca^{2+}]_i$ and Ca^{2+} transient, and results in arrthymias [76].

5. SL Ca^{2+}-Channel in Heart Failure

The L-type and T-type SL Ca^{2+}-channel are known to be present in the heart but the L-type Ca^{2+}-channel is predominant. It is via the SL Ca^{2+}-channel that extracellular Ca^{2+} influx occurs and triggers the Ca^{2+} release from the SR. There are several factors that influence the function of Ca^{2+}-channel (L-type current), as it is increased by activated

β-adrenergic receptors and PKA and is decreased by dihydropyridiens (DHPS), phenylalkylamines and bezothiazipines [77]. The molecular structure-function relation of the cardiac Ca^{2+}-channel has attracted some attention in the heart. The L-type Ca^{2+}-channel is believed to be a multimeric protein complexes with α_1, α_2, β, γ and δ subunits, which are encoded by separate genes [77]. The α_1 subunit contains the ion-conducting pore and the binding sites for channel blockers [78], and overexpression of α_1 subunit can significantly increases $[Ca^{2+}]_i$ [79], whereas α_2 subunit is thought to be located on the extracellular surface of the SL, and co-operates with δ subunit as $\alpha_2\delta$ subunit to accelerate channel opening and closing [78]. The β-subunit of the Ca^{2+}-channel is important in the assembly of the channel complex, and also in the regulation of channel activity by protein kinases. The γ subunit gene expression has been shown to be restricted to skeletal muscle [80,81]. SL Ca^{2+}-channel is also enhanced when stimulating cGMP, via the cGMP-dependent protein kinase (PKG) dependent phophorylation [82]. The contribution of altered L-type Ca^{2+}-channel function to heart failure is controversial [45]. While some researchers have reported that no change of peak L-type currents in failing rat heart following MI [36,83-85] and hypertension [86], others have reported significantly reduced L-type current [38], after the ascending aortic banding of the guinea pig. Nitrendipine binding is reduced in heart failure following MI [87]. The L-type current density was decreased in association with increasing myocyte membrane area, irrespective of any specific effects, hypertrophy and heart failure [88]. The DHP binding decreased in both SL vesicles and intact myocytes from MI rat but there was no change of I_{Ca}; forskolin and dibutyryl adenosine 3',5'-cyclic monophosphate, unlike isoproterenol, significantly increased I_{Ca} in MI myocytes [84]. On the other hand, pre-treatment with

Ca^{2+}-channel antagonist reduced infarct size and increased septum thickness, and mibefradil and amlodipine also prevented LV dilatation and cardiac fibrosis [89].

6. SL NCX and Ca^{2+}-pump in Heart Failure

The cloning of canine cardiac NCX is accomplished in the *Philipson's* lab [90], confirming a mature protein of 938 amino acids [91] and the nonglycosylated *Mr* 108 kDa [90]. Using monoclonal antibody R3F1 [90-92], there are three bands available at 160 kDa (at non-reducing gel condition), 120 kDa and 70 kDa (at SDS-PAGE); the 70 kDa band appears to be derived from the 120 kDa band, especially after chymotrypsin treatment of the sample. There are at least 2 NCX inhibitors. SEA0400 is a better cardiac protector than KB-R7943, which has side effects at high dose (> 1 μM). The side effects include depressions of heart rate and left ventricular systolic pressure (LVSP) as well as $\pm dP/dt$ [93]. In the failing human heart due to coronary artery disease, NCX mRNA level and protein content are significantly increased [58]. Also it is noted that sympathetic activation may enhance the expresson of NCX in end-stage heart failure patients [59]. In addition, isolated LV myocytes from 8 weeks infarcted rabbit heart exhibit an increase in the maximal NCX current ($I_{Na/Ca}$) density [38]. Opposite results are obtained in cardiomyocytes from 3 week post MI rats, reverse $I_{Na/Ca}$ (3 Na^+ out : 1 Ca^{2+} in) is greatly reduced in addition to the caffeine induced SR Ca^{2+}-release [85]. Neither hypothyroidism nor hyperthyroidism affects the cardiac NCX activities [71]. It is reported that, the protein level of NCX is not changed in hypertophied human heart [94], as well as in the failing human heart [95]. In our laboratory previous work has shown a reduction in the NCX activity [75,96] in MI induced failing heart, as well as depressed gene expression and

protein content (unpublished data). Nonetheless, treatments with L-carnitine attenuate the reduction of NCX function [75]. Although there are different observations regarding the SL NCX density and corresponding Ca^{2+}-current, *Hasenfuss* et al [45] have concluded that NCX is increased in failing hearts of both human patients and experimental models. In explanted hearts of patients with severe heart failure, thapsigargin (a SERCA2a inhibitor) abolishes the phasic component of action potential Ca^{2+} transient, as well as caffeine induced Ca^{2+} transient (from SR); whereas NCX inhibitor No7943 eliminates the tonic component of action potential Ca^{2+} transient and reduces the magnitude of the phasic component [97].

The Ca^{2+}-pump of the plasma membrane (PMCA) is widely expressed in human and rat tissues [98], and encoded by four different genes (PMCA1, PMCA2, PMCA3 and PMCA4). But in the heart tissue, only PMCA4 was found in humans and PMCA1 in rats [98]. Due to the very small amount of PMCA in most plasma membranes, the biochemical studies of PMCA have been very difficult; however, in the overexpression of PMCA4 rats heart, it is found that SL Ca^{2+}-pump has little relevance for beat-to-beat regulation of ECC, but likely to play a role in regulating myocardial growth, possibly through modulation of caveolar signal transduction [99]. Our laboratory has shown that there is no change of Ca^{2+}-pump activity at any time point after MI (4-, 8-, and 16-week) [96]. By contrast, there are reports of depressed Ca^{2+}-pump activity in different models including diabetic cardiomyopathy [100], perfused heart with oxygen free radicals [101]. In the hypothyroid heart, cardiac Ca^{2+}-pump activities are reduced, but no great changes in the hyperthyroid heart are observed [71].

7. SR Ca^{2+}-Channel in Heart Failure

SR Ca^{2+}-channel is also known as the ryanodine receptor (RYR), named due to the fact that a plant alkaloid, ryanodine, is found to both stimulate (low concentration <0.01 μM) and inhibit (high concentration > 10 μM) the Ca^{2+}-efflux from the SR to the cytosol [102]. Such inhibition is long lasting becasue removal of ryanodine from the perfusion medium does not recover the channel condition to a fully conducting state [103]. Generally, RYR can be activated by micromolar amounts of Ca^{2+} or millimolar amounts of ATP. The RYR is inhibited by millimolar amount of Mg^{2+} or micromolar amount of ruthenium red [104]. The cDNA of cardiac RYR is cloned in *Maclennan's* laboratory as 16,532 base pairs, which encodes a protein of 4,969 amnio acids with a M_r of 564,711 [105]. The electron microscopy revealed a four-leaf clover structure (feet) that spans the transverse tubule – SR junction [104,106]. This meets the requirement for its involvement in calcium induced calcium release (CICR) [107]. The developed force transients of the skinned fiber of MI rat is significantly reduced; this is associated with a depression in [^{3}H]-ryanodine binding activities in homogenates and SR-enriched fractions, while receptor affinity (K_d) is not changed [35,37]. Treatment with trandolapril attenuates the reduction of ryanodine binding activities [37]. *Periasamy's* laboratory has reported that the mRNA level of RYR was significantly reduced in both LV and RV from human failing heart [108]. By contrast, *Hasenfuss's* laboratory has reported that there is no change of RYR in failing human dilated cardiomyopathy by Western blot [109]. The reduction of SR function is significant for both Ca^{2+}-uptake by sarco-endoplasmic reticulum Ca^{2+}-ATPase (SERCA) and Ca^{2+}-release by RYR [37], because less Ca^{2+} is available in the SR lumen for release. A similar reduction of [^{3}H]-ryanodine binding

activities has been observed in volume overloaded cardiac hypertrophy model induced by aortocaval shunt [110], but it has been noted that the RYR density in cardiac hypertrophy model induced by pressure-overload is increased [111], but does not change in the prehypertrophic cardiomyopathic hamster heart [112].

8. SERCA in Heart Failure

The SERCA protein is uniformly distributed in the free SR membrane [113], and the SR Ca^{2+}-ATPase isoform 2 (SERCA2) gene encodes both SERCA2a (cardiac/slow-twitch muscle) [114-116] and SERCA2b (smooth/non-muscle and ubiquitously) proteins [114,115]. Two functional copies of the SERCA2 gene are necessary to maintain normal levels of SERCA2 mRNA, protein, and Ca^{2+}-sequestering activity, otherwise reported to result in impaired cardiac contractility and relaxation [117]. In addition to SERCA2, there are also SERCA1 (restricted to fast-switch striated muscle) and SERCA3 [118] (intestine, thymus and cerebellum) [115]. The decreased level of SERCA2a is regarded as the marker of ventricular dysfunction, which has been shown to occur in different models of CHF, *i.e.* marker of the transition from compensatory hypertrophy to heart failure in ascending aortic banding induced heart hypertrophy and heart failure model [119,120], streptozotocin-induced diabetic rat, as well as in hypothyroid mice [121]. In the overexpressed SERCA2a mouse, transgenic hearts show significantly higher contractile function and relax function. This is associated with a doubling in Ca^{2+} transient amplitude [122], even in the hypothyroid condition [121]. Furthermore, adenovirus gene transfer of SERCA2a improves LV systolic function of the failing heart in aortic-banded rats [123]. It is interesting to note that skeletal muscle SERCA1 overexpression in the heart has also

shown similar results [124,125].

Periasamy's laboratory has reported the depression of SERCA2a mRNA in both LV and RV from the human failing heart [108]. *Hasenfuss's* laboratory has found a significant depression (41%) in SERCA2a in failing human heart of dilated cardiomyopathy by Western blot, even relative to RYR (37%) and phospholamban (PLB) (28%) protein contents [109]. Also the protein levels of SERCA2a are closely related to the force-frequency behaviour of the human myocardium, suggesting that SERCA determines the systolic contractile reserve [126]. It has also been reported that SERCA is reduced and inversely related to the degree of the cardiac hypertrophy in both primary and secondary hypertrophied human myocardium [94]. In addition, cardiac SERCA2a protein and activity are significantly decreased in senescent hearts, associated with decrease in $-dP/dt$ [127]. By contrast, others have reported that the heart of human idiopathic dilated cardiomyopathy exhibits the same protein level of SERCA2a as normal heart [128-130], however, the depressed SR Ca^{2+}-uptake function is identified in the end-stage heart failure patient. This includes longer initial beat duration, depressed contraction amplitude following a rest interval, abolishment of positive staircase by treatment of thapsigargin (a SERCA2a inhibitor) [131]. Here, one point should be made that the mRNA level of SERCA2 is depressed in human heart failure [132], even in *Linck's* study in which the protein level of SERCA2a does not change [129]. Likewise, *Schwinger's* [130] has reported that Ca^{2+}-uptake, Ca^{2+}-ATPase activity and mRNA of SERCA2 are reduced in human dilated cardiomyopathy. Furthermore, both LV and RV SERCA2 mRNA to 18S RNA ratios show significant correlations with several indices of heart function [132]. Similar depression has been identified in animal models at 16 weeks after MI [34,40], SR Ca^{2+}-pump activity is depressed in LV, without changes in the affinities

of the enzyme for Ca^{2+} and ATP; SR Ca^{2+}-pump activity in the presence of both PKA and Ca^{2+}-calmodulin stimulation are significantly reduced and the ^{32}P incorporation in the presence of PKA or Ca^{2+}-calmodulin is depressed [34]. The reduction of Ca^{2+}-pump activity is confirmed at 4 weeks in infarcted rats, and associated with the depression of SERCA2 gene expression at the mRNA level [43,62], and such reductions become worse at 8 and 16 weeks post MI [62]. At 8 weeks after MI, rat heart shows decreased SERCA activity, protein contents and gene expression [61]. In failing rat heart following MI, thapsigargin induced relaxation time is significantly shortened compared to sham groups [36]. Similarly, in explanted hearts of patients with severe heart failure, thapsigargin abolishes the phasic component of action potential Ca^{2+} transient, as well as caffeine induced Ca^{2+} transient (from SR). On the other hand, NCX inhibitor No7943 eliminates the tonic component of action potential Ca^{2+} transient and reduces the magnitude of the phasic component as well [97]. There are also controversial opinions about SERCA2a undergoing a depression [40] or no change [26,29] in MI model. It is interesting that *Tajima, et al* [26] have reported that SERCA is not depressed in failing heart following MI but growth hormone improves these failing hearts function by increasing gene expression and protein contents of SERCA. On the other hand, SR exhibits increased Ca^{2+}-uptake at 8 weeks, but not 15 weeks in RV of infarcted rabbit hearts after MI [133]. Furthermore, overexpressed SERCA2a in human ventricular myocytes from failing heart has produced an increase in both protein expression and pump activity of SERCA, associated with a faster contraction velocity, enhanced relaxation velocity, and reduced diastolic Ca^{2+} [134]. Overexpression of SERCA2a significantly improves the heart function, otherwise depressed in senescent rat [127]. In the human RV, no statistically different changes in SERCA2a are found in end-stage heart failure [132]. Post-translation

regulation of SERCA2a function involves $[K^+]_i$ and ATP, which stimulates the enzyme activity [135] as well as the inhibition effect of PLB [136].

9. PLB and CQS in Heart Failure

PLB is a small homopentameric SR membrane protein with 52 amino acids (M_r 6,000) [136]. Actually, PLB localized in SR has a direct interaction with SERCA2a and inhibits it in the non-phosphorylated state whereas the phosphorylation of PLB reverses this inhibition [136]. The phosphorylation of PLB can be initiated by PKA [137,138] as well as calmodulin [138], another Ca^{2+}-binding protein. For example, in transgenic hearts overexpressing a non-phosphorylatable form of PLB (S16A, T17A), the maximal inhibition of SERCA is achieved [139]. Similarly, negative mutant of PLB in mouse enhances SERCA2 activity and myocyte contractility as well as heart contractility [140]. In patients with idiopathic dilated cardiomyopathy, the protein level of PLB is same as in normal heart [128-130], and there is no change of PLB between hypertrophied and normal human heart [94]. Laboratories of both *Linck* and *Schwinger* have reported depression of PLB mRNA in human failing heart [108,129,130,141] and *Hasenfuss's* laboratory has reported that PLB protein level (pentameric form) is decreased by 18% ($P < 0.05$) in failing human dilated cardiomyopathy [109]. *Periasamy* has reported the depression of PLB in RV of the failing human heart [108]. In addition, *Gwathmey's* laboratory has reported that SERCA and PLB are not changed in failing human heart, but cAMP-dependent phosphorylation level of PLB is significantly reduced [142].

In the failing rat heart following MI, PLB protein contents and gene expression are markedly reduced in LV; these changes are associated with the reduction of heart

function and SERCA activity [61]. Our previous work has shown depressed PLB in failing heart associated with reduced SERCA2a gene and protein expression [40]. It is interesting to note that at 3 weeks after MI, PLB protein and mRNA level are sustained but not basal levels of p16-PLB and p17-PLB, which are significantly reduced, associated with increased protein phosphatase 1 activity. Stimulation of β-adrenergic receptor or adenyly cyclase attenuates these changes [143]. One more important finding is that infection of cultured rat neonatal cardiomyocytes with antisense expression of PLB significantly reduces the PLB mRNA level and protein contents in 48 and 72 hours by 30% and 24% respectively and these reductions are associated with improvement of heart function [144]. On the other hand, catheter-based *in vivo* gene transfer of PLB significantly increases the PLB expression at protein level and also depresses LV contractility [145]. It should be mentioned that in patients with idiopathic dilated cardiomyopathy, the protein level of calsequestrin (CQS) is identical with normal human heart [109,128]. Moreover, in hypertrophied human heart [94], failing rat heart [40] and failing human heart [95], there is no change in CQS but *Periasamy* reported the reduction of CQS in LV of failing human heart [108]. Our previous works have not found change of CQS in failing heart following MI [40].

10. MHC and MLC in Heart Failure

Cardiac myosin heavy chain (MHC) isoforms play a key role in defining the dynamic contractile behaviour of the heart during development. In addition, propylthiouracil (0.6%) induced hypothyroid rats exhibits a transition in the ventricular cardiac MHC isoforms expression from α-myosin heavy chain (α-MHC) to β-myosin

heavy chain (β-MHC), while there is a significant desensitization in the Ca^{2+}-sensitivity of tension development in β-MHC-expressing ventricular myocytes, indicating the activation properties of the thin filament are in part MHC isoform dependent [146]. Also, hearts from transgenic mice expressing removal of the myosin light chain (MLC) binding domain in the lever arm of MHC are asymmetrically hypertrophied with increases in mass primarily located to the cardiac anterior wall while there is marked cellular hypertrophy, myocyte disorganization, small vessel coronary disease, and severe valvular pathology, decreased Ca^{2+} sensitivity of tension and decreased relaxation rate [147]. However, *Holt's* study has not revealed the changes in the calcium-myofilament sensitivity in the failing heart following MI [36]. The switching of MHC isforms from α-MHC to β-MHC has been regarded as the marker of ventricular dysfunction, which occurs in different models of heart diseases, such as streptozotocin-induced diabetic rat [148] and MI induced CHF in rats [29,39]. From the study of transgenic mice, it is found that even small shifts in the myosin isoform compostion of the myocardium can result in physiologically significant changes in cardiac contractility [149]. However, it is interesting to note that the relative increase of β-MHC expression is significant at 1 day compared to 1 week and 6 weeks after MI [29]. On the other hand, dexamethasone induced cardiac hypertrophy in newborn rats is accompanied by increased expression α-MHC by 83% at one day and 148% at 7 days after injection of dexamethasone (1 mg/kg/day), while the steady state level of β-MHC mRNA declines by 25% at day one and shows a maximum decrease of 54% at day seven [150]. Although, some reports indicate no change [141] or reduction [108] of β-MHC gene expression in failing human heart, it is now accepted that increase of β-MHC is a marker of heart failure. In our

previous studies, the shift between α-MHC and β-MHC in both LV and RV is significant post MI; this is associated with the depressed myofibrillar Ca^{2+}-ATPase activity and heart function [39]. This remodeling of MHC can be attenuated by the treatment of imidapril, in addition to the improvement of both myofibrillar Ca^{2+}-ATPase activity and heart function.

The protein and gene expression of MLC remains at the normal level in the failing heart following MI [39], which is in agreement with the observation in human idiopathic dilated cardiomyopathic hearts [151]. The regulatory mechanism of MLC is via the phosphorylation by Ca^{2+}/calmodulin-dependent MLC kinase (MLCK) and is considered to play a modulatory role in the activation of myofibrillar Ca^{2+}-stimulated ATPase. At 8 weeks following MI, the MLC phosphorylation (measured as MLC kinase and ratio of phosphorylated MLC) has increased significantly in the RV and septum but decreased markedly in the viable LV [152]. Similarly, *Bing's* laboratory has reported a striking decline in phosphorylation of regulatory MLC in both infarcted and non-infarcted portions of the LV [153]. On the other hand, isoproternol significantly increases the phosphorylation of regulatory MLC [153]. In the streptozotocin induced diabetic cardiomyopathy in rats, MLC, MLCK, MLC phosphorylation are significantly reduced, which is associated with the reduction of myofibrillar Ca^{2+}-stimulated ATPase as well as the depression of heart function [154], which can be partially prevented by the insulin treatment.

11. RAS in Cardiovascular System

RAS is one of the major mechanisms for the regulation of cardiovascular function

and includes several components (see Fig. 2). Angiotensinogen, a 452 amino acid globular glycoprotein of 55-56 kD, is the precursor of Ang II and is mainly localized in the pericentral zone of the liver lobules. The plasma is the major reservoir of angiotensinogen and thus is the major determinant of RAS activity [155]. Renin, a glycoproteolytic single-chain aspartyl protease of 37-40 kD, is highly specific for its substrate, angiotensinogen, and is generated mainly in the juxtaglomerular cells of the afferent arterioles of kidney. In fact, the renin mRNA is found in almost all organs of the body but its level is rather low in the heart. Renin cleaves a leucine-valine bond in the N-terminal region of angiotensiongen for the generation of angiotensin I (Ang I) [155,156]. Ang I is composed of 10 amino acids and does not have any significant effect of its own; however, it is converted by angiotensin-converting enzyme (ACE) to Ang II. ACE, a dipeptidyl carboxypeptidase, is a member of the family of zinc metallopeptidases, derived from the lung and other organs in the body. ACE is predominately attached to the endothelial cells [15], and in addition to converting Ang I to Ang II, it inactivates a well-known vasodilator, bradykinin. Recently, a novel ACE-related carboxypeptidase (ACE2) has been identified in failing heart [157]. Ang II shows almost all the effects of RAS activation when it combines with its receptor. Ang II receptor (AR) heterogenity has been defined primarily by the use of non-peptides to show that there are two distinct types of AR (see Fig. 2). One of these receptors is Ang II type 1 receptor (AT_1R), which is composed of 359 amino acids and divided into AT_{1a} ($AT_{1a}R$) and AT_{1b} ($AT_{1b}R$) subtypes; bovine and rat have a high degree of sequence identity of AT_1R with human [158]. It mediates most of physiological and pathophysiological effects of Ang II, involves the translocation of PKC from the cytosol to the membranes and is blocked by the specific

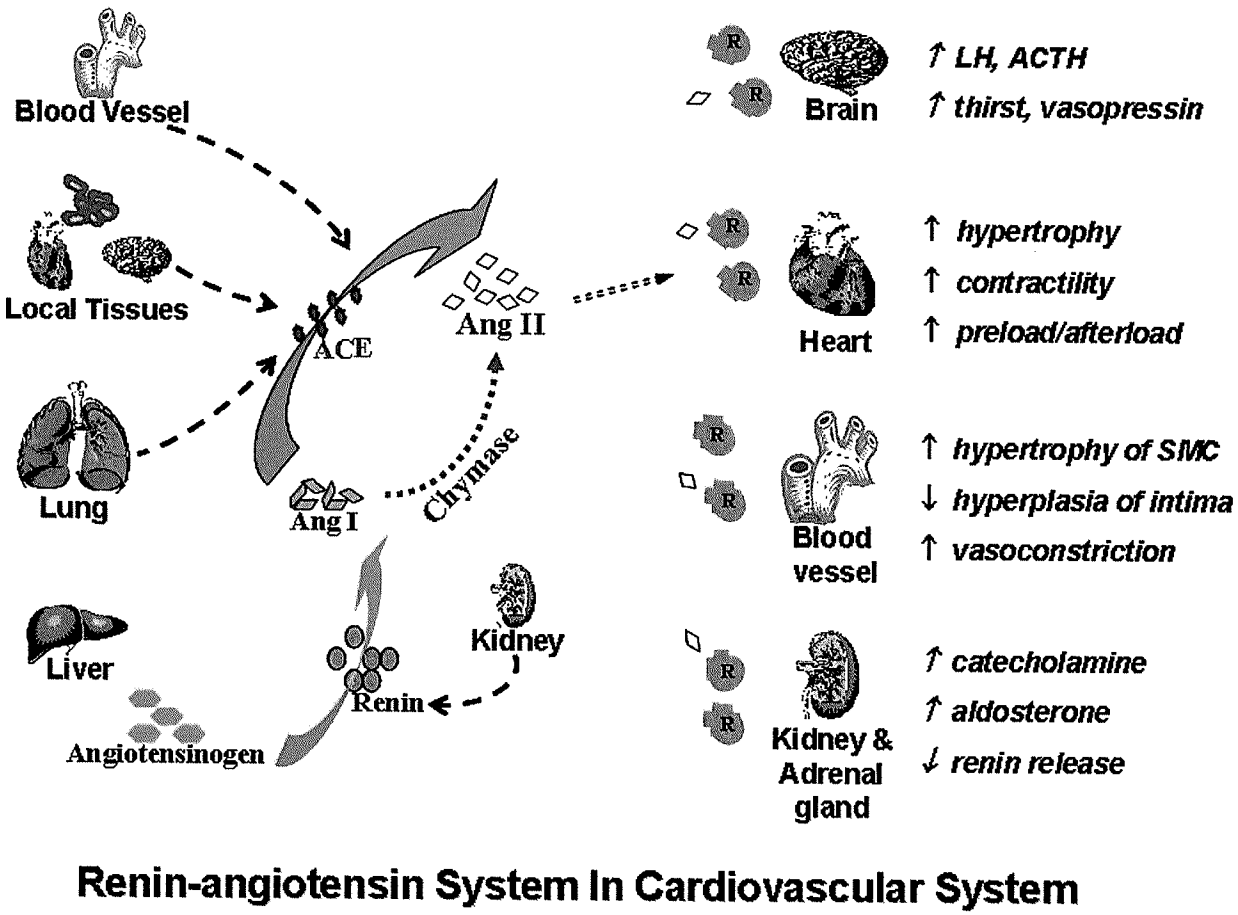

Figure 2. Renin-angiotensin system in cardiovascular system. ACE: angiotensin converting enzyme; Ang I: angiotensin I; Ang II: angiotensin II; R: angiotensin II receptor.

AT_1R antagonist, losartan [15,159]. The other receptor is the Ang II type 2 receptor (AT_2R), which is present in the heart during fetal development and is blocked by PD123177 [160]. Activation of AT_2R is fully capable of activating G_i [161] and inducing cardiac hypertrophy. Furthermore, enhancement of β-adrenergic receptor upregulation by ACE inhibitor (captropril) treatment is thought to be mediated by activation of bradykinin B_2 receptors and PKC, while it is abolished by B_2 receptor antagonist, but not AT_1R antagonist [162]. In addition, AT_2R is not found in skeletal muscle in human with CHF [163]. AT_1R subtype is considered to play a major role in adult ventricular myocytes [15].

There is now evidence available for the existence of a local RAS in the heart [164]; the tissue RAS in the heart is indicated by showing the presence of mRNA for angiotensinogen, ACE and pro-renin in cardiomyocytes [15]. Cardiac ACE has been observed mainly around the cardiac valves, the adventitial and endothelial layers of major arteries, and very minutely in the endocardium [165]. An alternative pathway for cardiac Ang II generation is through a chymotrypsin-like porteinase (chymase), which is not regulated by ACE inhibition [166]. There is no difference in chymase activity or mRNA levels between normal and failing hearts, while chymse levels are highest in both LV and RV [167]. AR is widely distributed throughout the heart and each receptor subtype accounts for about 50% of the specific binding by losartan or PD123177. The density of AR is high in the atrioventricular node [160]; the ratio of AT_2R:AT_1R in the human atria is about 2:1 and the ratio in rats is about 7:3. Most of the Ang II effects are mediated by the AT_1R only [159]. But in rats, AT_1R and AT_2R are equally distributed over the myocardium, and a twofold increase in the density after birth reaching the maximum on day 2 and decreasing towards prenatal values thereafter, suggest that these are

developmentally regulated [160]. Myocardial hypertrophy induced by oxirane carboxylates is belived to occur via the activation of AT_1R, independent of changes in systemic hemodynamics [168]. The stimulation of AT_1R activates phospholipase C (PLC) to produce phosphatidylinosital 4,5-bisphosphate (PIP_2), which forms diacylglycerol (DAG) and phosphatidylinositol 1,4,5-triphosphate (IP_3). IP_3 has been shown to induce Ca^{2+}-release from SR and increase cardiac contractile force development [169,170]. DAG activates PKC and thus stimulates cardiac growth [170]. Ang II is observed to increase the $[Ca^{2+}]_i$ in rat cardiomyocytes as measured by Fura-2/AM fluorescence spectroscopy; this increase is dependent on the concentration of Ang II (0.01 to 10 μM), as well as both losartan and PD 123319 attenuated this increase of $[Ca^{2+}]_i$ [171]. In cardiac hypertrophy, AT_2R is upregulated and associated with antiproliferative effects counteracting the growth-promoting effects of the AT_1R, whereas inhibition of AT_2R by PD 123319 amplies the immediate LV growth response to Ang II [172].

It should be mentioned that Ang II has multiple effects on the heart and peripheral vasculature, acting directly or indirectly on myocytes for the regulation of growth, vascular resistance and contractile force development. The effects of Ang II are mediated via its receptors, which are located on ventricular and smooth muscle cells and are linked to guanine nucleotide-binding proteins (G-proteins) that control the generation of various downstream second messenger pathways [15]. Mechanical stretch has been shown to initiate the release of Ang II from cardiomyocyte which acts as an initial mediator of the hypertrophic response in cardiac myocytes [173]. Cardiac local RAS interacts with the SNS; Ang II modifies the release of norepinephrine from sympathetic nerve endings and promotes presynaptic norepinephrine release. In addition, Ang II blocks presynaptic

norepinephrine re-uptake, increases catecholamine synthesis and potentiates postsynaptic actions of norepinephrine [164]. In cardiac fibroblasts, Ang II has been shown to decrease the activity of metalloproteinase I, which is the key enzyme for interstitial collagen degradation [30].

12. Activation of RAS in MI

Neurohormonal activation occurs almost immediately after the patient experiences acute MI as well as there is a positive relationship between these elevation of plasma neurohormones, including atrial natriuretic peptid (ANP), Ang II, aldosterone, catecholamines and size of infarction [174]. The degree of neurohumoral activation during the first period after MI may be crucial to the resulting degree of LV dilatation [164]. It has been suggested that the RAS and its primary effecter peptide, Ang II, play an important role in the pathophysiology of MI, cardiac hypertrophy and heart failure [175]. Decreased cardiac output following MI leads to a reduction in renal blood flow and therefore promotes the release of renin from the kidney. Renin acts on angiotensinogen to form Ang I, which reacts with the ACE from the lungs and produces Ang II. The RAS has been traditionally thought of a circulating system which is involved in the regulation of blood pressure and fluid homeostasis [176]. However, accumulating evidence indicates that locally synthesized Ang II within the cardiac tissue may be an autocrine/paracrine modulator of cardiac function and structure [177]. It has been indicated that most Ang I within the heart is produced *in situ*, and most of cardiac Ang II is synthesized by the conversion of local Ang I, instead of the systemic one [178]. In addition, both Ang I and Ang II levels are much higher in the interstitial fluid and intravascular space of dog heart,

which were over 100 folds of that in blood plasma. As well as the cardiac Ang I and Ang II levels were not affected by circularing Ang I concentration [179]. This suggested that Ang II production and/or degradation in the heart is compartmentalized and mediated by different enzymatic mechanism in the interstitial and intravascular spaces. In the first six hours after MI, plasma Ang I and Ang II are increased but thereafter only minor increase is observed. In LV, however, Ang I is gradually increased in the first 8-9 weeks, while Ang II increases in the first two weeks only. This phenomenon explained as local production, plays the major role in the increases in cardiac Ang II post-MI [180]. ACE activity was found higher in atria than ventricles, and higher in RV than in LV [181]. Furthermore, the cardiac RAS is thought to be capable of regulating Ang II levels locally within the heart [179,182]. Ang II increases aldosterone release from the adrenal cortex and causes peripheral vasoconstriction. The vasoconstriction as well as sodium and water retention enhance both preload and afterload, which may further increase the remodeling process in compromised myocardium [183]. Ang II also has characteristics as a local growth factor and may contribute to the compensatory LV hypertrophy following MI [183]. Once formed, Ang II may potentiate the effects of other vasoconstrictor hormones in heart failure, specifically by facilitating the central and peripheral effects of the SNS and by enhancing the release of vasopressin from the pituitary; all these three systems may then act in concert to greatly exacerbate loading conditions in the failing heart [44].

In the rat model of acute MI, the angiotensinogen mRNA levels are significantly elevated in the non-infarcted portion of the LV within 5 days of MI, and shows a significant correlation with infarct size and increased LVEDP. However, such alterations in LV disappear at 25 days after acute MI, without significant changes in RV and atria [42]. In this experimental model of acute MI, an increased expression of *c-myc* and *c-jun*

is demonstrated in the viable myocytes of RV and LV at 2 to 3 days after MI while the myocyte volume increases [15]. ACE is increased in the infarct area and in fibrous tissue from the viable areas in the infarcted rat heart [18]. The cardiac ACE activity is increased markedly in the infarcted area and moderately in the viable hypertrophied myocardium without any alteration of the affinity to the inhibitors [184]. The up-regulation of ACE mRNA has been shown in the MI-induced heart failure [15]. In addition, it has been reported that ACE activity is upregulated in LV aneurysms in patients with MI [181]. This upregulation of ACE in the hypertrophied heart induced by chronic aortic stenosis has been documented to be associated with an increased intracardiac conversion of Ang I to Ang II, and such an increased conversion can be blockade over 70% by enalapril [185]. As well as, cardiac bradykinin-(1-9) is increased and braykinin-(1-7) is reduced after MI, due to the activation of cardiac ACE [186]. On the other hand, there is evidence to indicate that AR expression in the heart is regulated in MI and heart failure. The AR, mainly located on the non-myocytes and fibroblasts [159], is found to be elevated in rats after MI; the $AT_{1a}R$ mRNA level is increased while the $AT_{1b}R$ mRNA did not change [43]. Increased mRNA expression in $AT_{1a}R$ and AT_2R has been demonstrated in the infarcted and non-infarcted areas of LV subsequent to coronary ligation in rats, but the increase of AT_1R (3.2 fold) and AT_2R (3.5 fold) receptors density is not associated with any change of receptor affinities [187]. One week after MI, the ventricular myocytes are found to possess the AT_1R subtype exclusively. On the other hand, the Ang II-stimulated phosphoinositol turnover is enhanced 3.7-fold and 2.5-fold in the LV and RV myocytes, respectively [188]. In addition, cardiomyocytes isolated from post-infarcted failing rat heart show increased AT_1R density in both LV and RV by 1.84- and 1.85- fold without the changes of affinity of AR, which may explain the enhanced susceptibility to Ang II in

both LV and RV [188]. It is pointed out that RAS in involved in pathologic myocardial fibrosis because Ang II was reported to increase the collagen synthesis and inhibit the collagenase activity in cultured adult cardiac fibroblasts [15]. The evidence at hand suggests that the RAS may be of potential physiological and clinical importance for remodeling of the infarcted LV. In fact, inhibition of the RAS has become the therapeutic strategy used in clinical practice (see Fig. 3). The inhibition of the RAS can be achieved either by reduction of Ang II by using ACE inhibitors or by blockade of AR [189].

13. Blockade of RAS in MI

The most important development in the treatment of MI and heart failure is the emergence of agents which are used to limit cardiac remodeling and dysfunction via neurohumoral blockade (see Fig. 3). In particular, there has been considerable interest in the role of ACE inhibition on LV remodeling. ACE inhibitors are introduced in 1980 for the treatment of hypertension [190]. Twenty years later, ACE inhibitors have become the main agents for treatment of MI and CHF. These have been found to improve ventricular function and long-term survival after MI [191-194] (see Table 4).

Although it is understood that ACE inhibitors decrease both plasma and LV Ang II content following MI [180], the mechanisms of action, time frame for the beneficial effects and duration of therapy with ACE inhibitors are still unknown [190]. ACE inhibitors are considered to affect heart failure following MI as a consequence of a combination of neurohormoanl, hemodynamic, LV structural remodeling and other effects [17,37,195-199](see Table 4). First, ACE inhibitors directly decrease the circulating and tissue effects of Ang II by reducing its production and may suppress the

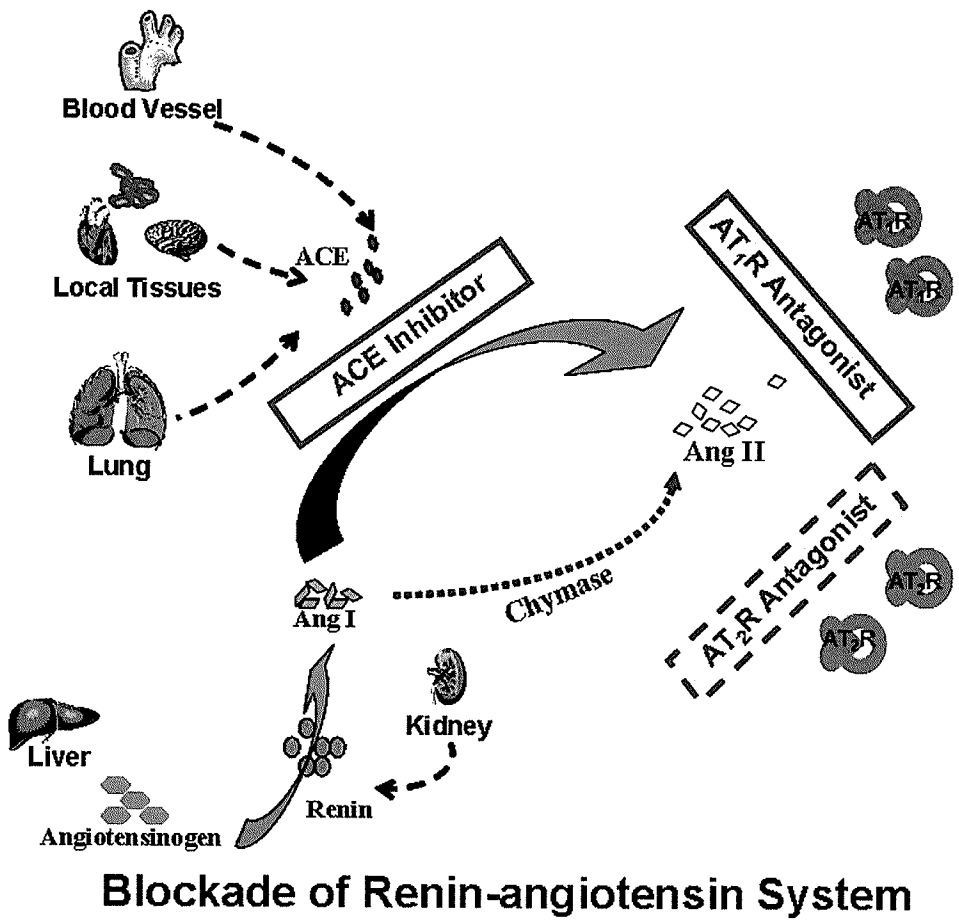

Figure 3. Blockade of rening-angiotensin system. ACE: angiotensin converting enzyme; Ang I: angiotensin I; Ang II: angiotensin II; AT_1R: angiotensin II type 1 receptor; AT_2R: angiotensin II type 2 receptor.

Table 4. Possible beneficial effects of RAS blockade after MI

A. Effects on left ventricle only

- Decreased left ventricular wall stress
- Decreased intracavity pressures
- Decreased infarct expansion
- Improved left ventricular geometric shape

B. Hemodynamic effects

- Reduced afterload
- Reduced preload
- Absence of chronotropic stimulation

C. Neurohormonal effects

- Decreased circulating angiotensin II level
- Decreased tissue angiotensin-converting enzyme activity
- Decreased catecholamine level
- Decreased aldosterone and secondary fluid retention
- Decreased bradykinin degradation

D. Anti-ischemic effects

- Improved coronary flow distribution
- Potential plaque stablilization and vascular protection

E. Other effects

- Inhibition of cell growth due to angiotensin II
- Possible direct cellular effects of angiotensin-converting enzyme (a carboxypeptidase inhibitor)

sympathetic-mediated ventricular dilation due to increased cardiac workload or direct inotropic effects on the myocardium [15,190,195]. ACE inhibitors are tested to be safe in treatment of MI patients and suitable to be combined with other drugs (recombinant tissue-type plasminogen activator) [200]. For example, in serial echocardiographic measurements of MI patients, early treatment with captopril (first generation ACE inhibitor) is found to attenuate infarct expansion and favourably influence early LV remodeling [201]. Long-term treatment with zofenopril markedly reduces the LV cavity volume in rats with moderate-to-large infarctions which is accompanied by a significant reduction in the total heart wt to body wt ratio [202]. Short-term treatment with zofenopril, however, neither prevents cardiac hypertrophy nor improves heart function [202]. It is also reported that there is no positive effect of acute administration of enalapril after MI [203],

As measured in the perindopril treated aorta-constricted rabbit, plasma ACE activity is inhibited by 93 to 95%, compared to placebo-treated animals or sham controls [204]. On the other hand, ramipril significantly reduces the uptake of ^{3}H-noradrenalin into the varicosities of the heart by 10%, associated with the decrease in neuronal and extraneuronal uptake of catecholamines [205]. In the pacing-induced heart failure pig model, benazeprilat alone or combined with valsartan significantly reduces plasma norepinephrine, which is not affected by valsartain sole treatment [206]. These drugs may also diminish the level of plasma aldosterone and prevent secondary sodium retention and fluid accumulation [15,190,195]. The circulatory catecholamines are reduced, while the degradation of bradykinin is diminished by ACE inhibitors [15,195]. However, ACE inhibitors do not completely inhibit the production of Ang II because it is also produced through non-ACE pathway [170]. Secondly, these drugs can induce veno- and arteriolar

dilation resulting in improved stroke volume and reduce atrial and ventricular diastolic volume without chronotropic stimulation [15,190,195]. In patients treated with captopril, ischemia-related events are reduced during the first 3 to 12 months after MI but there is a rebound phenomenon after the withdrawal of the treatment [207]. ACE inhibitors containing sulfhydryl groups may have additional beneficial effects in scavenging free radicals in reducing reperfusion damage [208]. Accumulating evidence supports the idea that chronic ACE inhibition reduces cardiac hypertrophy and chamber dilatation while improving long-term survival in MI animal models (Table 5) [195,197,209]. ACE inhibitors not only reduces the LV filling pressure and ventricular distension but also reduces the dilatation of LV (Table 6) without reducing the infarct size [37]. Irrespective of early versus delayed ACE inhibition in rats after MI, LVSP, LVEDP and central venous pressure (CVP) are reduced; LV wt, cavity size and collagen density are decreased [197]. In addition, ACE inhibitors are found to decrease the transmural wall stress, compensatory dilatation and compensatory increase of end-diastolic and end-systolic volume. ACE inhibitors directly or indirectly alter remodeling process of the LV and improve the coronary flow distribution in both surface and transmural areas [15,190,195]. On a long-term basis (6 to 8 weeks), treatment with ACE inhibitors also reduces the abnormal accumulation of myocardial collagen in MI rats [15]. Blockade of RAS by trandolapril attenuates the reduction of SR function and heart fuction in MI induced heart failure [37]. In addition to the cardiovascular benefits, ACE inhibition improves the respiratory and skeletal muscle performance [204].

Clinical studies have been carried out to evaluate the effects of ACE inhibition following MI (see Table 5). It has been shown that ACE inhibitors attenuated ventricular remodeling, minimized the subsequent development of severe CHF and ultimately

Table 5. Clinical trials for ACE inhibitors in heart failure

Drug	Dose in Human	Major Clinical Trial	Therapeutic Effects
Captopirl	12.5-2.5 (up to 50) mg t.i.d.	SAVE [210]	Improvement in survival and reduction in morbidity and mortality, as well as reduction of both fatal and nonfatal major cardiovascular events.
		ISIS-4 [211]	Significant (7%) reduction in 5-week mortality, especially in high-risk patients.
	25 mg t.i.d.	CATS [212]	Very early treatment with captopril after MI significantly reduces the occurrence of early dilation and the progession to heart failure.
Enalapril	2.5-20 mg/day	SOLVD [191,194]	Improves clinical symptoms and reduces mortality and recurrence of MI
	2.5-40 mg/day	CONSENSUS I [192]	Reduces mortality and improves symptoms.
	2.5-20 mg/day	CONSENSUS-II [203]	No improvement of survival in first 180 days after MI
Fosinopril	5-20 mg/day	FAMIS [213]	Fosinopirl shows a 30% reduction in the 2-year incidence of death or moderate-to-severe CHF in MI patients.
Lisionpril	20 mg/day divided does	GISSI-3 [214]	Improves prognosis in terms of survival rate and ventricular dysfunction
Ramipril	5 mg b.i.d.	AIRE [215]	Ramipril reduces premature death from all causes of MI patients MI (27% reduction of observed risk)

Table 5 (Cont'd)

Drug	Dose in Human	Major Clinical Trial	Therapeutic Effects
Ramipril	10 mg/day	HOPE [216]	Ramipril lowers the risk of MI by 22%, cardiovascular death by 37% in high risk patients
Trandolapril	2-4 mg/day	TRACE [217]	Reduces the risk of overall mortality, mortality from cardiovascular causes, sudden death, and the development of severe heart failure
Zofenopril	7.5-30 mg/day	SMILE [218]	Zofenopril improves both short-term and long-term outcome, significantly reduced death or severe CHF

AIRE: Acute Infarction Ramipril Efficacy Study; CATS: Captopril and Thrombolysis Study; CHF: congestive heart failure; CONSENSUS: Cooperative New Scandinavian Enalapril Survival Study; FAMIS: Fosinopril in Acute Myocardial Infarction Study; GISSI-3: the Third Gruppo Italiano per lo Studio della Sopravivenza nel Infarto Miocardico; HOPE: Heart Outcomes Prevention Evaluation; ISIS-4: the Fourth International Study of Infarct Survival; MI: myocardial infarction; SAVE: Survival and Ventricular Enlargement; SMILE: Survival of Myocardial Infarction Long-Term Evaluation; SOLVD: Studies of Left Ventricular Dysfunction; TRACE: Trandolapril Cardiac Evaluation.

Table 6. ACE inhibitors in MI model

Drug	Model	Dose	Beneficial Effects
Captopril	Female Wistar rats	2 g/L drinking water	The captopirl treatment starting at 14 days after MI, significantly improves LV function and lessened dilatation, as well as improved the one yeart survival [209].
	Female Wistar rats	2 g/L drinking water	Attenuates LV dilation, rightward shift of the pressure-volume relation; and lowers LV filling pressures and LV dilatation, as well as prolongs survival rate [17].
	Male Wistar rats	500 μg/kg/hr	Early captopril treatment (one day to 21 days after MI) had tachycardia together with a decreased stroke volume [219].
	Male Wistar rats	500 μg/kg/hr	Later captopril treatment (starting at 21 days after MI) improves cardiac function, without effects on MAP, central venous pressure and heart rate [219].
	Male SD rats	2 g/L drinking water	Captopril has similar effect with losartan in survival rate for MI [220].
	Male Wistar rats	10 mg/kg/day	Decreases MAP and LVEDP, increases cardiac output and stoke volume; reverses the reduction in ATP, creatine phosphate, creatine and the mitochondrial oxygen consumption rate [196].
	Male SD rats	2 g/L drinking water	Captopril reduces LVEDP and increases venous compliance [199].
	Female SD rats	2 g/L drinking water	Captopril improves heart function, reduces LV volume and lower left and right ventricular weights, without effects on scar size [221].
	Male SD rats	2 g/L drinking water	Captopril improves heart function, SR Ca^{2+}-uptake and SERCA activities; as well as attenuates the depression of SERCA and PLB at both protein and gene expression level [61].
	SD rats	2 g/L drinking water	Captopirl prevents the hypertrophy in both LV and RV, by reducing the increased cell length at LV free wall, septum and RV [222].
	Wistar rats	2 g/L drinking water	Captopril prevents the reduction of toall, MM-, and mitochondrial creatine kinase activity, as well as the depression of total cratine, phosphocratine and CK velocity [223].

Table 6 (Cont'd)

Drug	Model	Dose	Beneficial Effects
	Female SD rats	10 μg/ml drinking water	Enalapril produces thicker and less expanded scar in MI rat, which may be due to the hypertrophy of viable myocytes.[224].
	SD rats	25 mg/L drinking water	Enalapril prevents LV and RV hypertrophy, as well as the increase in white blood count, neutrophils and lymphocyte count. There is significant increase in the T helper:suppressor ratio, and attenuates T cells and immunoglobulin G antibody [225].
	Female SD rats	2 g/L drinking water	Captopril attenuates LV remdoeling, decreases interstitial fibrosis and prevents the increase of TGF-β1 mRNA expression [226].
	Male Wistar rats	30 mg/kg, daily, intraperitoneally	Captopril reduces similary postinfarction hypertrophy and collagen depostition in viable myocardium [227].
Enalapril	Male Wistar rats	10 mg/kg/day	Decreases MAP and LVEDP, increases cardiac output and stoke volume; reverses the reduction in ATP, creatine phosphate, creatine and the mitochondrial oxygen consumption rate [196].
	Male SD rats	10 mg/kg/day	Enalapril inhibits nonmyocyte proliferation and limits myocardial hypertrophy, as well as diminished collagen content [198].
	Male SD rats	0.5 mg/kg/day	Enalapril reduces cardiac hypertrophy, restores minimal coronary vascular resistance, attenuates the development of myocardial interstitial fibrosis in the noninfarcted LV [19]
	Female SD rats	2 mgkg/day	Enalapril prevents LV dilation by limiting infarct expansion [228].
Lisinopril	Male Wistar rats	10 mg/kg/day	Both early versus delayed treatment increase survival rate, lower LVEDP, cntral venous pressures; meanwhile accompanying with reduction of systolic pressure and LV wt, LV cavity circumference, and LV collagen density [197].
	Male SD rats	0.5 mg/kg/day	Low dose of lisinopril attenuates the desease in skeletal muscle capillary density and capillary-to-muscle fiber ratio [20].

Table 6 (Cont'd)

Drug	Model	Dose	Beneficial Effects
		5 mg/kg/day	High dose of lisionpril reduces the increased media thinckness of intramuscular resistance vessels, in addition to attenuation of the skeletal muscle capillary density and capillary-to-muscle fiber ratio [20].
Ramipril	Male albino Wistar rats	1 mg/kg/day	Ramipril improves contraction rate, and suppresses the development of hypertrophy [229].
Imidapril	Male SD rats	1 mg/kg/day	Imidapril attenuates the changes of SL PLC isoenzymes [230].
Trandolapril	Male Wistar rats	3 mg/kg/day	Decreases MAP and LVEDP, increases cardiac output and stroke volume; reverses the reduction in ATP, creatine phosphate, creatine and the mitochondrial oxygen consumption rate [196].
Quinapril	Male Wistar rats	6 mg/kg/day	Quinapril improves cardiac performance and reduces LV wt [231].
	Male Wistar rats	3 mg/kg/day	Decreases LVEDP and improves the developed force transients of the skinned fibre and attenuates the reduction of RYR [37].
Zofenopril	Male Wistar rats	12 ~ 15 mg/kg/day	Long-term (42 days) treatment with zofenopril reduces the LV cavity volume in rats with moderate-to-large infarctions, and also reduces the septal wall thickness in both sham and MI rats [202].

improved survival after MI [232]. The Cooperative North Scandinavian Enalapril Survival Study I (CONSENSUS I) is the first clinical trial to demonstrate the beneficial effects of the ACE inhibitor on survival [192]. In the Fourth International Study of Infarct Survival (ISIS-4), captopril is reported to be associated with significant improvement in the overall survival rate in acute MI patients [233]. The Survival and Ventricular Enlargement (SAVE) Trial demonstrated that use of captopril in the post-infarction period is associated with a decrease in sudden death, recurrent MI, fewer ventricular arrhythmias and a reduction of infarct expansion [210]. The results in the Acute Infarction Ramipril Efficacy (AIRE) Study shows that ramipril substantially reduces premature death, severe heart failure and recurrent MI after it has been administered to the patient with heart failure following MI [215]. AIRE Study also demonstrates that ramipril significantly decreases SVR, lowers LV filling pressure and improves LV function. Based on these clinical trials, ACE inhibitors have been utilized in hemodynamically stable patients within the first 24 hours after acute MI, asymptomatic LV dysfunction after MI, and CHF [215,218]. However, an experimental study in rats with MI differs from these clinical results [219]. There is no significant benefit when the ACE inhibitor is given within the first 3 weeks after MI; captopril therapy in chronically infarcted rats improves cardiac function when therapy is started after completion of the healing process. Nonetheless, recent studies from our laboratory have revealed the beneficial effects of captopril and imidapril on cardiac dysfunction when these ACE inhibitors are administered within 1 to 3 hours after the induction of MI in rats [61,234]; imidapril is also observed to attenuate MI-induced arrhythmias [235]. It is pointed out that the major side effects of ACE are cough, renal dysfunction and first dose hypotension, which are due to ACE inhibitor-induce bradykinin formation but there are still some patients having

poor LV function despite ACE inhibitor treatment [236]. Some of the ACE inhibitors which have been evaluated clinically for their beneficial effects in CHF are shown in Table 6.

An important discovery occurred in 1990 in terms of the biological activity of the first orally active antagonist (losartan potassium, old name was DuP 753) of AR [237], which has effects on Ca^{2+}-transport, as blockade of Ang II-induced Ca^{2+} efflux in rat aortic smooth muscle cell, without partial agonistic effect [237]. Several AR antagonists, including valsartan, candesartan cilexetil, irbesartan, telmisartan and losartan, are currently used for the treatment of patients with hypertension [238]. The AT_1R antagonist are more specific than ACE inhibitor in that these block the Ang II actions at the receptor level and could inhibit the effects of Ang II formed through both the RAS and non-RAS pathways as well [239]. In addition, AT_1R blockers do not affect bradykinin metabolism as do the ACE inhibitors, therefore, they do not cause cough. It has been reported that AR blockers are not as effective as ACE inhibitors in preventing cardiac remodeling, but AT_1R antagonists do have the same effect in attenuating cardiac hypertrophy and long-term mortality as compared to ACE inhibitors in ligated rats [220] and other beneficial effects [198,199,240] (see Table 7 and 8). However, the therapeutic effect of losartan on nonmyocyte proliferation and collagen deposition are limited [198]. Losartan improves the symptoms in CHF after MI or other diseases [241]. Furthermore, losartan is reported to enhance the peak exercise capacity and alleviate the clinical symptoms [242] in CHF patients who are severely symptomatic even during treatment with optimal doses (maximally recommend or tolerated) of ACE inhibitors. In normal rat cardiomyocytes, losartan is shown to block the increase of $[Ca^{2+}]_i$ and cell beating due to Ang II [171]. It is demonstrated that either losartan alone or combined with enalapril could limit cardiac

Table 7. Clinical trials for AT_1R antagonists in MI

Drug	Dose in Human	Major Clinical Trial	Beneficial Effects
Losartan	50 mg/day	OPTIMAAL [243]	Losartan has non-significant difference in total mortality in favour of captopril, but losartan has better tolerance than captopril.
	50 mg/day	ELITE [244]	In elderly heart-failure patients (65 years old or more), losartan treatment has a lower mortality and better tolerated, compared with captopril.
	25 or 50 mg/day	166 CHF patients [245]	Losartan and enalapril are of comparable efficacy and tolerability in short-term treatment of moderate or severe CHF.
	50 mg/day	20 CHF patient [246]	Losartan blunts the hypertensive response to exercise, increasing exercise tolerance and improves quality of life.
Candesartan	8 mg/day	23 CHF patients [247]	Candesartan decreases plasma levels of TNFα, IL-6, sICAM-1 and sVCAM-1, without significant alteration of hemodynamic parameters.
		218 CHF patients [248]	Candesartan demonstrates significant short-term and long-term improvements in hemodynamic, neurohormonal, and symptomatic status and was well tolerated in patients with CHF.
Eprosartan	400-800 mg/day	ADEPT [249]	There is no change in left ventricle ejection fraction after 2 months of therapy with eprosartan.

CHF: congestive heart failure; OPTIMAAL: The Optimal Therapy in Myocardial Inarction with the Angiotensin II Antagonist Losartan; ELITE: Evaluation of Losartan in the Elderly Study; ADEPT: Addition of the AT_1 receptor antagonist eprosartan to ACE inhibitor therapy in chronic heart failure trial

Table 8. AT_1R antagonists in MI model

Drug	Model	Dose	Beneficial Effects
Losartan	Male SD rat	40 mg/kg/day	Losartan limits the collagen deposition, and limits the increase of heart wt/body wt ratio, without therapeutic effecs on nonmyocyte and collagen deposition [198].
	Male SD rats	40 mg/kg/day	Dup 753 reduces LVEDP and increases venous compliance [199].
	Male Wistar rats	15 mg/kg/day	Losartan reduces cardiac hypertrophy, and completely inhibits collagen deposition [240].
	Male SD rats	2 g/L drinking water	Losartan has the same effect as captopril in survival rate for MI, but associated with increase in heart rate and decreae in peak developed pressure [220].
	Male SD rats	3 mg/kg/day	Losartan reduces cardiac hypertrophy, restores minimal coronary vascular resistance, attenuates the development of myocardial interstitial fibrosis in the noninfarcted LV [19].
	Male Wistar rats	10 mg/kg/day	Losartan initiates 1 week after MI attenuates LV dilation and limited the thinning of the scar [250].
	Female SD rats	2 g/L drinking water	Losartan attenuates LV remodeling, decreases interstitial fibrosis and prevents the increase of TGF-β1 mRNA expression [226].
	Male SD rats	15 mg/kg/day	Losartan attenuates the activation of TGF-β1 in target tissue, normalize total Smad2 overexpression in scar and viable tissue, as well as Smad4 in scar [251].
	Male SD rats	2 g/L drinking water	Losartan decreases LV and RV weights as well as MAP and LVSP, and associated with the reduction of interstitial fibrosis [21].
Irbesartan	Male SD rats	40 mg/kg/day	Irbesartan attenuates the cardiac hypertrophy, prolonged time constant of isovolumic relaxation (*tau*), and increases ANP expression [252].
Candesartan	Male Wistar rats	1 mg/kg/day	Attenuates the mRNA changes in both LV and RV, including β-MHC, α-skeletal actin, ANP, collagens I and III, NCX, and SERCA [47].

hypertrophy in acute MI rats; however, losartan does not have marked effects on non-myocyte cellular proliferation [198]. The SL L-type Ca^{2+}-channel and SERCA densities are reduced in the failing pig heart induced by rapid pacing, and these changes are attenuated by a combination therapy with benazeprilat and valsartan; neither ACE inhibitor nor AT_1R blocker alone has such effects [253].

Although only a small improvement in cardiac output in the rat MI model is observed in losartan treated group, losartan does reduce LV hypertrophy and completely prevents cardiac interstitial collagen accumulation [240]. When losartan is administered locally in the coronary circulation of dogs, there is a greater increase in coronary corss-section area and coronary blood flow than the results observed in the ACE inhibitor (enalapril) trial [254]. It has been suggested that nitric oxide released from endothelial cells of epicardial vessels may be involved in this vasodilatory effect of losartan because the response is blocked by L-NAME [239]. Although Ang II may rise during the treatment with losartan, the deleterious effects of the increased Ang II still remain blocked by losartan. Additionally, the available circulating Ang II may stimulate the unblocked AT_2R, which is thought to regulate several beneficial cardiovascular processes, including vasodilation and antiproliferation through the production of cGMP and protein dephosphorylation [255-257], as well as inhibition of growth factor-induced proliferation [255], and offset the growth promoting effects mediated by the AT_1R [256]. The postulated benefits of AR blocker over ACE inhibitors have not been clearly proven, but preliminary data indicates that AR blocker may be at least as effective as ACE inhibitors in terms of their therapeutic effect on patients with heart failure [244].

It has already been shown that ACE inhibitors and AR antagonist have comparable efficacy and tolerability in patients with moderate and severe CHF [245],

reducing cardiac hypertrophy in acute MI rats, and restoring minimal coronary vascular resistances, as well as attenuating the development of myocardial interstitial fibrosis in viable LV tissue [19]. In the Optimal Therapy in Myocardial Infarction with the Ang II Antagonist Losartan (OPTIMAAL) study [258], losartan has been compared with captopril in high risk patients with acute MI. Losartan is found to be significantly better tolerated than captopril, associated with significantly fewer discontinuations, but a non-significant difference in total mortality is in favour of captopril [243]. In order to answer the question whether the combination of ACE inhibitors and AR blockade will provide benefits over using ACE inhibitor or AR antagonist alone, both experimental animal models of CHF and clinical studies have been designed with combination of ACE inhibitor/AR blocker therapy and the preliminary results indicate that the agents may be additive with respect to reduction of circulating endothelin level [206,253]. A large clinical trial, Valsartan in Heart Failure, is being carried out to investigate the benefits of combining treatment of patient of heart failure. It has been suggested that by adding an AT_1R antagonist to the ACE inhibitor therapy, more benefits will be provided to the patients both from the bradykinin actions and a complete blockade of Ang II [259].

Some researchers have found that the combination of ACE inhibitor and AT_1R antagonist is more beneficial than monotherapy for treatment of heart failure. In Dahl salt-senstive (DS) rats, the combination of ACE inhibitor benazepril (5 mg/kg) and AT_1R antagonist valsartan (15 mg/kg), independent of the hypotensive effect, improves LV phenotypic change and increased LV endothelin-1 production and collagen accumulation, diastolic dysfunction, and survival in a rat heart failure model more effectively than either agent (benazepril 10 mg/kg or valsartan 30 mg/kg) alone [260].

14. RAS Blockade and Subcelluar Remodeling

Although pharmacological therapy with ACE inhibitors and AT_1R has proven to be effective in humans with CHF, the experimental basis of this effect has not yet been addressed clearly. Treatment of CHF patients with ACE inhibitors and AR antagonists is commonly considered to produce beneficial effects by attenuating cardiac remodeling in terms of changing the shape and size of cardiomyocytes. These actions are primarily attributed to alteration in the extracellular matrix. Extensive studies in rats have revealed marked changes in SL Na^+-K^+ ATPase, Ca^{2+}-channels, NCX and G-protein activities, SR Ca^{2+}-uptake and -release activities as well as myofibrillar ATPase activities in failing hearts due to MI [74,87,96,261,262]. Accordingly, it is proposed that there occurs remodeling of cardiac membranes and contractile proteins during the development of heart failure [263] and it is likely that this remodeling of subcellular organelles is affected by RAS blockade. This view is supported by the fact that different ACE inhibitors have been observed to prevent changes in SR, extracellular matrix and myocardial metabolism in the failing rat hearts due to MI [61,196,264]. It should be mentioned that remodeling of subcellular organelles should be viewed in terms of changes in their molecular structure. It appears that remodeling of subcellular organelles during the development of CHF is occurring at the level of gene expression and both ACE inhibitiors and AR antagonists may be acting to prevent these molecular alterations in the failing heart. Such an effect of RAS blockade may not be limited to cardiomyocytes but vascular myocytes have also been shown to be affected by treatment of MI rats with losartan [265].

15. Summary

From the foregoing discussion, it is evident that MI results in cardiac hypertrophy and subsequent CHF, but the exact mechanisms of these pathophysiological alterations are still not fully understood. For the phenotypic alterations following MI, immediate early genes [29], contractile proteins [39], Ca^{2+}-regulating proteins [40], and signal transduction pathway proteins [41] are significantly changed. These alterations are associated with the ventricular remodeling and heart function, while different pharmacological intervention are considered to modify them and improve the heart function [39-41]. Although not all the proteins are studied (as it is impossible and not practicable at current condition), it is possible and necessary to investigate the key proteins, which are involved in the ECC in the heart following MI, the major cause of CHF.

An immediate induction of the fetal/embryonic transcriptional gene program [29], is followed by myocyte hypertrophy and CHF in rats with post-MI. In failing hearts due to MI in rats, the diastolic $[Ca^{2+}]_i$ is increased and the systolic peak $[Ca^{2+}]_i$ is decreased. However, alterations of SL Ca^{2+}-channel, SL Na^{+}-K^{+}-ATPase, SL NCX, and SL Ca^{2+}-pump are not well defined following MI. Since RV is part of the whole heart, a study of gene expression in RV in comparison to that in LV can be seem to yield valuable information. Factors such as neurohumoral activation, including RAS, are crucial in terms of ventricular topographic changes during the development of cardiac hypertrophy and heart failure. RAS affects not only structural remodeling of the LV but also the myocyte function following MI. In clinical studies and animal experiments, blockade of RAS with different ACE inhibitors or AR antagonists has been shown to produce beneficial effects in MI-induced CHF. The blockade of RAS following MI is still of critical importance even if new therapeutic methods including cell transplantation [266-268] have been

emerged for research and clinical trial, The beneficial actions of RAS blockade on cardiac function in CHF are considered to be due to its ability to limit infarct size, enhance scar formation and reduce infarct expansion to decrease ventricular wall stress as well as prevent the ventricular remodeling after MI. It has been shown that various ACE inhibitors and AR antagonists have comparable efficacy and tolerability in patients with moderate and severe CHF. Since alterations in subcellular organelles such as SL, SR and myofibrils in CHF are attenuated by ACE inhibitors and AR antagonists, it is suggested that the beneficial effects of RAS blockade in heart failure may be due to the actions of these agents on subcellular remodeling.

II. STATEMENT OF THE PROBLEM AND HYPOTHESES TO BE TESTED

MI is known to cause cardiac remodeling (changes in cardiomyocyte size and shape) and leads to cardiac hypertrophy and subsequent CHF [191]. Following MI, it is clearly evident that there is activation of the RAS in the failing heart, which may contribute to the subcellular and molecular changes that occur in cardiomyocytes during the cardiac remodeling process. Thus, it is hypothesized that the blockade of the RAS may prevent the cardiac remodeling at gene expression and protein level, associated with improvement of heart function.

Cardiac remodeling has been shown to be associated with alterations in SL Na^+-K^+-ATPase [269]. For example, in the failing rat heart post MI, the activity of Na^+-K^+-ATPase is reduced and associated with the depressed LV contractility [74]. However, the mechanism of the reduced Na^+-K^+-ATPase activity has not been fully elucidated. SL Na^+-K^+-ATPase manipulates intracellular homeostasis of $[Na^+]_i$ and $[K^+]_i$ as well as myocardial function regulating movements of the Na^+ and K^+ across cell membrane [49,270]. Generally, Na^+-K^+-ATPase is composed of one α isoform and one β isoform, while there are 3 α and 3 β isoforms of Na^+-K^+-ATPase in rats [271]. The increase in the Na^+-K^+-ATPase α_3 isoform (low affinity for Na^+) is involved in cardiac remodeling in the aortic constriction induced hypertrophied heart [272], the ischemic-reperfused heart [273] as well as in the failing human heart [274]. However, there is not enough information regarding the status of the SL Na^+-K^+-ATPase subunits in CHF post MI. Thus, it is proposed that examination of alterations in the different subunits of Na^+-K^+-ATPase in

heart failure will yield the required information about the cardiac remodeling that occurs following MI. In addition, the gene expression of different Na^+-K^+-ATPase subunits will also be tested.

The RAS is vital to cardiac remodeling in clinical studies as well as in animal experiments and blockade of the RAS has become the major therapeutic method in CHF [2]. However, the mechanism of the effects of RAS on SL Na^+-K^+-ATPase during CHF has not been fully investigated. In order to study the therapeutic mechanisms of RAS blockade, changes in enzyme activities, protein content and steady state mRNA levels of SL Na^+-K^+-ATPase need to be evaluated upon treatment with enalapril, an ACE inhibitor, and/or losartan, an AT_1R antagonist following MI.

Since the RAS is activated in CHF and its blockade has been shown to prevent cardiac remodeling and improve cardiac function in CHF due to MI in humans [191,215] and animal models [39,40,61,196,275], it is likely that SL Na^+-K^+-ATPase remodeling in the failing heart is prevented by the blockade of RAS. Although enalapril and losartan have been reported to produce beneficial actions on cardiac remodeling and heart failure [40,260,276], the effects of enalapril and losartan on changes in SL Na^+-K^+-ATPase activity and different isoforms in CHF remain to be determined. Thus, the present study was undertaken to test the hypothesis that improvement of LV cardiac function is associated with prevention of changes in gene and protein expression as well as activities of Na^+-K^+-ATPase isoforms in the failing heart upon treatment with enalapril or losartan. Combination therapy with enalapril and losartan was used to treat infarcted animals in order to test the hypothesis that the effects of enalapril and losartan are additive.

Alterations in SL Ca^{2+}-transport in different types of failing heart are due to changes in the expression of genes specific to SL Ca^{2+}-regulatory proteins; however, the

understanding of the SL NCX changes following MI is controversial. Furthermore, SL Ca^{2+}-pump and Ca^{2+}-channel have not been examined previously. Due to the increased diastolic $[Ca^{2+}]_i$ and reduced activity of SERCA2a following MI, it is hypothesized that the SL Ca^{2+}-pump may be upregulated to compensate for the reduction in SR function. It is therefore proposed that the protein level of cardiac PMCA1 in the failing heart post MI be examined. The gene expression of PMCA1 will also be measured at the same time. On the other hand, the decrease in systolic $[Ca^{2+}]_i$ and reduced amount of SL Ca^{2+}-current following MI gives rise to the hypothesis that reduced L-type Ca^{2+} channel current is due to the remodeling of the SL Ca^{2+}-channel. Therefore, different subunits of cardiac SL Ca^{2+}-channel will be assessed at the protein level. Furthermore, the gene expression and protein level of NCX will also be tested in this study. Interestingly, due to the significant therapeutic effects of RAS blockade in SR remodeling in our previous work [40], it is logically assumed that activation of the RAS also involves the remodeling of SL Ca^{2+}-regulatory proteins. Nonetheless, the effects of enalapril and losartan, alone and in combination, on gene expression and protein contents of SL Ca^{2+}-regulatory proteins will be examined in failing heart due to MI.

Although the heart is an integrated organ composed of LV and RV, the inter-relationship and interaction of these two ventricles is critical for cardiac function. The RV is significantly different from the LV in both anatomical and physiological parameters, as well as its alterations in the failing heart following MI. There is some data related to changes in RV cardiac gene expression after MI but such information is limited. Moreover, all the studies examined LV or RV independently without showing the relationship between them. It is therefore logical to hypothesize that there is a difference between LV and RV gene expression. The screening of available ECC related cardiac

gene mRNA level will give general information about cardiac gene expression in both LV and RV from the normal heart as well as the differential response of cardiac genes in LV and RV following MI. The blockade of RAS by enalapril and/or losartan in the failing heart post MI has shown beneficial effects with regarding to different cardiac gene expression in different studies, however, no link between the differential changes has been established. Therefore, our study will provide an integrated picture of the RAS blockade during cardiac remodeling at the gene expression level.

III. MATERIALS AND METHODS

1. Experimental Model

All animal experiments were conducted in St. Boniface General Hospital Research Centre, in accordance with the "Guide to the Care and Use of Experimental Animals" issued by the Canadian Council of Animal Care. All experimental protocols were approved by the Animal Care Committee of the University of Manitoba. MI was induced in male Sprague-Dawley rats (175-200g) by surgical occlusion of the left coronary artery as described earlier in our laboratory [40,61,87,261,277]. In brief, rats were anesthetized with isofluorane mixed with 95% oxygen and 5% carbon dioxide under intermittent positive pressure ventilation. A left thoracotomy was performed, and following the incision of skin and muscle, a purse string suture was prepared without closure. The fourth and fifth ribs were incised left of and adjacent to the sternum; the pericardial sac was then removed and the heart was exteriorized from the chest cavity gently. The left coronary artery was then quickly ligated at about 2 mm from origin of the aorta with a 6-0 silk suture. The heart was repositioned back in the chest and the incision was closed with a purse string suture as described previously. Sufficient suction was accomplished with a 100 mL syringe to restore negative pressure in the chest cavity. Additional suture closure was made for the chest skin.

Mortality of experimental rats was 30-35% within the first 48 hr and rats surviving the first week following operation were expected to live until the end of the experiments. Sham operated rats were treated in the same way however, that the coronary artery was not ligated and the sutures were removed immediately. Electrocardiography (EKG) was performed before and after the procedure to test the success of the ligation, as

well as at 3 weeks and 8 weeks as required by the CHF protocol. All animals were given standard care, kept at 12 hr day/night cycle, fed regular rat chow and provided with water *ad libitum*. The assessment of cardiac function and measurement of the histological and biochemical changes was carried out 8 weeks after the coronary artery ligation.

2. Treatment with Enalapril and Losartan

All rats were randomly divided into 5 groups: sham control (sham), infarcted (MI), enalapril treated infarcted (ENP), losartan treated infarcted (LOS), and combined enalapril and losartan treated infarcted (COM). Three weeks after the operation, enalapril (10 mg/kg/day) and/or losartan (20 mg/kg/day), or tap water were given orally via an oral gavage to sham and infarcted groups for 5 weeks. Enalapril and losartan are both water soluble and were administered once a day in tap water. These two drugs, however, cannot be mixed together before administration since a white cotton-like precipitation develops. This precipitation can be dissolved by heating or vigorous stirring. Usually, there was 20 to 30 min interval between the deliveries of enalapril and losartan in the combined therapy group. The selection of the doses for enalapril and losartan was based on our previous study [40] in which enalapril and losartan exhibited therapeutic effects on the SR protein and gene expression in MI induced CHF model without significant alteration in vascular function, such as systolic pressure and diastolic pressure in the aorta. Both enalapril and losartan were supplied by Merck Research Laboratories (Rahway, NJ, USA).

3. EKG Measurement and Analysis

The EKG recordings of the operated rats were performed in stabilized animals

under isoflurane anesthesia with computer software (AcqKnowledge for Windows 3.0., Harvard Apparatus, Montreal, Canada). Six lead electrocardiograms (limb leads I, II, III, aVR, aVL and aVF) were recorded simultaneously at four time points: before opening the chest, after closure of chest, just before starting the therapy (3 weeks after operation) and 8 weeks after the surgery. According to the modified method of QRS scoring system in humans [278-282], only the amplitude of Q wave in lead I, -aVR and aVL were measured in mV to estimate the gross size of MI in the rats. The presence of Q (> 1 mV) waves in the limb (I, -aVR and aVL) was used as the criteria for a large MI, this method is over 95% correct and in accordance with previous studies [199].

4. Hemodynamic Studies

All animals were assessed hemodynamically before sacrificing. The animals were anesthetized with an intraperitoneal injection of a mixture of ketamine (60 mg/kg) and xylazine (10 mg/kg). The hemodynamic condition of rats became stable at 5 to 10 min after the injection and usually the analysis was performed 10 min later. The right carotid artery was exposed and a cannula with a microtip pressure transducer (model SPR-249, Millar Instruments, Houston, TX) was introduced through proximal arteriotomy [39-41,87,261,277]. The catheter was advanced carefully through the lumen of the carotid artery, until it entered the LV (confirmed by the characteristic changes of pressure and dP/dt curves), and was then secured with a silk ligature around the artery. The readings were recorded with a computer software (AcqKnowledge for Windows 3.0., Harvard Apparatus, Montreal, Canada). The LVSP, LVEDP, heart rate, +dP/dt, -dP/dt, aorta systolic and diastolic pressure were measured and MAP was calculated [39-

41,61,87,261,277].

5. General Assessment and Tissue Preparation

After finishing of the hemodynamic measurements, the abdominal cavity was opened and blood was taken from the descending aorta and hearts were quickly removed. The LV (including septum) and RV as well as the scar tissue were quickly dissected out, washed twice with a solution containing 10 mM 3-[N-morpholino]-propanesulfonic acid (MOPS) and 10 mM sodium ethylenediaminetetraacetate (EDTA), weighed, frozen in liquid nitrogen and stored at -70°C. All procedures were carried out on top of an ice-pad within 3 min to protect the tissue during handling. The lung wet/dry wt ratio, an index of pulmonary congestion, as well as the heart wt/body wt ratio (including both ventricles and infarct scar), an index of cardiac hypertrophy, were measured in these animals. The scar of the LV was removed and kept separately from viable LV tissue. The infarct size was determined while the viable myocardium (including septum) was used for a biochemical study. Scar wt/total LV wt (including septum and infarcted tissue) ratio was found to exhibit a linear relationship with infarct size (as measured morphometrically) [40,275]. Therefore, the scar wt was used as a marker to determine the extent of scar size [40,61,87,261,277]. Generally, 10% of the total infarcted rats showed a small infarct (scar wt/total LV ratio < 15% corresponding to scar size < 30% of the free LV wall). The hemodynamic data from these animals showing small infarct were not included and the cardiac tissue from these animals was discarded. The noninfarcted LV (including septum) and RV tissues from the infarcted animals were employed in this study. From previous studies [39], the average scar wt/LV wt ratio in the untreated and imidapril treated

animals were 24.4 ± 0.8 and 23.6 ± 0.6, respectively; these values were not statistically different ($P > 0.05$) from each other and corresponded to infarct size of about 40% of the free LV wall area.

6. Isolation of Cardiac SL Membrane

Isolation of cardiac SL membrane was performed according to a modified method of *Pitts* [283]. Generally, all the procedures were performed in cold room (4°C), and the frozen viable LV tissue without scar was ground by crushing with mortar and pestle in liquid nitrogen. The powdered samples were suspended in 15 mL ice cold buffer containing 0.6 M sucrose and 10 mM imidazole-HCl (pH 7.0) and homogenized with a Polytron (Polytron PT-MR3000, Brinkmann Instruments; Mississauga, Ontario, Canada) at 12,000 rpm, 20 sec × 5 with 1 min intervals in between. The resulting homogenate was centrifuged at 12,000 × g, compensation -1 (model J2-HS, Beckman Instruments Canada Inc; Mississauga, Ontario, Canada), for 30 min at 4°C. The supernatant was collected and diluted with 3 volume of 20 mM MOPS and 160 mM KCl (pH 7.4), centrifuged at 100,000 × g (model L70 ultracentrifuge, Beckman Instruments Canada Inc; Mississauga, Ontario, Canada) for 60 min. The supernatant was discarded, and the pellet was re-suspended in 5 mL 20 mM MOPS and 160 mM KCl (pH 7.4), and layered over 20 mL 0.88 M sucrose buffer with 100 mM Tris/HCl, 50 mM Na_2pyrophosphate and 300 mM KCl (pH 8.3), and centrifuged at 100,000 × g for 90 min. The white layer of SL at the interface between upper and lower layers was carefully collected with a disposable glass pipette, and diluted with 3 times 20 mM MOPS and 160 mM KCl (pH 7.4). The homogenate was centrifuged at 100,000 × g for 30 min, and pellet was collected and

suspended in 0.5 mL 250 mM sucrose with 10 mM L-histidine (pH 7.0). Isolated sample were divided into 50 μL each tube and stored at -70°C.

7. Measurement of Na^+-K^+-ATPase Activity

Cardiac SL Na^+-K^+-ATPase activity was measured by the method described before [74,273] with some modification. After the protein assay with *Lowry's* method, 10 μg of isolated SL membrane was incubated at 37 °C for 5 min with 61 mM L-histidine (pH 7.4), 1.2 mM ethylene glycol-bis(β-aminothyl ether)-N,N,N'-Tetra-acetic acid (EGTA)-Tris (pH 7.4), 6.1 mM NaN_3, 6.7 mM $MgCl_2$, 111.1 mM NaCl, and 11.1 mM KCl. The reaction was initiated by adding 25 μL 80 mM Na_2ATP (pH 7.4), and terminated 10 minutes later with 0.5 mL ice-cold 12% trichloroacetic acid (TCA). After centrifuging at 1,159 × g (model GS-15R, Beckman Instruments Canada Inc; Mississauga, Ontario, Canada) at 4 °C for 10 min, the liberated phosphate was measured by the method of *Taussky* and *Shorr* [284]; reading absorbance at 691 nm by SPECTRAmax® PLUS^{384} (Molecular Devices, Sunnyvale, CA, USA). Na^+-K^+-ATPase activity was calculated as the difference between activities with and without Na^+ plus K^+ and Mg^{2+}-ATPase activity was estimated as the difference between the activities with and without Mg^{2+} in the absence of Na^+ and K^+ in the reaction medium. All reaction samples were carried out in duplicate.

8. Analysis of SL Protein Content

The relative protein contents of SL Na^+-K^+-ATPase subunits, NCX, Ca^{2+}-channel isoforms, and PCMA1 was obtained by running 10% or 12% mini sodium dodecyl sulfate

polyacrylamide gel electrophoresis (SDS-PAGE), with a 4% stacking gel followed by Western blot analysis with isolated cardiac SL membrane from viable LV tissue [40,273]. The SL membranes (1 mg/mL) were added to the SDS-PAGE loading buffer containing 0.25 M Tris-HCl (pH 6.8), 8% (w/v) sodium dodecyl sulfate (SDS), 45% glycerol, 20% β-mercaptoethnol, and 0.006% bromophenol blue in a ratio of 3:1. The sample loads for each group were of the same volume as 15 μg total SL protein in each lane. The SDS-PAGE was carried out at 200 voltage for 45 to 60 minutes. The separated proteins were then electroblotted to polyvinylidene difluoride (PVDF) Western blotting membrane (Roche Diagnostics GmbH; Inaianapolic, IN, USA) in a transfer buffer containing 25 mM Tris-HCl, 192 mM glycine and 4% methanol (v/v) at 0.5 mA. The transferred membranes were shaken for 2 hr in blocking buffer containing Tris-buffered saline (TBS, 10 mM Tris-HCl, 150 mM NaCl) and 5% fat-free powdered milk.

The membranes were incubated for 1 hr at room temperature with a) protein G-purified mouse monoclonal IgG anti-rabbit Na^+-K^+-ATPase α_1 antibody (1:5,000, Upstate Biotechnology; Lake Placid, NY, USA), b) rabbit polyclonal antiserum anti-rat Na^+-K^+-ATPase α_2 antibody (1:1,000, Upstate Biotechnology; Lake Placid, NY, USA), c) protein A-purified rabbit polyclonal IgG anti-rat Na^+-K^+-ATPase α_3 antibody (1:1,000, Upstate Biotechnology; Lake Placid, NY, USA), d) protein G-purified mouse monoclonal $IgG2_{a/k}$ anti-rabbit Na^+-K^+-ATPase β_1 antibody (1:5,000, Upstate Biotechnology; Lake Placid, NY, USA), e) recombinant rabbit polyclonal antiserum anti-rat Na^+-K^+-ATPase β_2 antibody (1:1,000, Upstate Biotechnology; Lake Placid, NY, USA), f) protein A-purified rabbit polyclonal IgG anti-rat Na^+-K^+-ATPase β_3 antibody (1:1,000, Upstate Biotechnology; Lake Placid, NY, USA), g) lyophilized, affinity-purified mouse

monoclonal IgG anti-canine NCX antibody (1:5,000, Swant; Bellinzona, Switzerland), h) anti-NCX R3F1 antibody (1:5,000, courtesy of Dr. K. D. Philipson, UCLA, Los Angles, CA, USA), j) mouse monoclonal anti-rabbit Ca^{2+}-channel α_1-subunit antibody (1:3,000, Swant; Bellinzona, Switzerland), k) mouse monoclonal anti-rabbit Ca^{2+}-channel α_2-subunit antibody (1:3,000, Swant; Bellinzona, Switzerland), l) mouse monoclonal anti-rabbit Ca^{2+}-channel β-subunit antibody (1:3,000, Swant; Bellinzona, Switzerland), and m) lyophilized whole serum rabbit monoclonal anti-rabbit Ca^{2+}-ATPase (PMCA1) antibody (1:3,000, Swant; Bellinzona, Switzerland). Then the membranes were subsequently incubated for 1 hr with second goat anti-mouse IgG (H+L)-horseradish peroxidase (HRP) conjugate antibody (1:3,000, Bio-Rad Laboratories Canada Ltd; Mississauga, Ontario, Canada) or goat anti-rabbit IgG (H+L)-HRP conjugate antibody (1:3,000, Bio-Rad Laboratories Canada Ltd; Mississauga, Ontario, Canada) respectively. The blots were rinsed in the TBS-T (TBS and 0.2% Tween 20) buffer 4 times (10 min each time) between each of the preceding steps. For chemiluminescent detection, the membrane sheets were dipped into the luminal substrate solution (ECL kit, Amersham Biosciences Inc; Baie d'Urfe, Quebec, Canada) and the chemilumigrams were developed on ECL-hyperfilm (Amersham Biosciences Inc; Baie d'Urfe, Quebec, Canada) to visualize each protein. The bands were analyzed by the model GS-800 Calibrated Densitometer (Bio-Rad Laboratories Canada Ltd; Mississauga, Ontario, Canada) with the Quantity One software (version 4.4.0, Bio-Rad Laboratories Canada Ltd; Mississauga, Ontario, Canada) and were expressed in relation to sham control values as a percentage. A purified microsomal preparation from a rat brain (Upstate Biotechnology; Lake Placid, NY, USA) was used a positive control to identify different Na^+-K^+-ATPase subunits.

9. RNA Isolation

Total myocardial RNA was extracted from the viable LV and RV of sham, MI, ENP, LOS, COM rats by the acid guanidinium thiocyanate-phenol-chloroform method (TRIzol reagent, GIBCO-BRL Life Technologies; Burlington, Ontario, Canada) with modification to the manufacturer's instructions, which is compatible with the original *Chomczynski's* method [285]. Briefly, frozen samples were chopped around 100 mg from each heart ground with mortar and pestle while immersed in liquid nitrogen. Powdered samples were suspended in 1.5 mL TRIzol Reagent and subjected to polytron homogenization (Polytron PT3000, Brinkmann Instruments; Mississauga, Ontario, Canada) at 12,000 rpm, 15 sec × 2 with 20 sec intervals in between. The mixture was cooled on ice for an additional 15 min and was centrifuged at 12,000 × g (model J2-HS, Beckman Instruments Canada Inc; Mississauga, Ontario, Canada) for 10 min at 4°C. The clear supernatant homogenate solution was transferred to a fresh capped tube and kept for 5 minutes at room temperature (22.5°C), and 0.3 mL/sample chloroform was added followed by vigorously hand shaking for 15 sec and incubation at room temperature for another 5 minutes. Mixture was centrifuged at <12,000 × g for 15 min at 4°C. The RNA-containing colorless upper aqueous phase was transferred to a fresh 1.5 mL capped-tube, mixed with 0.75 mL of isopropyl alcohol and kept at -20° C for at least 4 hrs. Following centrifuge at <12,000 × g (Eppendorf Centrifuge 5415C, Brinkmann Instruments; Mississauga, Ontario, Canada) for 10 min at 4°C, gel-like RNA pellets were suspended in 75% ethanol (molecular biology grade diluted with DEPC-treated water). After sedimentation at <12,000 × g for 10 min at 4°C, RNA pellets were washed for a second time in 75% ethanol, centrifuged at <12,000 × g for 10 min at 4°C and vacuum dried by

Speed Vac (SC110, Savant Instruments Inc. Farmingdale, NY). Samples were dissolved in DEPC-treated water and the RNA concentration was calculated from the absorbance at 260 and 280 nm with SPECTRA$_{max}$® PLUS^{384} (Molecular Devices, Sunnyvale, CA, USA).

10. Northern Blot Analysis

Steady-state levels of different cardiac proteins mRNA were determined by Northern hybridization analysis; 20 μg of total RNA was denatured in 50% formamide, 7% formaldehyde, 20 mM MOPS (pH 7.4), 2 mM EDTA (pH 8.0), 0.1% SDS and was subjected to electrophoresis in a 1.2% agarose/formaldehyde gel to size fractionate the mRNA transcripts. The fractionated RNA was transferred (capillary) to nylon transfer membranes (NYTRAN® supercharge, Schleicher & Schuell, Keene, NH, USA). After 24 to 48 hr, the filter was removed and nucleic acids were covalently crosslinked to the matrix using UV radiation (UV Stratalinker 2400, Stratagene, Cedar Creek, TX, USA). After 5 to 12 hr prehybridization at 42°C in an Innova 4080 incubator (New Brunswick Scientific; Edison, NJ, USA) with continuous oscillation at 65 rpm the ^{32}P-labeled cDNA probes were added to the prehybridization solution, and each membrane was hybridized at 42°C for 24 hr. Following cardiac protein cDNA probes and glyceraldehydes-3-phosphate dehydrogenase (GAPDH) cDNA probes were radio-labeled with α-[^{32}P]dCTP (DuPont NEN™ Life Sciences Products; Boston, MA, USA) by a Random Primer DNA Labeling System using Klenow fragment (GIBCO-BRL Life Technologies; Burlington, Ontario, Canada) [286]. Specific isoform cDNA probes derived from rat brain sequences were used to identify specific isoforms of Na^+-K^+-ATPase as follows [273]: a) 0.332-kb cDNA fragment (nucleotides, abbreviated as nt 89-421) from rat brain for α_1-isoform

(American Type Culture Collection, Rockville, MD, USA); b) 0.381-kb cDNA fragment (nt 121-502) from rat brain for α_2-isoform (American Type Culture Collection, Rockville, MD, USA); c) 0.278-kb cDNA fragment (nt 53-331) from rat brain for α_3-isoform (American Type Culture Collection, Rockville, MD, USA); and d) 0.271-kb cDNA fragment (nt 913-1,184) from rat brain for β_1-isoform (American Type Culture Collection, Rockville, MD, USA). In addition, e) 1.0-kb cDNA fragment from the dog heart for the NCX (courtesy of Dr. K. D. Philipson, UCLA, Los Angeles, CA, USA). Specific isoform cDNA probes were employed for SR Ca^{2+}-regulation proteins as follows: f) 2.2-kb cDNA fragment (nt 7,900-10,090) from rabbit origin for RYR2 (courtesy of Dr. D. H. Maclennan, University of Toronto, Toronto, Ontario, Canada); g) 0.762-kb cDNA fragment from rabbit origin for SERCA2a (courtesy of Dr. A. K. Grover, McMaster University, Hamilton, Ontario, Canada); h) 0.507-kb cDNA fragment (-177 to +330 nt) from rabbit origin for PLB (courtesy of Dr. D. H. Maclennan, University of Toronto, Toronto, Ontario, Canada); i) 2.5-kb cDNA fragment from rabbit origin for CQS (courtesy of Dr. A. Zilberman, University of Cincinnati, Cincinnati, OH, USA). For myofibrillar proteins, j) 0.607-kb cDNA fragment from human fetal muscle for MLC (American Type Culture Collection, Rockville, MD, USA); and k) 1.1-kb cDNA fragment from Homo sapiens hippocampus for β-actin (American Type Culture Collection, Rockville, MD, USA). For internal standard, s) 1.2-kb fragment from human for GAPDH (American Type Culture Collection, Rockville, MD, USA) was utilized.

For cardiac myofibrillar α-MHC, a 39-meroligonucleotide derived from the 3′-untranslated region of the rat α-MHC gene is as follows: 5′-GGG ATA GCA ACA GCG AGG CTC TTT CTG CTG GAC AGG TTA-3′ (American Type Culture Collection,

Rockville, MD, USA), and for the cardiac β-MHC probe, a 30-meroligonucleotide was derived from the 3′-untranslated region of the gene (rat genome) and was 5'-CAG GCA TCC TTA GGG TTG GGT AGC ACA AGA-3′ (American Type Culture Collection, Rockville, MD, USA). For 18S ribosomal RNA, a 25-mer synthetic oligonucleotide complementary to the rat 18S rRNA sequence (1,046-1,070 nt) (American Type Culture Collection, Rockville, MD, USA) was utilized. Synthetic oligonucleotide were 5'-end radio-labled with T4 Polynucleotide Kinase (GIBCO-BRL Life Technologies; Burlington, Ontario, Canada) and γ-^{32}P[ATP] (DuPont NEN^{TM} Life Sciences Products; Boston, MA, USA).

Following the washing in 1 × SSC/1% SDS at oscillation at 62 rpm for 20~40 min, filters were exposed to x-ray film (Biomax MS film, Eastman Kodak Company, Rochester, NY, USA) at -80°C with intensifying screens. Results of the autoradiographs from Northern blot analysis were quantified by densitometry (model GS-800 Calibrated Densitometer, Bio-Rad Laboratories Canada Ltd; Mississauga, Ontario, Canada) and the Quantity One software (version 4.4.0, Bio-Rad Laboratories Canada Ltd; Mississauga, Ontario, Canada). The densitometric values for all the bands were divided by the respective GAPDH value. Therefore, signals of Na^+-K^+-ATPase subunits (α_1, α_2, α_3 and β_1), NCX, RYR, SERCA2a, PLB, CQS, α-MHC, β-MHC, MLC, and β-actin mRNA were normalized to that of corresponding GAPDH mRNA to account for differences in loading and/or transfer. All of these signals were also tested with 18S signal. The signal for GAPDH mRNA in infarcted hearts did not change when normalized with respect to that for the 18S or 28S. The mRNA signal for each band was expressed as a percentage of the mean value observed for the sham control group.

11. Semi-quantitative PCR

Reverse transcription (RT) was conducted for 45 min at 48°C using the Superscript Preamplification System for First Strand cDNA Synthesis (GIBCO-BRL Life Technologies; Burlington, Ontario, Canada) as described elsewhere [287]. One primer for rat PMCA1 RT-PCR was from *Mamic's* paper in 2000 [288], which amplified a 120-bp amplicon and was as follows: forward primer 5'-GGC GAC TTT GGC ATC ACA CT-3' and reverse primer 5'TTT CAA CTT GGT GCA AAT TCC A-3'. Another PMCA1 primer, which amplifing a 177-bp (nt 642-818) was designed from rat PMCA1 genome (gene bank) with Primer3 online software (http://frodo.wi.mit.edu/cgi-bin/primer3/primer3_www.cgi) as forward primer 5'-ATT GCC CAA GTG AAG TAC GG-3' and reverse primer 5'CAT CCT TCC AGA ACC TTC CA-3'. Amplification of the cDNA of PMCA1 gene was performed using specific primers and the Superscript Preamplification System (GIBCO-BRL Life Technologies; Burlington, Ontario, Canada). Temperatures used for PCR were as follows: denaturation at 94°C for 30 sec, annealing at 60°C for 60 sec, and extension at 68°C for 120 sec with a final extension for 7 min. 30 amplification cycles for each individual primer sets were carried out by thermal cycler (Techne Genius®, Fisher Scientific, Nepean, ON, Canada). GAPDH primers, 5'-TGA AGG TCG GTG TCA ACG GAT TTG GC-3' (forward) and 5'-GCA TGT CAG ATC CAC AAC GGA TAC-3' (reverse) were utilized as internal standards to normalize of the data and to amplify GAPDH gene as a multiplex with the PCMA1 gene. The PCR products were analysed by 2% agarose gel electrophoresis for 35 min at 50 mA. The intensity of the bands was photographed and quantified with a Molecular Dynamics STORM860 scanning system (Amersham Biosciences Inc; Baie d'Urfe, Quebec, Canada)

as a ratio of PMCA1 gene over GAPDH.

12. Data Analysis

Data are expressed as mean ± SE. The differences among various groups were evaluated statistically by one-way ANOVA followed by the Newman-Keuls test. A P value < 0.05 was taken to represent a significant difference.

IV. RESULTS

1. SL Na^+-K^+-ATPase Remodeling in Failing Rat Heart

Occlusion of the left coronary artery resulted in scar formation in the LV as shown in the histological study (Fig. 4), while the remaining cardiac muscle in the 8 weeks infarcted animals underwent hypertrophy as indicated by increased ventricular wt compared to sham control values (Table 9). A significant increase in wet wt/dry wt ratio of the lungs indicated the presence of pulmonary congestion in MI rats. The liver wet wt/dry wt ratio was not altered. The depression in contractile function in the 8 weeks untreated MI group was evident from a significant increase in LVEDP and a depression in both $+dP/dt$ and $-dP/dt$ (Table 9). Changes in the general characteristics and hemodynamics were partially prevented by treatment with enalapril, losartan or combination of enalapril and losartan. In addition, MAP in the untreated and treated groups was not different from the sham control rats (Table 9). The alterations in treated and untreated MI groups observed in this study were similar to those reported earlier [39,40,61]. It was interesting that the combination therapy did not produce any additive effects as these values were not different from those obtained by treatments with either enalapril or losartan alone (Table 9). The scar wt in the untreated MI group was not different from the treated groups.

SL preparation isolated from the viable LV of infarcted hearts exhibited a lower (14.4 ± 1.5 μmol Pi/mg/hr) Na^+-K^+-ATPase activity compared to sham-operated rats (24.3 ± 2.0 μmol Pi/mg/hr). Blockade of RAS with enalapril and/or losartan partially ($P < 0.05$) normalized the Na^+-K^+-ATPase activity (19.5 ± 1.1, 19.8 ± 1.4, and 18.7 ± 1.7 μmol

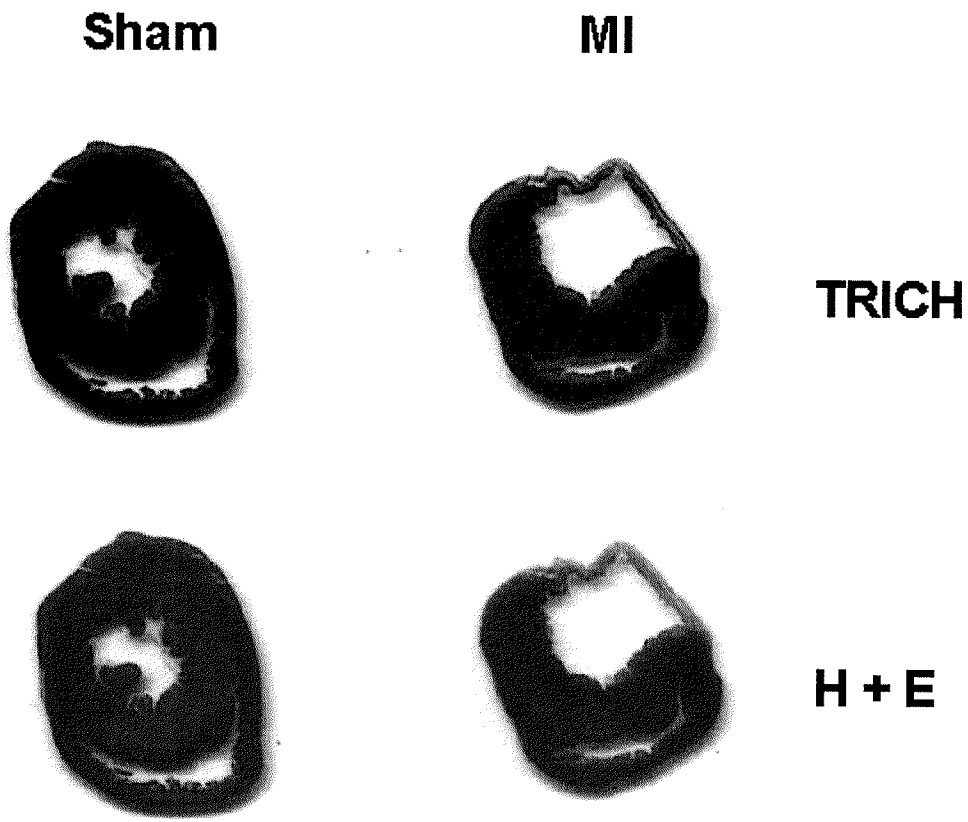

Figure 4. Histological alterations at 8 weeks after coronary artery ligation in rats. Sham: sham control rats; MI: myocardial infarcted rats; TRICH: Masson's trichrome stain; H + E: hematoxylin and eosin stain.

Table 9. General characteristics and hemodynamic parameters in myocardial infarcted rats with or without enalapril, and/or losartan treatment for 5 weeks starting at 3 weeks after coronary occlusion.

	Sham (n = 24)	MI (n = 30)	ENP (n = 21)	LOS (n = 22)	COM (n = 25)
Body wt (BW; g)	514 ± 8.1	512 ± 5.6	507 ± 7.3	509 ± 7.7	504 ± 8.5
Heart wt (mg)	1101 ± 18.8	1262 ± 23.7 *	1142 ± 22.3 #	1160 ± 16.0 #	1126 ± 27.0 #
Scar wt (mg)	ND	233 ± 11.9	211 ± 12.7	224 ± 9.8	210 ± 10.5
Heart wt/BW (mg/g)	2.15 ± 0.03	2.47 ± 0.04 *	2.26 ± 0.04 #	2.29 ± 0.04 #	2.24 ± 0.05 #
Lung wet/dry wt	4.50 ± 0.09	4.88 ± 0.06 *	4.69 ± 0.06 #	4.65 ± 0.07 #	4.72 ± 0.05 #
Liver wet/dry wt	2.89 ± 0.06	3.00 ± 0.04	2.97 ± 0.05	2.91 ± 0.06	2.95 ± 0.04
Heart rate (beat/min)	251 ± 3.8	250 ± 6.3	250 ± 5.2	251 ± 5.9	251 ± 5.3
LVSP (mm Hg)	128 ± 3.8	125 ± 3.5	119 ± 4.5	123 ± 3.2	119 ± 5.1
LVEDP (mm Hg)	5.4 ± 0.8	14.9 ± 1.2 *	9.1 ± 0.9 #	10.2 ± 0.6 #	10.8 ± 0.9 #
+d*P*/d*t* (mm Hg/sec)	11917 ± 328	9185 ± 296 *	10356 ± 288 #	10157 ± 274 #	10255 ± 360 #
-d*P*/d*t* (mm Hg/sec)	12604 ± 449	9641 ± 316 *	10785 ± 260 #	10831 ± 353 #	10882 ± 375 #
MAP (mm Hg)	103 ± 2.4	100 ± 2.9	97 ± 2.4	99 ± 2.8	96 ± 3.3

Values are mean ± SE of 21 to 30 (n) animals in each group. MI: myocardial infarcted; ENP: myocardial infarcted treated with enalapril; LOS: myocardial infarcted treated with losartan; COM: myocardial infarcted treated with both enalapril and losartan; ND: not detected; LVEDP: left ventricular end diastolic pressure; LVSP: left ventricular systolic pressure; MAP: mean arterial pressure; * $P < 0.05$ compared with sham group; # $P < 0.05$ compared with MI group.

Pi/mg/hr) in ENP, LOS and COM groups, respectively (Fig. 5). Furthermore, no significant alterations of SL Mg^{2+}-ATPase activity (34.5 ± 3.8, 39.1 ± 2.4, 39.5 ± 3.3, 40.3 ± 4.1 and 36.4 ± 4.2 μmol Pi/mg/hr) were found among different groups ($P > 0.05$) (Fig. 5).

The relative protein content of SL Na^+-K^+-ATPase was determined from immunoblots using anti-Na^+-K^+-ATPase antibodies (Table 10). In the MI group, the protein content for Na^+-K^+-ATPase α_2 isoform was reduced significantly while that for α_3 isoform was increased markedly (Fig. 6); Na^+-K^+-ATPase α_2 isoform content was reduced by 21% compared to sham-control rats ($P < 0.05$) while that of α_3 isoform increased by 34% ($P < 0.05$) as shown in Fig. 6 and Table 10. On the other hand, protein content for Na^+-K^+-ATPase β_2 and β_3 decreased significantly by 26% and 33% respectively in MI groups (Fig. 7). No changes in the protein contents for Na^+-K^+-ATPase α_1 and β_1 isoforms were evident in the infarcted rats. Blockade of RAS with ENP, and/or LOS partially prevented the decrease in Na^+-K^+-ATPase α_2, β_2 and β_3 isoforms as well as the increase in Na^+-K^+-ATPase α_2 isoform due to MI. However, the combination therapy did not show any additive effects.

The steady-state mRNA levels for Na^+-K^+-ATPase subunits were determined by Northern blot analysis (Fig. 8 and 9). Northern blot analysis showed that in the failing heart following MI, the level of Na^+-K^+-ATPase α_2-subunit was reduced by 31% while that of α_3-subunit was increased by 66% without significant changes in α_1- and β_1-subunits compared to sham control groups. These changes were partially reversed by treatment with ENP, LOS and COM.

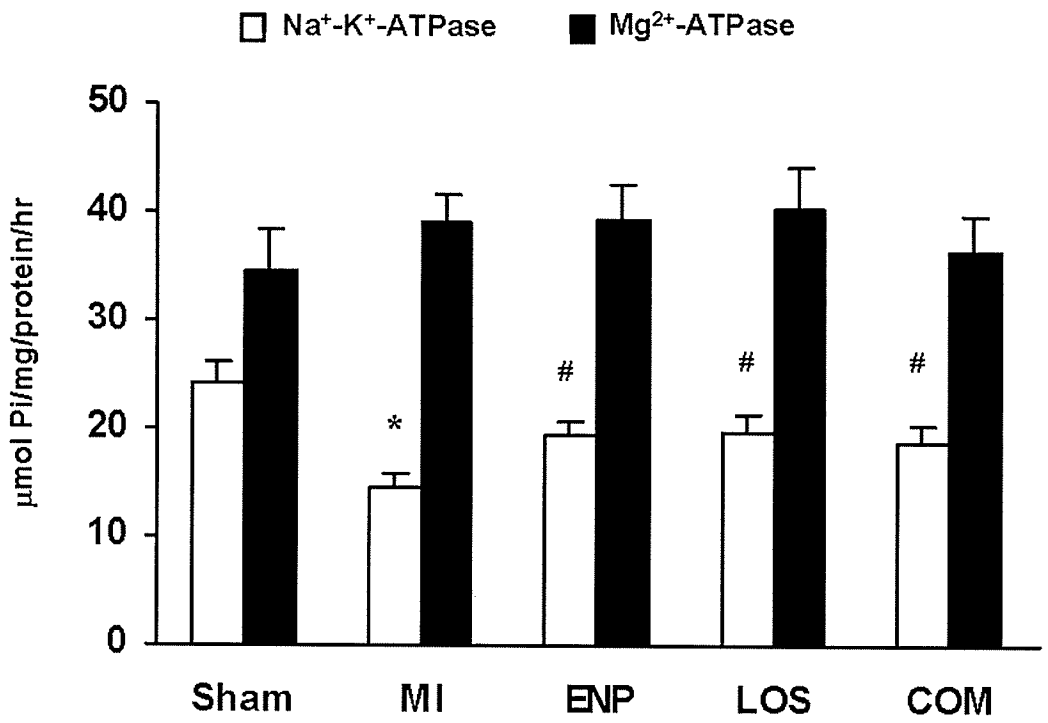

Figure 5. Changes in cardiac sarcolemmal Na^+-K^+-ATPase and Mg^{2+}-ATPase activities of the left ventricles from sham, infarcted (MI), enalapril (10 mg/kg/day) treated infarcted (ENP), losartan (20 mg/kg/day) treated infarcted (LOS), and combined enalapril and losartan treated infarcted (COM) rats. ENP and/or LOS were given orally for 5 weeks starting at 3 weeks after inducing MI. Values are means ± SE of 5 experimental samples for each group. * $P < 0.05$ *vs* Sham; # $P < 0.05$ *vs* MI.

Table 10. Modification of Na^+-K^+-ATPase Isoforms in myocardial infarcted rats with or without enalapril, and/or losartan treatment for 5 weeks starting at 3 weeks after coronary occlusion.

	Sham	MI	ENP	LOS	COM
Na^+-K^+-ATPase α_1 isoform	100%	-4.6 ± 4.1%	-10.7 ± 2.2%	-10.8 ± 3.1%	-12.4 ± 4.7%
Na^+-K^+-ATPase α_2 isoform	100%	-21.4 ± 3.4% *	-10.1 ± 1.6% #	-7.1 ± 2.5% #	-12.9 ± 2.1% #
Na^+-K^+-ATPase α_3 isoform	100%	+34.0 ± 5.2% *	+14.7 ± 4.2% #	+13.6 ± 5.5% #	+6.6 ± 8.3% #
Na^+-K^+-ATPase β_1 isoform	100%	-16.4 ± 14.5%	-14.1 ± 9.4%	+1.9 ± 9.8%	-19.0 ± 6.0%
Na^+-K^+-ATPase β_2 isoform	100%	-26.4 ± 3.1% *	-1.4 ± 8.5% #	-0.8 ± 8.5% #	-13.3 ± 8.6% #
Na^+-K^+-ATPase β_3 isoform	100%	-33.2 ± 1.6% *	-18.9 ± 4.5% #	-9.7 ± 6.7% #	-15.8 ± 3.6% #

Values are mean ± SE of 5 experimental samples in each group as shown in Fig. 2 and 3. MI: myocardial infarcted; ENP: myocardial infarcted treated with enalapril; LOS: myocardial infarcted treated with losartan; COM: myocardial infarcted treated with both enalapril and losartan; +: increase; -: decrease. * $P < 0.05$ compared with sham group; # $P < 0.05$ compared with MI group.

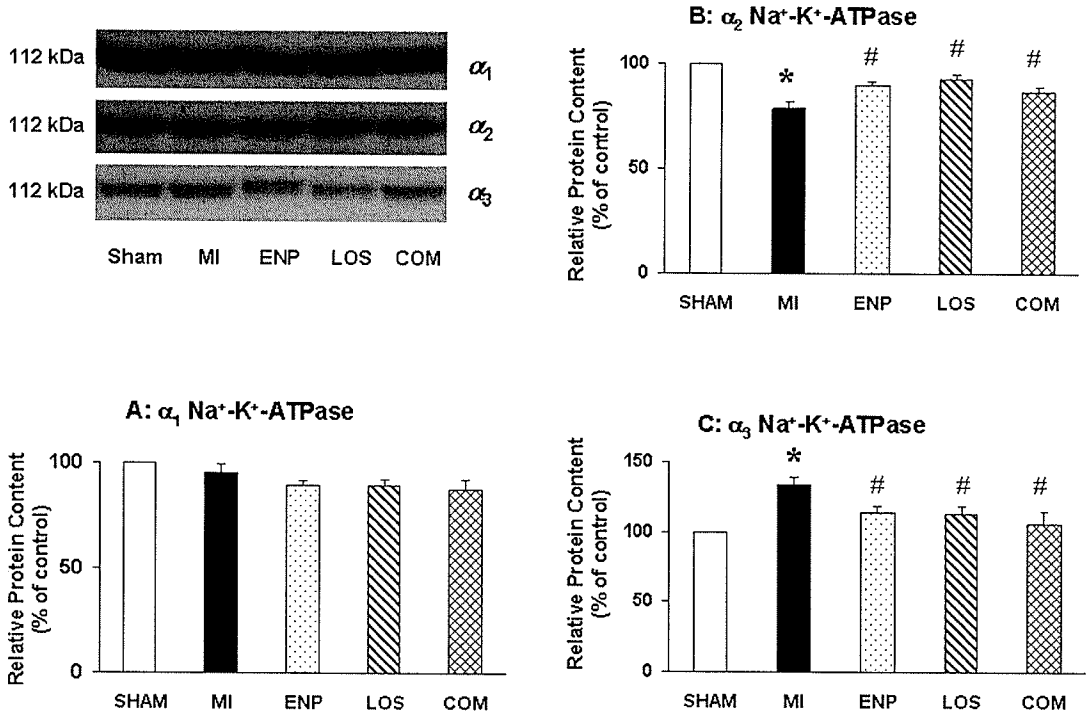

Figure 6. Typical immunoblots and protein contents of cardiac sarcolemmal Na^+-K^+-ATPase different α isoforms α_1 (A), α_2 (B), and α_3 (C), in the left ventricles from sham, infarcted (MI), enalapril (10 mg/kg/day) treated infarcted (ENP), losartan (20 mg/kg/day) treated infarcted (LOS), and combined enalapril and losartan treated infarcted (COM) rats. ENP and/or LOS were given orally for 5 weeks starting at 3 weeks after inducing MI. Values are means ± SE of 5 experimental samples for each group. * $P < 0.05$ *vs* Sham; # $P < 0.05$ *vs* MI.

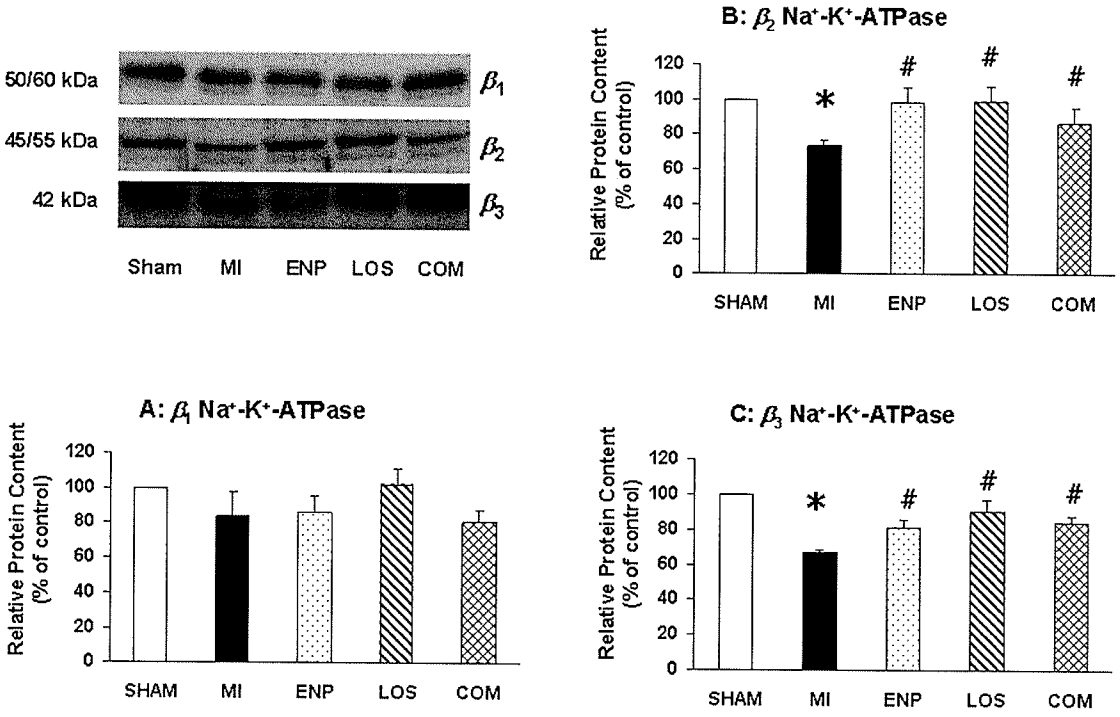

Figure 7. Typical immunoblots and protein contents of cardiac sarcolemmal Na^+-K^+-ATPase different β isoforms β_1 (A), β_2 (B), and β_3 (C), in the left ventricles from sham, infarcted (MI), enalapril (10 mg/kg/day) treated infarcted (ENP), losartan (20 mg/kg/day) treated infarcted (LOS), and combined enalapril and losartan treated infarcted (COM) rats. ENP and/or LOS were given orally for 5 weeks starting at 3 weeks after inducing MI. Values are means ± SE of 5 experimental samples for each group. * $P < 0.05$ *vs* Sham; $^{\#}$ $P < 0.05$ *vs* MI.

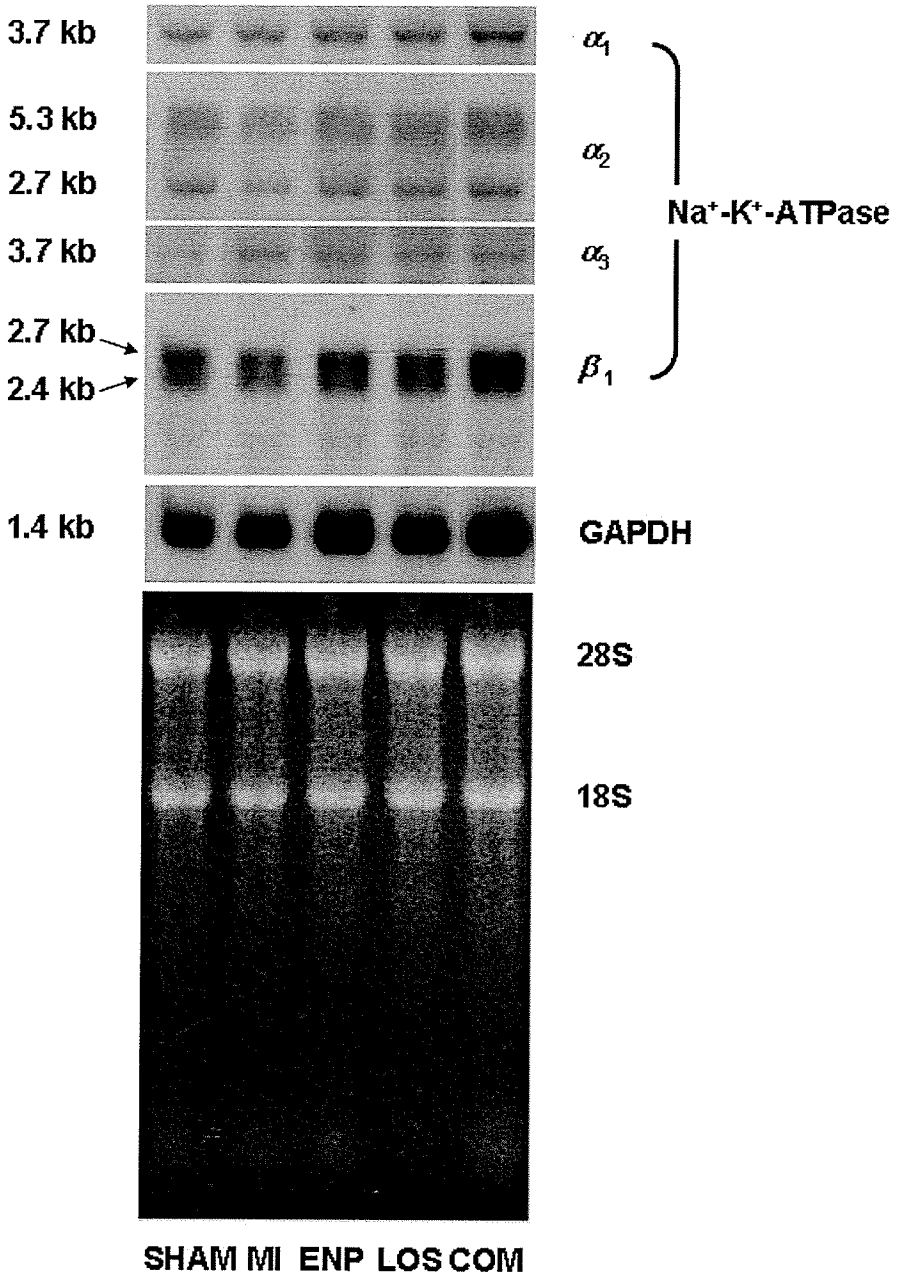

Figure 8. Typical Northern blots of cardiac sarcolemmal Na^+-K^+-ATPase different isoforms α_1, α_2, α_3, and β_1, in the left ventricles from sham, infarcted (MI), enalapril (10 mg/kg/day) treated infarcted (ENP), losartan (20 mg/kg/day) treated infarcted (LOS), and combined enalapril and losartan treated infarcted (COM) rats. ENP and/or LOS were given orally for 5 weeks starting at 3 weeks after inducing MI. Blots for α_1, α_2, α_3, and β_1 Na^+-K^+-ATPase mRNA were obtained by using specific molecular probes. GAPDH: mRNA blot for glyceraldehydes-3-phosphate dehydrogenase; 28S/18S: the quality of mRNA preparation is evident from the ethidium bromide staining of the 28S and 18S ribosomal RNA.

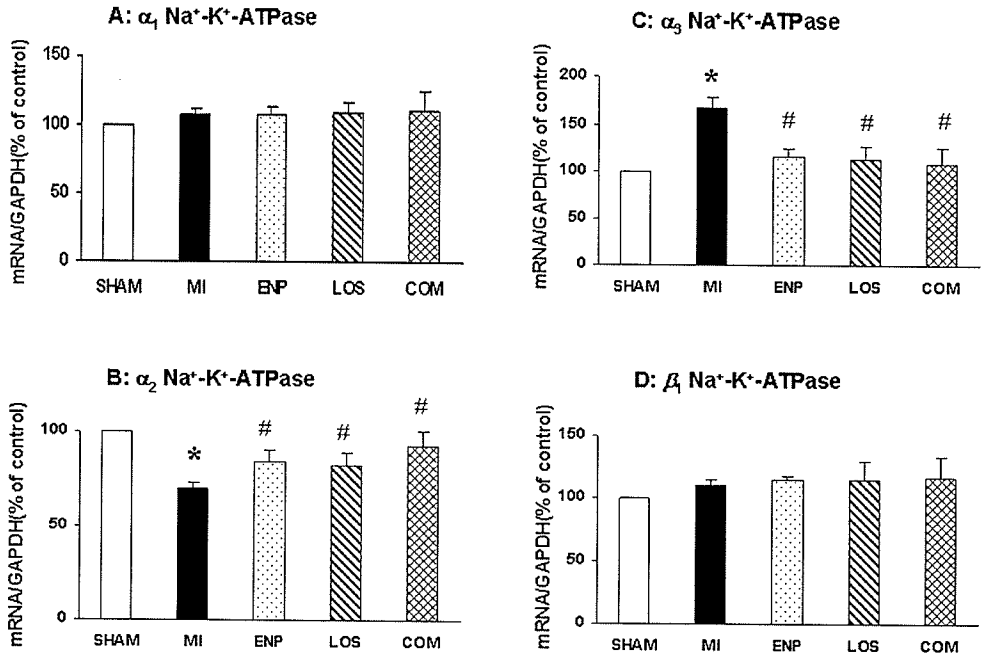

Figure 9. mRNA abundance for cardiac sarcolemmal Na^+-K^+-ATPase different isforms α_1 (A), α_2 (B), α_3 (C), and β_1 (D), in the left ventricle from sham, infarcted (MI), enalapril (10 mg/kg/day) treated infarcted (ENP), losartan (20 mg/kg/day) treated infarcted (LOS), and combined enalapril and losartan treated infarcted (COM) rats. ENP and/or LOS were given orally for 5 weeks starting at 3 weeks after inducing MI. The values were normalized with respect to glyceraldehydes-3-phosphate dehydrogenase (GAPDH) mRNA levels and were expressed as a percentage of values for sham. Values are means ± SE of 8 animals for each group. * $P < 0.05$ *vs* Sham; $^{\#}$ $P < 0.05$ *vs* MI.

2. SL Ca^{2+}-regulatory Proteins Expression in Failing Rat Heart

In another set of experiments, both treated and untreated animals were also assessed hemodynamically before monitoring the Ca^{2+}-regulatory protein expression. Occlusion of the left coronary artery resulted in extensive LV infarction and the viable tissue of both LV and RV underwent marked hypertrophy at 8 weeks post-ligation. These changes are associated with the presence of a large scar, as indicated by the 23% ~ 24 % scar wt-to-total LV wt ratio in different infarcted groups, corresponding to the average scar size value in the range of 45% ~ 47% of the LV wall [40]. The heart wt (including LV, RV and scar) and heart wt/body wt ratio were markedly increased, which were due to the cardiac hypertrophy post MI, but there was no significant difference in the body wt of different groups as shown in Table 11. In addition, the average scar wt (and corresponding scar size) ranged from 209 g to 233 g without a significant difference in the different groups of infarcted animals. Therefore, the differential alterations of heart wt in infarcted hearts with or without treatment were due to the alteration of viable myocardium. In contrast, there were significant increases in lung wet/dry wt ratio in the infarcted group (MI) compared to the sham group, indicating the presence of pulmonary edema (Table 11). This increase in the lung wet/dry wt ratio was attenuated by ENP, LOS and COM groups. There was no great difference in the liver wet/dry wt ratio in this study. An increase in LVEDP as well as a decrease in both $+dP/dt$ and $-dP/dt$ was observed in infarcted animals at 8 weeks post-ligation; however, no difference in heart rate, LVSP or MAP between the infarcted and sham groups was observed (Table 11). Treatment with enalapril and/or losartan (ENP, LOS and COM) showed beneficial effects for attenuating the depression in contractile function of LV, including changes in $+dP/dt$, $-dP/dt$ and

Table 11. General characteristics and hemodynamic parameters of myocardial infarcted rats with or without enalapril, and/or losartan treatment for 5 weeks starting at 3 weeks after coronary occlusion.

	Sham (n = 17)	MI (n = 23)	ENP (n = 21)	LOS (n = 21)	COM (n = 22)
Body wt (BW; g)	507 ± 8.2	513 ± 6.3	504 ± 7.2	506 ± 8.2	512 ± 9.3
Heart wt (mg)	1099 ± 22.7	1269 ± 27.8 *	1160 ± 24.2 #	1164 ± 16.3 #	1148 ± 28.2 #
Scar wt (mg)	ND	233 ± 15.1	210 ± 12.9	223 ± 10.4	209 ± 9.6
Heart wt/BW (mg/g)	2.17 ± 0.04	2.48 ± 0.06 *	2.30 ± 0.04 #	2.31 ± 0.05 #	2.25 ± 0.05 #
Lung wet/dry wt	4.61 ± 0.04	4.90 ± 0.08 *	4.70 ± 0.06 #	4.68 ± 0.07 #	4.71 ± 0.06 #
Liver wet/dry wt	2.85 ± 0.05	2.97 ± 0.04	2.97 ± 0.04	2.88 ± 0.05	2.94 ± 0.03
Heart rate (beat/min)	252 ± 5.3	259 ± 5.9	251 ± 4.8	252 ± 6.2	249 ± 5.0
LVSP (mm Hg)	129 ± 4.2	127 ± 5.0	120 ± 4.8	123 ± 3.5	118 ± 5.6
LVEDP (mm Hg)	6.2 ± 1.0	15.3 ± 1.4 *	9.5 ± 1.0 #	10.2 ± 0.7 #	10.5 ± 0.8 #
+dP/dt (mm Hg/sec)	11952 ± 386	9019 ± 348 *	10119 ± 335 #	10042 ± 289 #	10107 ± 377 #
-dP/dt (mm Hg/sec)	12607 ± 461	9361 ± 322 *	10495 ± 328 #	10705 ± 376 #	10654 ± 399 #
MAP (mm Hg)	102 ± 3.2	98 ± 4.2	97 ± 2.4	98 ± 3.1	94 ± 3.7

Values are mean ± SE of 17 to 23 (n) animals in each group. MI: myocardial infarcted; ENP: myocardial infarcted treated with enalapril; LOS: myocardial infarcted treated with losartan; COM: myocardial infarcted treated with both enalapril and losartan; ND: not detected; LVEDP: left ventricular end diastolic pressure; LVSP: left ventricular systolic pressure; MAP: mean arterial pressure; * $P < 0.05$ *vs* Sham; # $P < 0.05$ *vs* MI.

LVEDP, without afffecting the LVSP and MAP. These results are similar to those described earlier and are consistent with previous observations in this experimental model [39-41]. The combination of enalapril and losartan did not result in an additive effect as no significant change was evident among ENP, LOS and COM groups of experimental animals.

In this study, Western blots of SL Ca^{2+}-regulatory proteins were obtained by employing specific antibodies for NCX, PMCA1 and Ca^{2+}-channel subunits in isolated SL samples from sham and infarcted animals with enalapril and/or losartan treatment. Densitometric analysis of the immunoblots (anti-NCX-antibody R3F1) revealed a significant increase (34.1 ± 7.0%) in the relative SL NCX protein content in the infarcted hearts (Fig. 10). Both bands at 116/112 kDa were regarded as NCX as explained by the developer of this antibody [92] in ECL exposure film. On the other hand, the 70 kDa band was not included in the calculation. Treatment with enalapril, with or without losartan significantly attenuated the increase of NCX; the values were 108.4 ± 4.2%, 107.4 ± 7.4%, and 112.7 ± 3.3% of that in non-infarcted animals in ENP, LOS and COM groups, respectively (Fig. 10). The mRNA level for NCX determined by Northern blot analysis (Fig. 11) showed a significant increase (136 ± 2.8% in MI group). Such changes were partially prevented in ENP, LOS and COM groups (118.5 ± 6.5%, 111.1 ± 9.3% and 105.6 ± 11.3% respectively).

In the isolated SL preparations, the relative protein level of PMCA1 was also tested (Fig. 12). Signals at the molecular mass range of the PMCA1 (130-135 kDa) were detected, similar results have been described in rat brain [289]. A marked increase as high as 264.9 ± 34.0% ($P < 0.01$), was identified in infarcted animal, This increase was

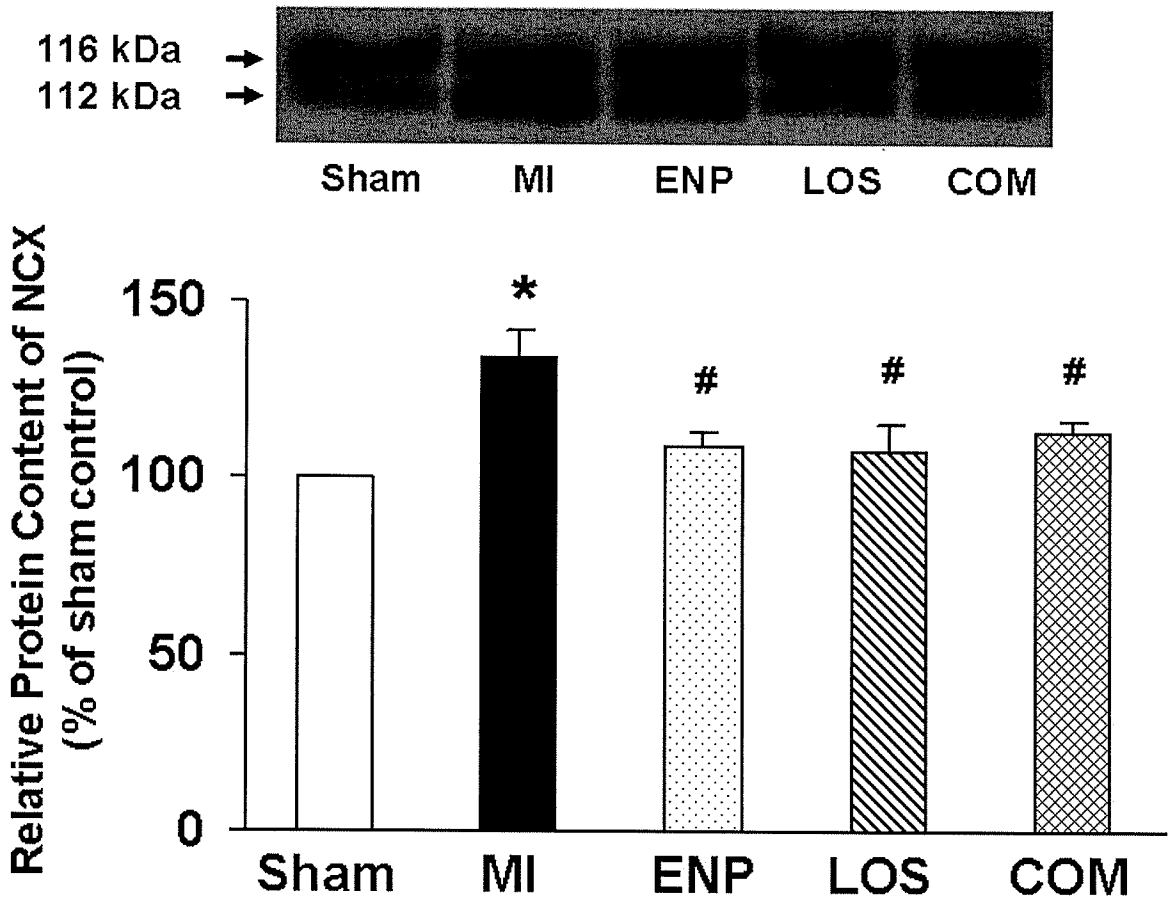

Figure 10. Typical immunoblots and protein contents of cardiac sarcolemmal Na^{+}-Ca^{2+}-exchanger (NCX) in the left ventricles from sham, infarcted (MI), enalapril (10 mg/kg/day) treated infarcted (ENP), losartan (20 mg/kg/day) treated infarcted (LOS), and combined enalapril and losartan treated infarcted (COM) rats. ENP and/or LOS were given orally for 5 weeks starting at 3 weeks after inducing MI. Values are means ± SE of 5 experimental samples for each group. * $P < 0.05$ *vs* Sham; $^{\#}$ $P < 0.05$ *vs* MI.

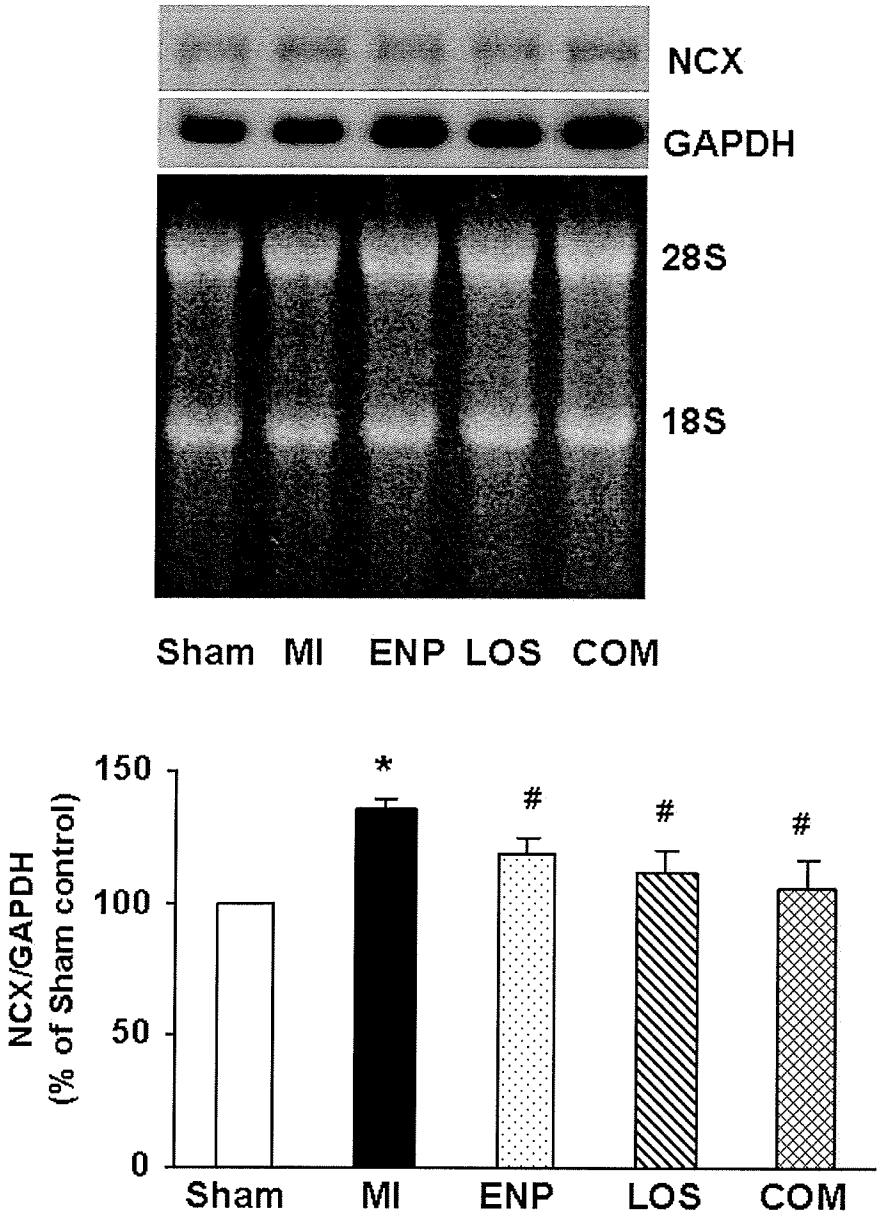

Figure 11. Typical Northern blots and mRNA abundance of cardiac sarcolemmal Na^+-Ca^{2+}-exchanger (NCX) in the left ventricles from sham, infarcted (MI), enalapril (10 mg/kg/day) treated infarcted (ENP), losartan (20 mg/kg/day) treated infarcted (LOS), and combined enalapril and losartan treated infarcted (COM) rats. ENP and/or LOS were given orally for 5 weeks starting at 3 weeks after inducing MI. The values were normalized with respect to glyceraldehydes-3-phosphate dehydrogenase (GAPDH) mRNA levels and were expressed as a percentage of values for sham. 28S/18S: the quality of mRNA preparation is evident from the ethidium bromide staining of the 28S and 18S ribosomal RNA. Values are means ± SE of 8 animals for each group. * $P < 0.05$ *vs* Sham; $^{\#}$ $P < 0.05$ *vs* MI.

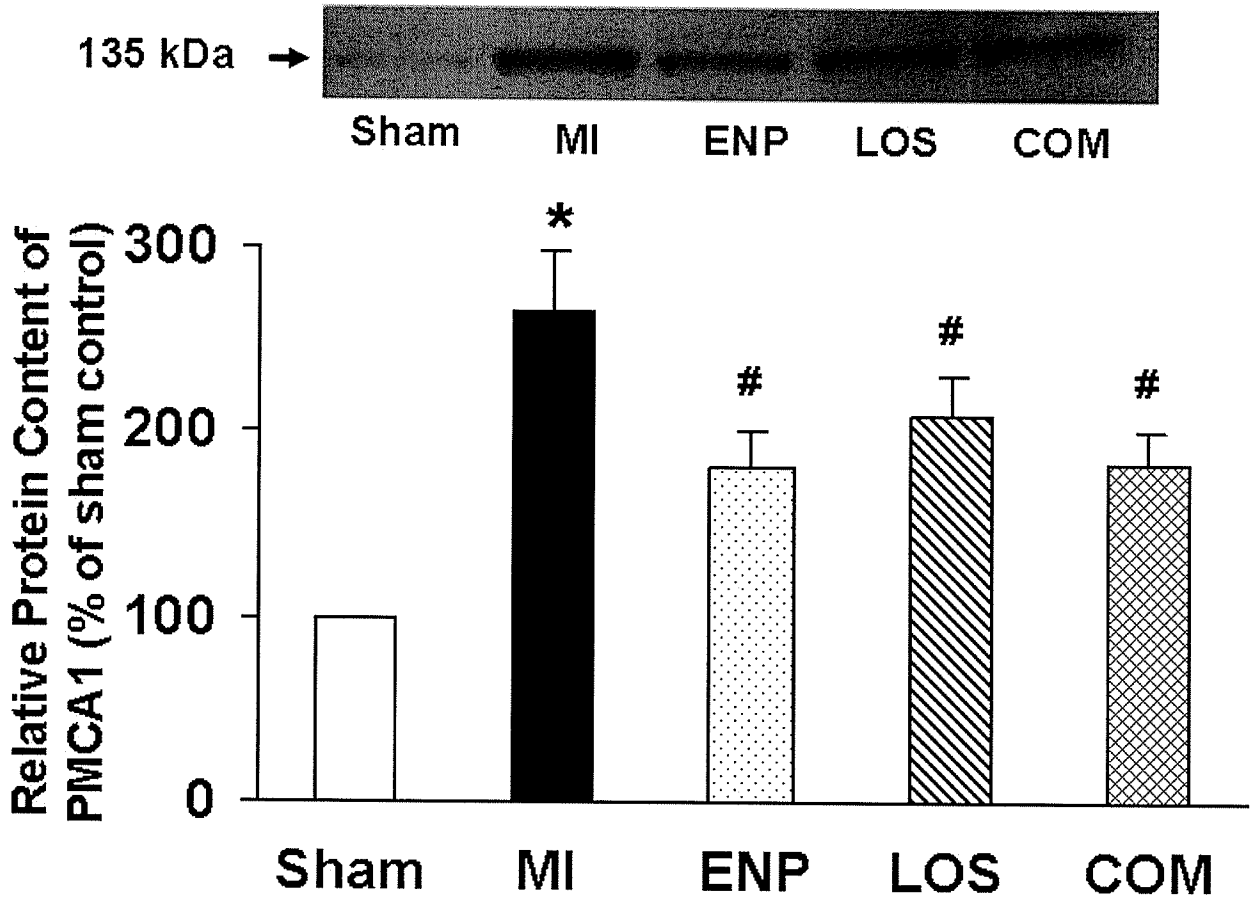

Figure 12. Typical immunoblots and protein contents of cardiac sarcolemmal Ca^{2+}-pump (PMCA1) in the left ventricles from sham, infarcted (MI), enalapril (10 mg/kg/day) treated infarcted (ENP), losartan (20 mg/kg/day) treated infarcted (LOS), and combined enalapril and losartan treated infarcted (COM) rats. ENP and/or LOS were given orally for 5 weeks starting at 3 weeks after inducing MI. Values are means ± SE of 5 experimental samples for each group. * $P < 0.05$ *vs* Sham; $^{\#}$ $P < 0.05$ *vs* MI.

significantly attenuated ($P < 0.05$) in each of the treatment groups (182.3 ± 17.6%, 209.1 ± 21.1, and 183.2 ± 18.5% for ENP, LOS and COM respectively). The mRNA level for PMCA1 was also determined using semi-quantitative PCR by isolated total RNA from viable tissues of animals from each group. As shown in Fig. 13, PMCA1 mRNA in ligated rats was significantly higher (162 ± 24.2%) than in sham animals ($P < 0.05$). Treatments with enalapril and/or losartan attenuated this increase (112.6 ± 2.6%, 116.3 ± 12.0% and 115.8 ± 20.5% in ENP, LOS and COM groups respectively). There was no difference in GAPDH mRNA in each experimental group.

The relative protein levels of SL Ca^{2+}-channel subunits were tested by Western blot (Fig. 14). It was observed that there is a significant decrease in the α_1 subunit ($P < 0.05$) and a marked decrease in the β subunit ($P < 0.05$) in the failing heart, without a significant change in the α_2 subunit. The results showed that the protein levels of α_1 subunit protein were 67.1 % ± 6.4%, 91.6 ± 4.8%, 96.5 ± 4.8%, and 95.1 ± 10.4% of that in sham animals in MI, ENP, LOS and COM groups respectively. Such changes were partially attenuated by enalapril and/or losartan treatments ($P < 0.05$). On the other hand, there was a significant increase in the SL Ca^{2+}-channel β subunit ($P < 0.05$) in the failing heart, which was attenuated by the treatment with enalapril and/or losartan. Compared to relative protein levels in the sham group, SL Ca^{2+}-channel β subunit was 148.6 ± 10.1%, 117.9 ± 4.7%, 126.8 ± 9.8% and 115.5 ± 5.5%; the values for treatment groups (ENP, LOS and COM) and MI were significantly different ($P < 0.05$). There was no change in the SL Ca^{2+}-channel α_2 subunit ($P > 0.05$) in this model as the relative protein contents in MI, ENP, LOS and COM were 93.9 ± 8.3%, 86.0 ± 5.2%, 101.6 ± 5.9%, and 110.4 ± 12.5% of that in sham animals.

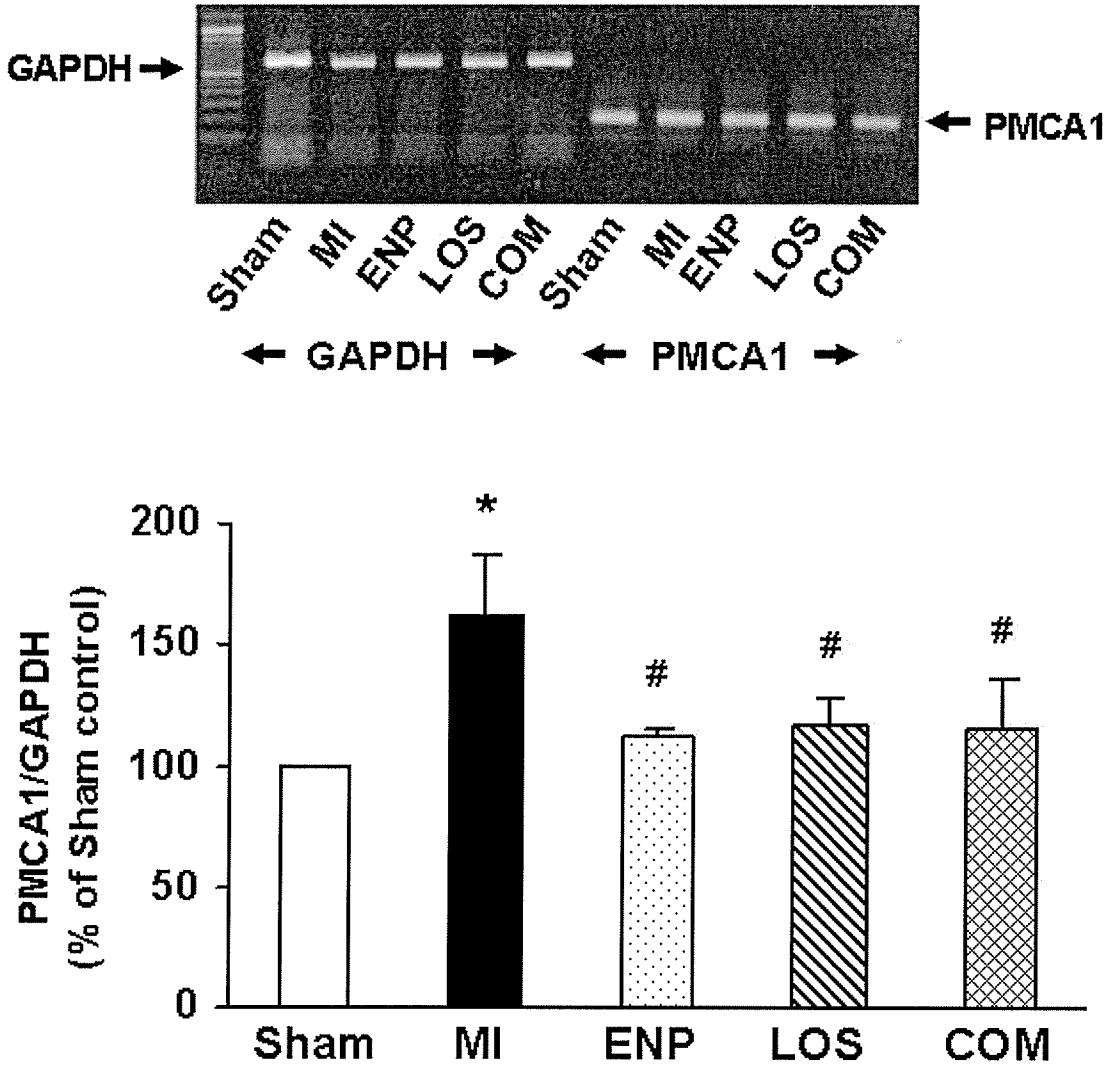

Figure 13. Typical RT-PCR and mRNA abundance of cardiac sarcolemmal Ca^{2+}-pump (PMCA1) in the left ventricles from sham, infarcted (MI), enalapril (10 mg/kg/day) treated infarcted (ENP), losartan (20 mg/kg/day) treated infarcted (LOS), and combined enalapril and losartan treated infarcted (COM) rats. ENP and/or LOS were given orally for 5 weeks starting at 3 weeks after inducing MI. The values were normalized with respect to glyceraldehydes-3-phosphate dehydrogenase (GAPDH) mRNA levels and were expressed as a percentage of values for sham. Values are means ± SE of 4 animals for each group. * $P < 0.05$ *vs* Sham; # $P < 0.05$ *vs* MI.

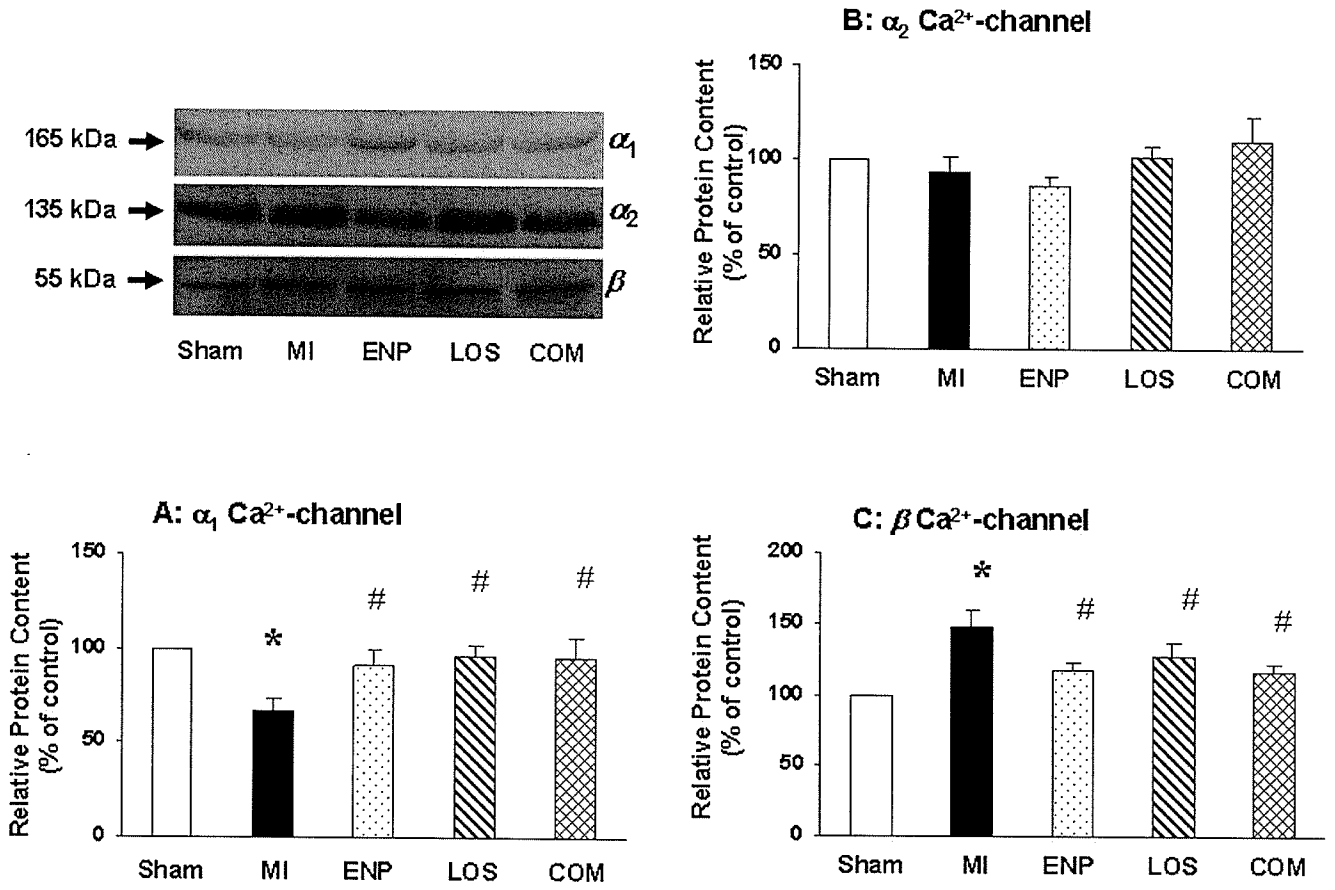

Figure 14. Typical immunoblots and protein contents of cardiac sarcolemmal Ca^{2+}-channel different subunits α_1 (A), α_2 (B), and β_2 (C), in the left ventricles from sham, infarcted (MI), enalapril (10 mg/kg/day) treated infarcted (ENP), losartan (20 mg/kg/day) treated infarcted (LOS), and combined enalapril and losartan treated infarcted (COM) rats. ENP and/or LOS were given orally for 5 weeks starting at 3 weeks after inducing MI. Values are means ± SE of 5 experimental samples for each group. * $P < 0.05$ *vs* Sham; # $P < 0.05$ *vs* MI.

3. Changes in Left and Right Ventricular Gene Expression in Heart Failure

In order to examine if changes in LV gene expression occur differently from that in the RV in heart failure due to MI, animals with and without drug treatments were assessed hemodynamically. As previously described, rats that underwent coronary artery ligation were treated with enalapril (10 mg/kg/day) and/or losartan (20 mg/kg/day) starting at 3 weeks after surgery for 5 weeks. The infarcted rats without treatment showed significant cardiac hypertrophy which was evident from the increased heart wt and increased heart wt/body wt ratio (Table 12). This kind of cardiac hypertrophy occurred in both LV and RV; RV wt increased 31% (272 ± 11.4 mg in MI group *vs* 208 ± 7.21 mg in Sham group, $P < 0.05$). The LV viable tissue also underwent significant hypertrophy but it was difficult to calculate the increase due to the loss of necrotic myocardium and replacement of scar tissue in the ligated animal. As shown in Table 12, the average amount of total heart wt (including LV viable tissue, scar and RV) in MI group (1314 ± 29.8 mg) was increased compared to the Sham group (1120 ± 17.4 mg)($P < 0.05$). However, there was no significant difference in scar wt among each group. Enalapril and/or losartan treatment significantly prevented the cardiac hypertrophy in both LV and RV. Total heart wt was reduced to 1199 ± 40.9, 1201 ± 35.0 and 1208 ± 34.4 mg, whereas RV wt was reduced to 233 ± 9.77, 240 ± 7.6 and 233 ± 10.9 mg, in ENP, LOS and COM groups respectively.

LV systolic and diastolic functions were significantly impaired in the MI group, including reduced +dP/dt and -dP/dt as well as increased LVEDP (Table 12). In addition, the lung wet wt/dry wt ratio was markedly increased in infarcted rats, 5.04 ± 0.14 *vs* 4.19

Table 12. General characteristics and hemodynamic parameters of myocardial infarcted rats with or without enalapril, and/or losartan treatment for 5 weeks starting at 3 weeks after coronary occlusion.

	Sham (n = 12)	MI (n = 12)	ENP (n = 11)	LOS (n = 9)	COM (n = 11)
Body wt (BW; g)	514 ± 12.5	510 ± 10.1	510 ± 10.6	520 ± 10.3	515 ± 10.0
Heart wt (mg)	1120 ± 17.4	1314 ± 29.8 *	1199 ± 40.9 #	1201 ± 35.0 #	1208 ± 34.4 #
Scar wt (mg)	ND	223 ± 11.8	222 ± 11.7	213 ± 11.3	221 ± 15.0
RV wt (mg)	208 ± 7.21	272 ± 11.4 *	233 ± 9.77 #	240 ± 7.6 #	233 ± 10.9 #
Heart wt/BW (mg/g)	2.19 ± 0.05	2.59 ± 0.08 *	2.35 ± 0.04 #	2.32 ± 0.08 #	2.35 ± 0.07 #
Lung wet/dry wt	4.19 ± 0.13	5.04 ± 0.14 *	4.57 ± 0.08 #	4.55 ± 0.08 #	4.56 ± 0.05 #
Liver wet/dry wt	2.87 ± 0.07	2.91 ± 0.06	2.94 ± 0.08	2.88 ± 0.07	2.91 ± 0.04
Heart rate (bpm)	249 ± 3.5	246 ± 7.2	248 ± 10.3	251 ± 7.5	247 ± 6.4
LVSP (mm Hg)	121 ± 4.4	120 ± 6.3	118 ± 6.2	121 ± 3.9	119 ± 8.6
LVEDP (mm Hg)	4.8 ± 0.5	14.1 ± 1.6 *	7.3 ± 0.9 #	8.7 ± 0.6 #	8.6 ± 0.9 #
+d*P*/d*t* (mm Hg/sec)	11617 ± 458	8970 ± 289 *	10200 ± 334 #	10008 ± 215 #	10186 ± 477 #
-d*P*/d*t* (mm Hg/sec)	12093 ± 528	9254 ± 225 *	10551 ± 358 #	10773 ± 266 #	10568 ± 436 #
MAP (mm Hg)	104 ± 3.5	98 ± 4.6	97 ± 3.0	106 ± 3.9	97 ± 6.9

Values are mean ± SE of 9 to 12 animals (n) in each group. MI: myocardial infarcted; ENP: myocardial infarcted treated with enalapril; LOS: myocardial infarcted treated with losartan; COM: myocardial infarcted treated with both enalapril and losartan; ND: not detected; LVEDP: left ventricular end diastolic pressure; LVSP: left ventricular systolic pressure; MAP: mean arterial pressure; * $P < 0.05$ *vs* Sham; # $P < 0.05$ *vs* MI.

± 0.13 as compared to Sham group ($P < 0.05$); this indicates the presence of pulmonary edema, which is the standard index of LV heart failure. In contrast, the RV cardiac function was preserved because there was no significant difference in liver wet wt/dry wt ratio among all the experimental groups ($P > 0.05$). Thus, it appeared that the LV of the infarcted heart was at the moderate stage of heart failure whereas the RV was in the hypertrophic stage without clinical signs of liver congestion. Enalapril and/or losartan treatment partially prevented the cardiac hypertrophy in both LV and RV as well as attenuated the LV dysfunction (Table 12). There was no change of MAP among each group after treatment with enalapril and/or losartan in failing heart ($P > 0.05$).

In this hemodynamically assessed MI model, a series of Northern blots for SL cation transporting proteins were performed for both LV and RV from the same heart (Fig. 15). These values were normalized with respect to GAPDH mRNA levels, expressed as a percentage of the value of the Sham group. The SL NCX mRNA level was significantly increased in both LV and RV (Fig. 16) by 32.1 ± 6.0 and 25.6 ± 5.4% respectively. The increase of NCX mRNA was partially attenuated with the treatment of ENP, LOS and COM ($P < 0.05$). For SL Na^+-K^+-ATPase isoforms, a significant increase in the α_3 isoform (37.0 ± 6.4%) and a marked decrease in the α_2 isoform (37.3 ± 4.7%) in the LV of MI rats ($P < 0.05$) were observed without significant changes in the α_1 and β_1 isoforms. On the other hand, there were no significant changes in the SL Na^+-K^+-ATPase isoforms (α_1, α_2, α_3, and β_1 isoforms) in the RV ($P > 0.05$).

The mRNA level for PMCA1 was determined using semi-quantitative PCR in both the LV and the RV. As shown in Fig. 17, PMCA1 expression in ligated rats was significantly increased to 162 ± 24.2% as compared to sham animals ($P < 0.05$), and

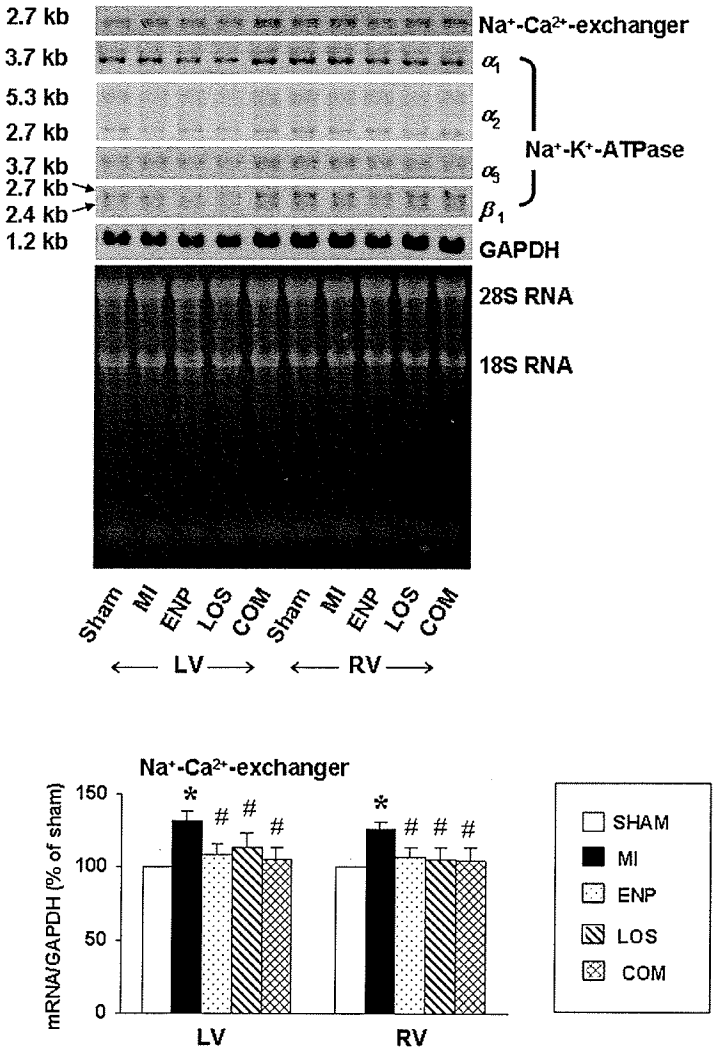

Figure 15. Typical Northern blots of cardiac sarcolemmal Na^+-Ca^{2+}-exchanger (NCX), Na^+-K^+-ATPase different α_1, α_2, α_3, and β_1 isoforms in the viable tissue of both left and right ventricles from the same heart in sham, infarcted (MI), enalapril (10 mg/kg/day) treated infarcted (ENP), losartan (20 mg/kg/day) treated infarcted (LOS), and combined enalapril and losartan treated infarcted (COM) rats. ENP and/or LOS were given orally for 5 weeks starting at 3 weeks after inducing MI. mRNA abundance for cardiac sarcolemmal Na^+-Ca^{2+}-excahnger in the viable tissue of both left and right ventricles from sham, infarcted (MI), enalapril (10 mg/kg/day) treated infarcted (ENP), losartan (20 mg/kg/day) treated infarcted (LOS), and combined enalapril and losartan treated infarcted (COM) rats. The values were normalized with respect to glyceraldehydes-3-phosphate dehydrogenase (GAPDH) mRNA levels and were expressed as a percentage of values for sham. 28S/18S: the quality of mRNA preparation is evident from the ethidium bromide staining of the 28S and 18S ribosomal RNA. Values are means ± SE of 6 animals for each group. * $P < 0.05$ *vs* Sham; $^{\#}$ $P < 0.05$ *vs* MI.

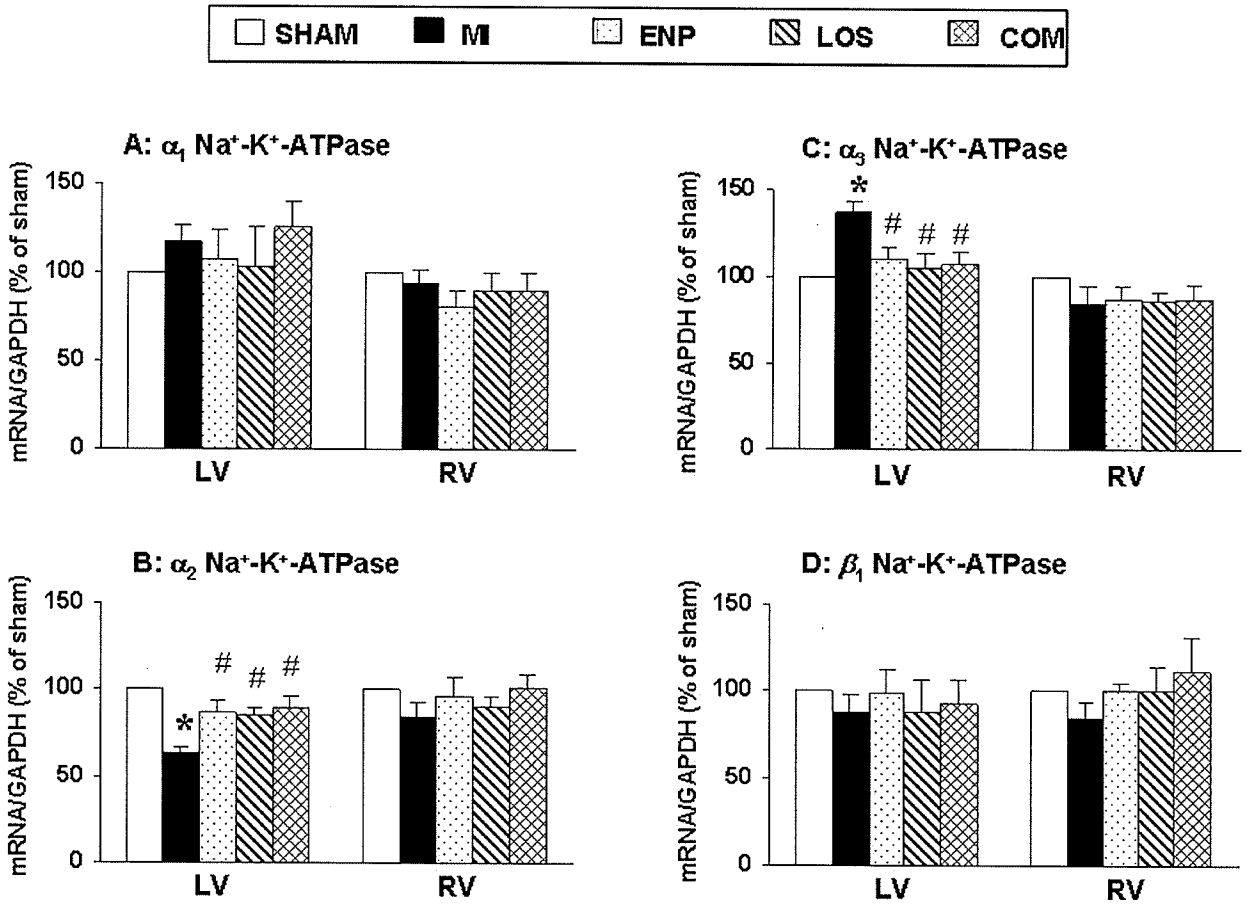

Figure 16. mRNA abundance for cardiac sarcolemmal Na^+-K^+-ATPase different isoforms α_1 (A), α_2 (B), α_3 (C), and β_1 (D), in the viable tissue of both left and right ventricles in sham, infarcted (MI), enalapril (10 mg/kg/day) treated infarcted (ENP), losartan (20 mg/kg/day) treated infarcted (LOS), and combined enalapril and losartan treated infarcted (COM) rats. ENP and/or LOS were given orally for 5 weeks starting at 3 weeks after inducing MI. The values were normalized with respect to glyceraldehydes-3-phosphate dehydrogenase (GAPDH) mRNA levels and were expressed as a percentage of values for sham. Values are means ± SE of 6 animals for each group. * $P < 0.05$ *vs* Sham; # $P < 0.05$ *vs* MI.

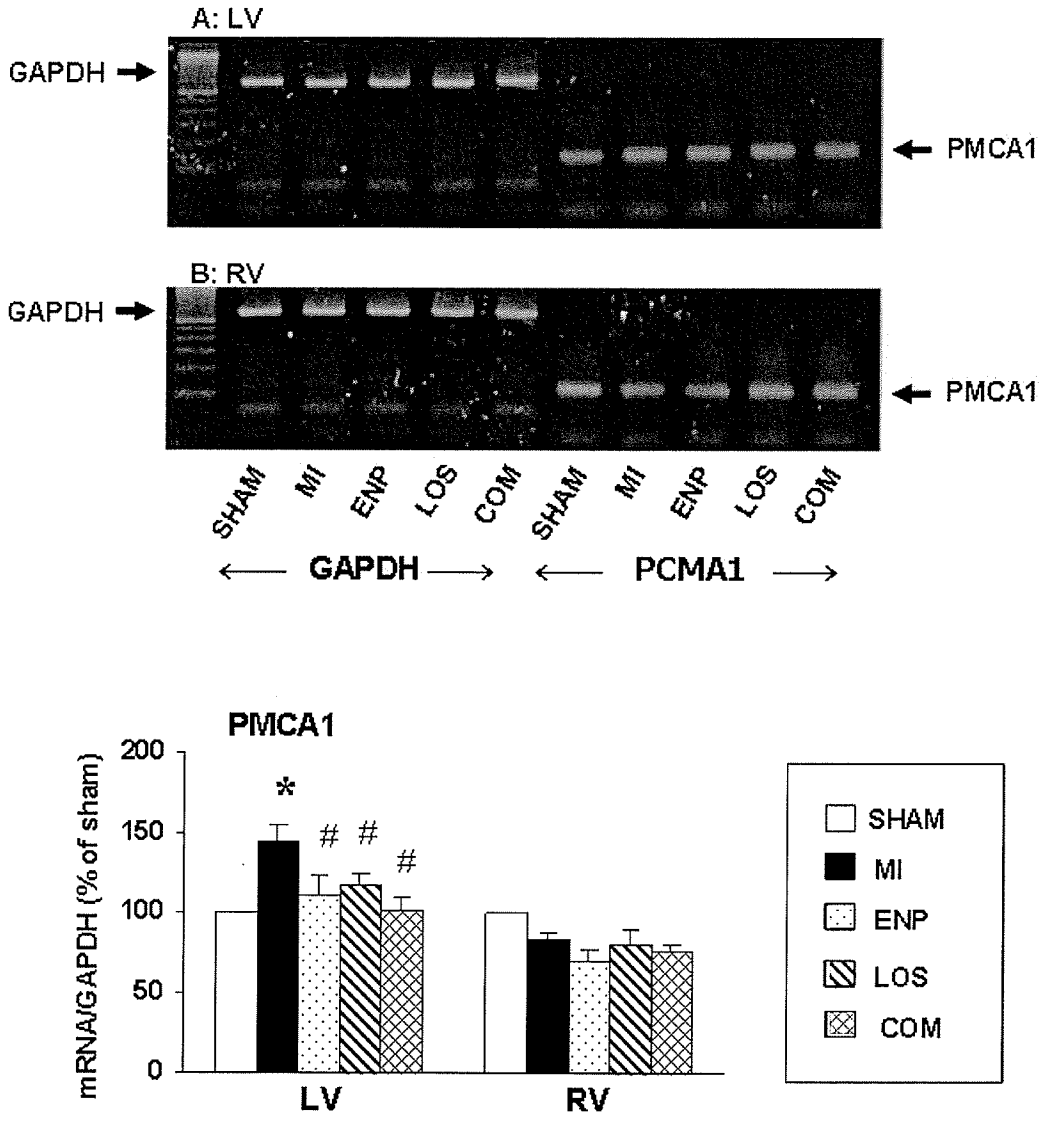

Figure 17. Typical RT-PCR and mRNA abundance of cardiac sarcolemmal Ca^{2+}-pump (PMCA1) tested in the viable tissue of both left (A) and right (B) ventricles from the same heart in sham, infarcted (MI), enalapril (10 mg/kg/day) treated infarcted (ENP), losartan (20 mg/kg/day) treated infarcted (LOS), and combined enalapril and losartan treated infarcted (COM) rats. The values were normalized with respect to glyceraldehydes-3-phosphate dehydrogenase (GAPDH) mRNA levels and were expressed as a percentage of values for left ventricle in sham. Values are means ± SE of 4 animals for each group. * $P < 0.05$ *vs* Sham; $^{\#}$ $P < 0.05$ *vs* MI.

treatments with enalapril and/or losartan attenuated this increase (113 ± 2.6, 116 ± 12.0% and 116 ± 20.5% in ENP, LOS and COM groups, respectively). On the other hand, there was a small reduction of PMCA1 expression in RV after MI but it was not significant ($P > 0.05$).

A second series of Northern blots was performed using the same RNA samples as used in the first series of studies. Gene expression from four myofibrillar genes α-MHC, β-MHC, MLC and β-actin were tested (Fig. 18). In the infarcted heart, a myosin "shift" was evident from a significant decrease in α-MHC and a marked increase in β-MHC in both LV and RV (Fig. 19). In LV, α-MHC in MI group reduced to 54 ± 5.8% whereas β-MHC increased to 374.0 ± 44.2% of that in the Sham group; similar but larger changes occurred in RV in α-MHC (81.1 ± 2.9%, $P < 0.05$) and β-MHC (575 ± 74.5%, $P < 0.01$). Treatment with enalapril and/or losartan significantly but not completely prevented the myosin "*shift*" in both LV and RV (the decrease in α-MHC and increase in β-MHC). There was no change in MLC or β-actin mRNA levels in both LV and RV. Although, the mRNA level of β-actin in LOS group was increased in LV samples, it did not reach the significant range ($P > 0.05$).

The gene expression for SR Ca^{2+}-regulating proteins (including RYR, SERCA2, PLB and CQS) was also examined in the same RNA sample as used earlier (Fig. 18). Significant reductions in RYR (77 ± 7.1%), SERCA2 (70 ± 5.4%) and PLB (79 ± 3.9%) were identified in the LVof post MI rats, compared to those in the Sham group (Fig. 20). PLB was also reduced in the RV to 70 ± 2.5%; however, RYR, SERCA2 and CQS were not changed in RV. The changes of RYR and SERCA2 in LV as well as PLB in both LV and RV were partially prevented by treatment with enalapril and/or losartan ($P <0.05$).

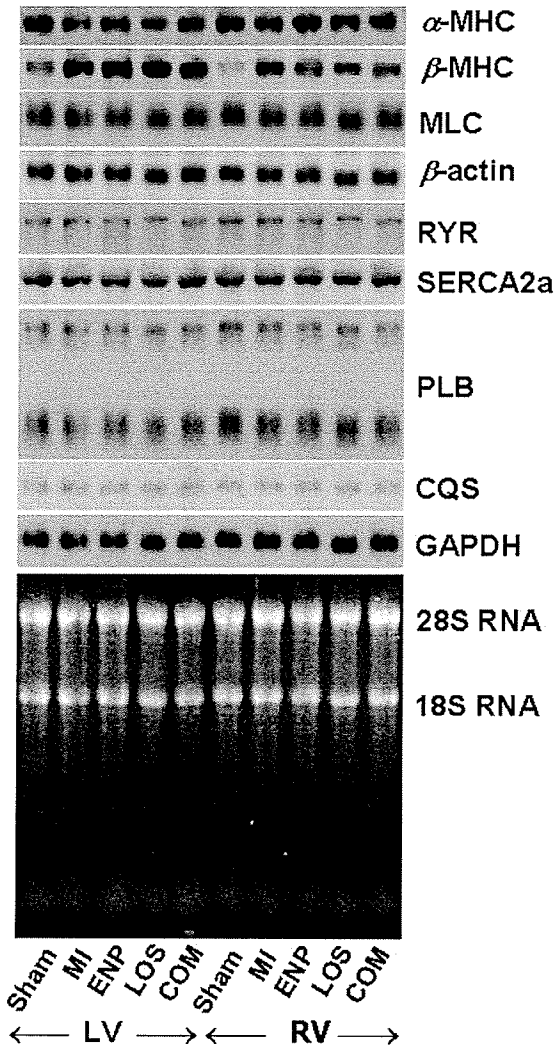

Figure 18. Typical Northern blots of cardiac myofibrillar protein α-myosin heavy chain (α-MHC), β-myosin heavy chain (β-MHC), myosin light chain (MLC), β-actin, and sarcoplasmic reticular proteins ryanodine receptor (RYR), sarco-endoplasmic reticulum Ca^{2+}-ATPase (SERCA2a), phospholamban (PLB) and calsequestrin (CQS) in the viable tissue of both left and right ventricles from the same heart in sham, infarcted (MI), enalapril (10 mg/kg/day) treated infarcted (ENP), losartan (20 mg/kg/day) treated infarcted (LOS), and combined enalapril and losartan treated infarcted (COM) rats. ENP and/or LOS were given orally for 5 weeks starting at 3 weeks after inducing MI. GAPDH: mRNA blot for glyceraldehydes-3-phosphate dehydrogenase; 28S/18S: the quality of mRNA preparation is evident from the ethidium bromide staining of the 28S and 18S ribosomal RNA.

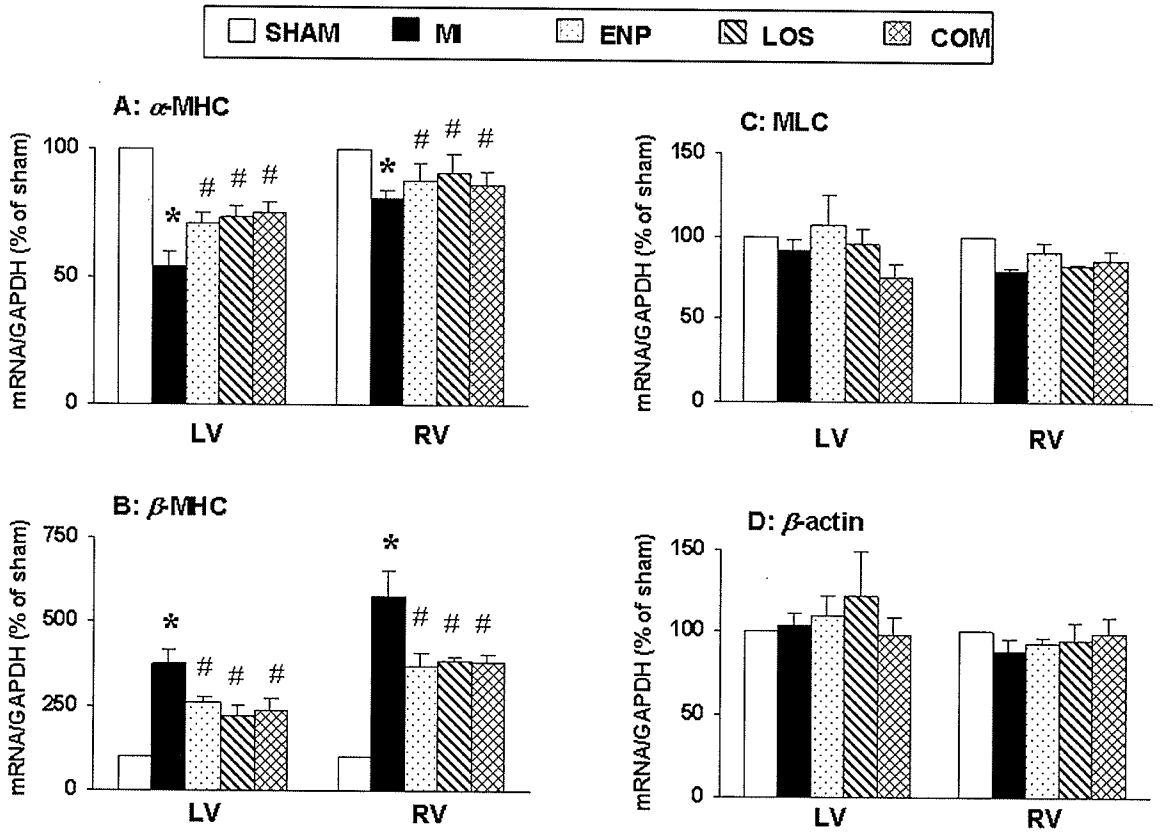

Figure 19. mRNA abundance for cardiac α-myosin heavy chain (α-MHC)(A), β-myosin heavy chain (β-MHC)(B), myosin light chain (MLC)(C), and β-actin (D), in the viable tissue of both left and right ventricles in sham, infarcted (MI), enalapril (10 mg/kg/day) treated infarcted (ENP), losartan (20 mg/kg/day) treated infarcted (LOS), and combined enalapril and losartan treated infarcted (COM) rats. ENP and/or LOS were given orally for 5 weeks starting at 3 weeks after inducing MI. The values were normalized with respect to glyceraldehydes-3-phosphate dehydrogenase (GAPDH) mRNA levels and were expressed as a percentage of values for sham. Values are means ± SE of 6 animals for each group. * $P < 0.05$ *vs* Sham; # $P < 0.05$ *vs* MI.

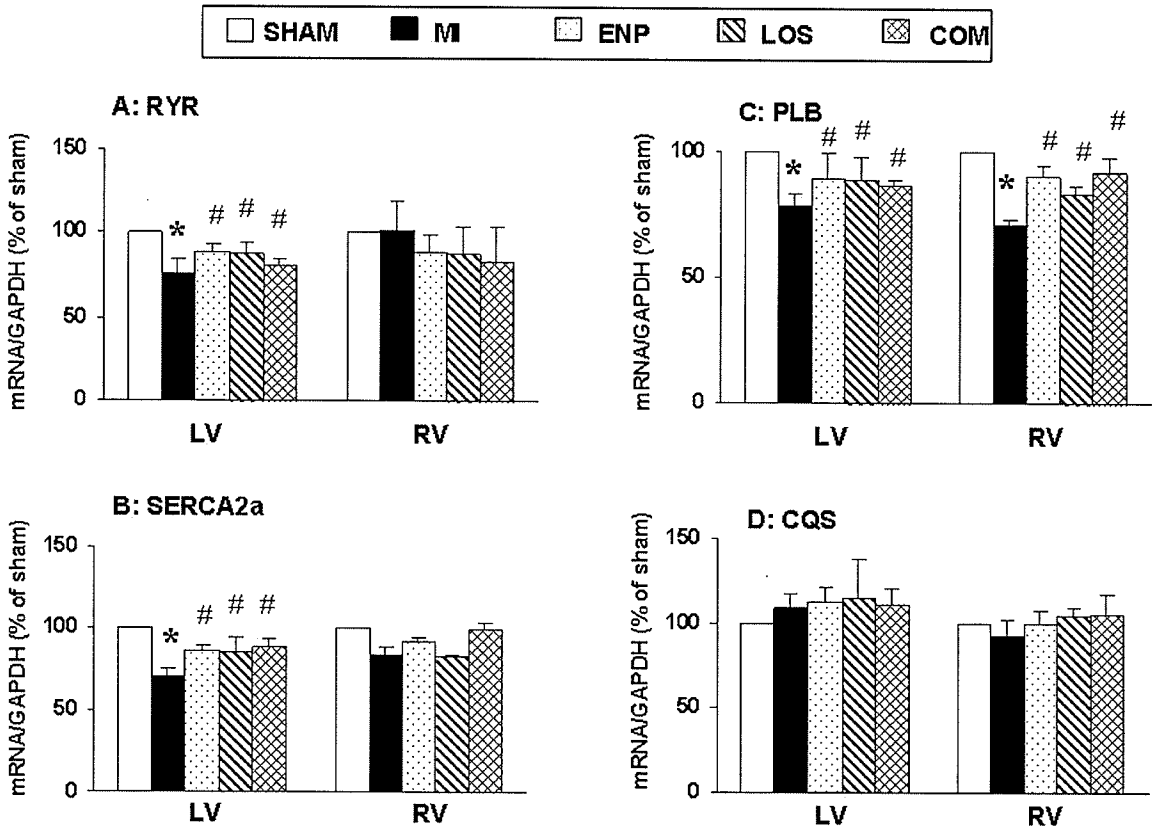

Figure 20. mRNA abundance for cardiac ryanodine receptor (RYR)(A), sarco-endoplasmic reticulum Ca^{2+}-ATPase (SERCA2a)(B), phospholamban (PLB)(C) and calsequestrin (CQS)(D), in the viable tissue of both left and right ventricles in sham, infarcted (MI), enalapril (10 mg/kg/day) treated infarcted (ENP), losartan (20 mg/kg/day) treated infarcted (LOS), and combined enalapril and losartan treated infarcted (COM) rats. ENP and/or LOS were given orally for 5 weeks starting at 3 weeks after inducing MI. The values were normalized with respect to glyceraldehydes-3-phosphate dehydrogenase (GAPDH) mRNA levels and were expressed as a percentage of values for sham. Values are means ± SE of 6 animals for each group. * $P < 0.05$ *vs* Sham; $^{\#}$ $P < 0.05$ *vs* MI.

The loading of both LV and RV samples into one gel provided an opportunity to directly compare the LV and RV cardiac gene expression. Analysis of the data of Northern blots from both LV and RV was carried in comparison to the LV and expressed as a percentage of the value of Sham LV. Results of the Sham and MI groups are shown in Fig. 21, 22, and 23; NCX was expressed at almost the same level in both LV and RV (102 ± 4.2%, $P > 0.05$), and as reported previously, the NCX mRNA levels were significantly increased in both LV and RV post MI (Fig. 21). There were no differences in mRNA levels for Na^+-K^+-ATPase α_1, α_2, and β_1 isoforms in the LV and RV (Fig. 21); however, the gene expression of Na^+-K^+-ATPase α_3 isoform was higher in RV (126 ± 10.5%) but not significant ($P > 0.05$). By contrast, the gene expression in PMCA1 (Fig. 21) of Sham animals was much higher in the RV (187 ± 24.6%, $P < 0.05$). As stated previously, there was a small reduction in PMCA1 in the RV following MI, but the MI value in the LV was higher than that of Sham group ($P < 0.05$).

In the sham group, there was no difference in α-MHC between LV and RV (101 ± 8.2%); however, β-MHC was about one third in RV (27.9 ± 4.8%, $P < 0.05$) of that in LV (Fig. 22). Even as shown in Fig. 19, β-MHC increased almost six fold in RV post MI ($P < 0.001$), but this value in the LV group was lower. No significant difference in mRNA level for MLC from Sham or infarcted groups was observed between the LV and RV; however, RV post MI had signficantly lower content of MLC ($P < 0.05$) as compared to Sham LV. β-actin gene expression was significant lower in RV (81.9 ± 3.8%) than in LV ($P < 0.05$).

Although there was lower expression of PLB and higher expression of RYR and CQS in the RV, the differences were not significant ($P > 0.05$). The RV had similar

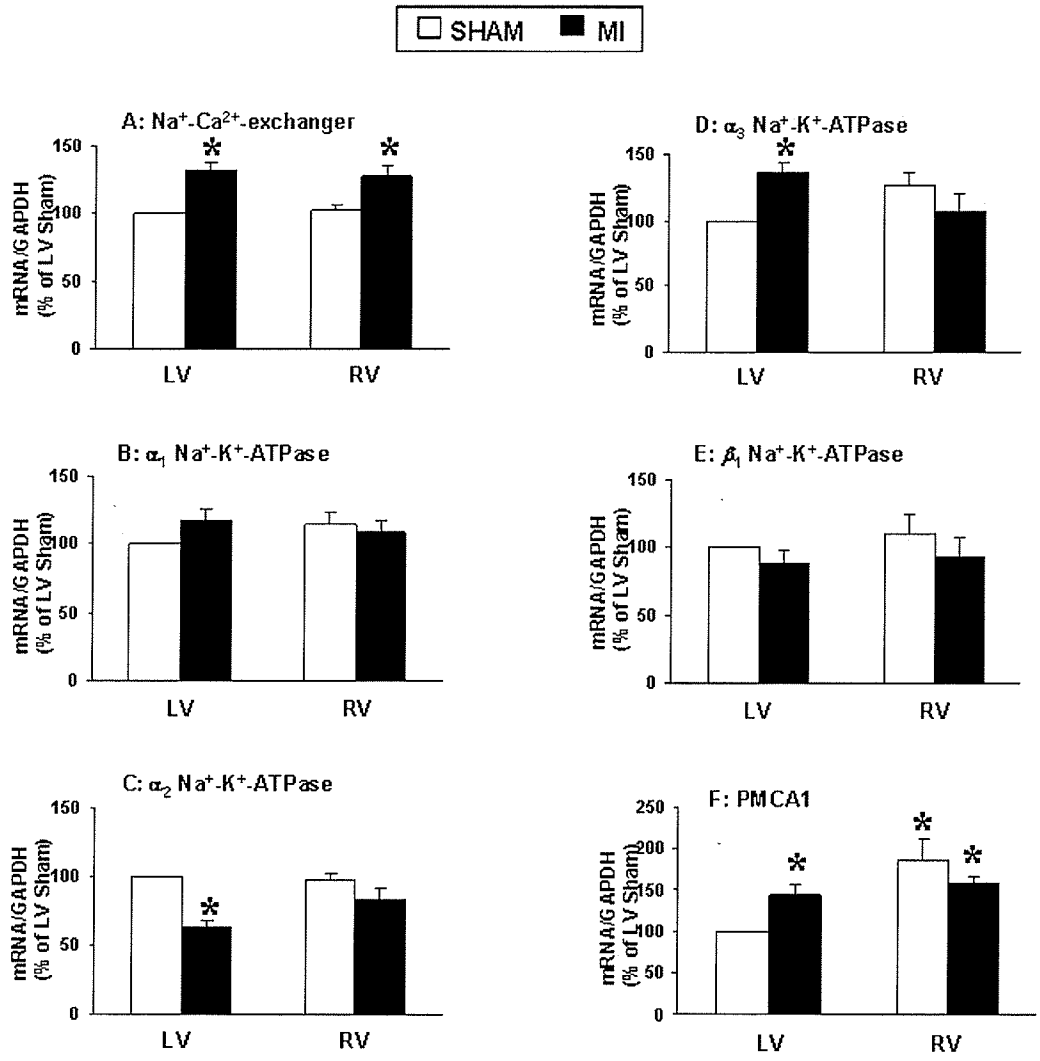

Figure 21. Comparison of mRNA abundance for cardiac sarcolemmal Na^+-Ca^{2+}-exchanger (NCX)(A), Na^+-K^+-ATPase different isoforms α_1 (B), α_2 (C), α_3 (D), and β_1 (E), and Ca^{2+}-pump (PMCA1)(F) in the viable tissue of both left and right ventricles from sham and infarcted (MI) rats. The values were normalized with respect to glyceraldehydes-3-phosphate dehydrogenase (GAPDH) mRNA levels and were expressed as a percentage of values for left ventricle in sham. Values are means ± SE of 6 animals for each group (except 4 for PMCA1). * $P < 0.05$ *vs* Sham LV.

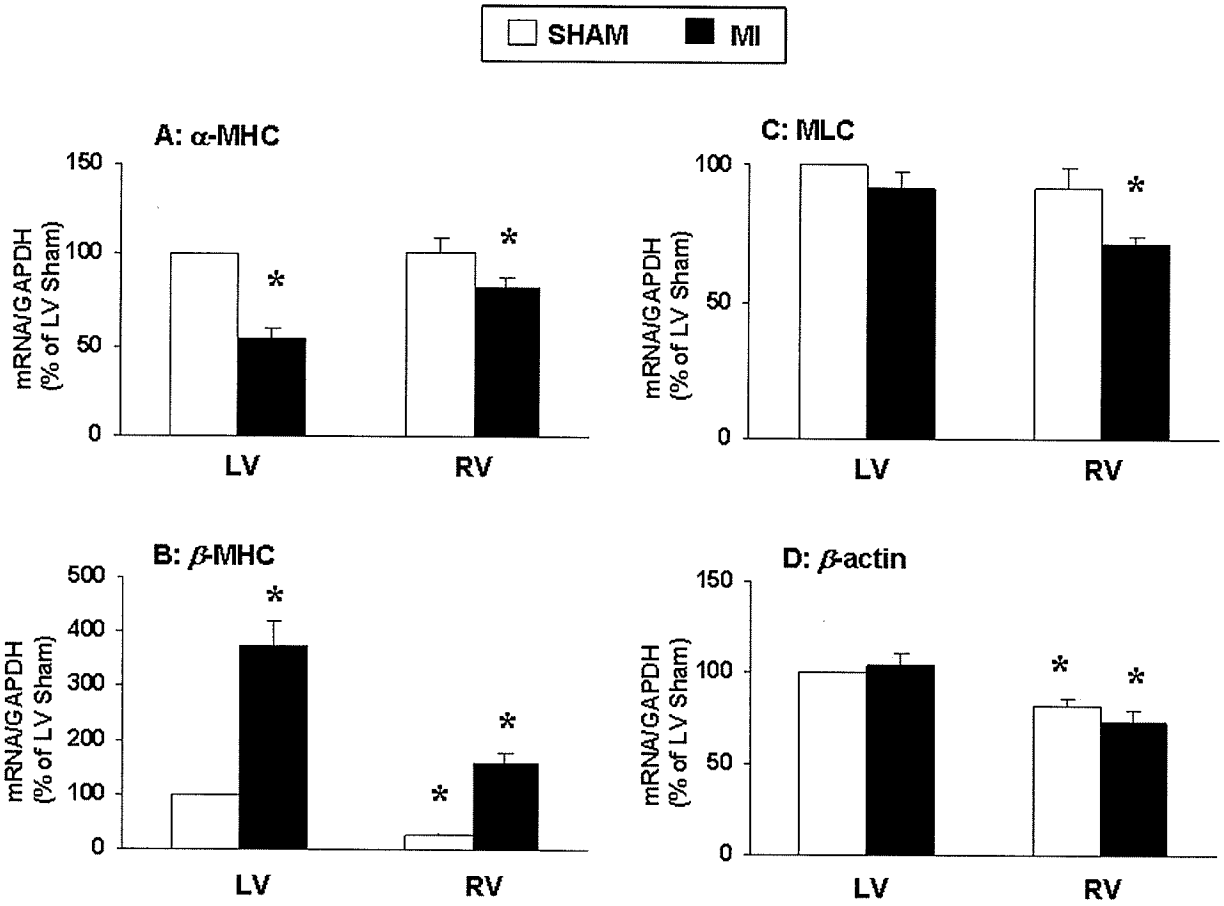

Figure 22. Comparison of mRNA abundance for cardiac α-myosin heavy chain (α-MHC)(A), β-myosin heavy chain (β-MHC)(B), myosin light chain (MLC)(C), and β-actin (D), in the viable tissue of both left and right ventricles from sham and infarcted (MI) rats. The values were normalized with respect to glyceraldehydes-3-phosphate dehydrogenase (GAPDH) mRNA levels and were expressed as a percentage of values for left ventricle in sham. Values are means ± SE of 6 animals for each group. * $P < 0.05$ *vs* Sham LV.

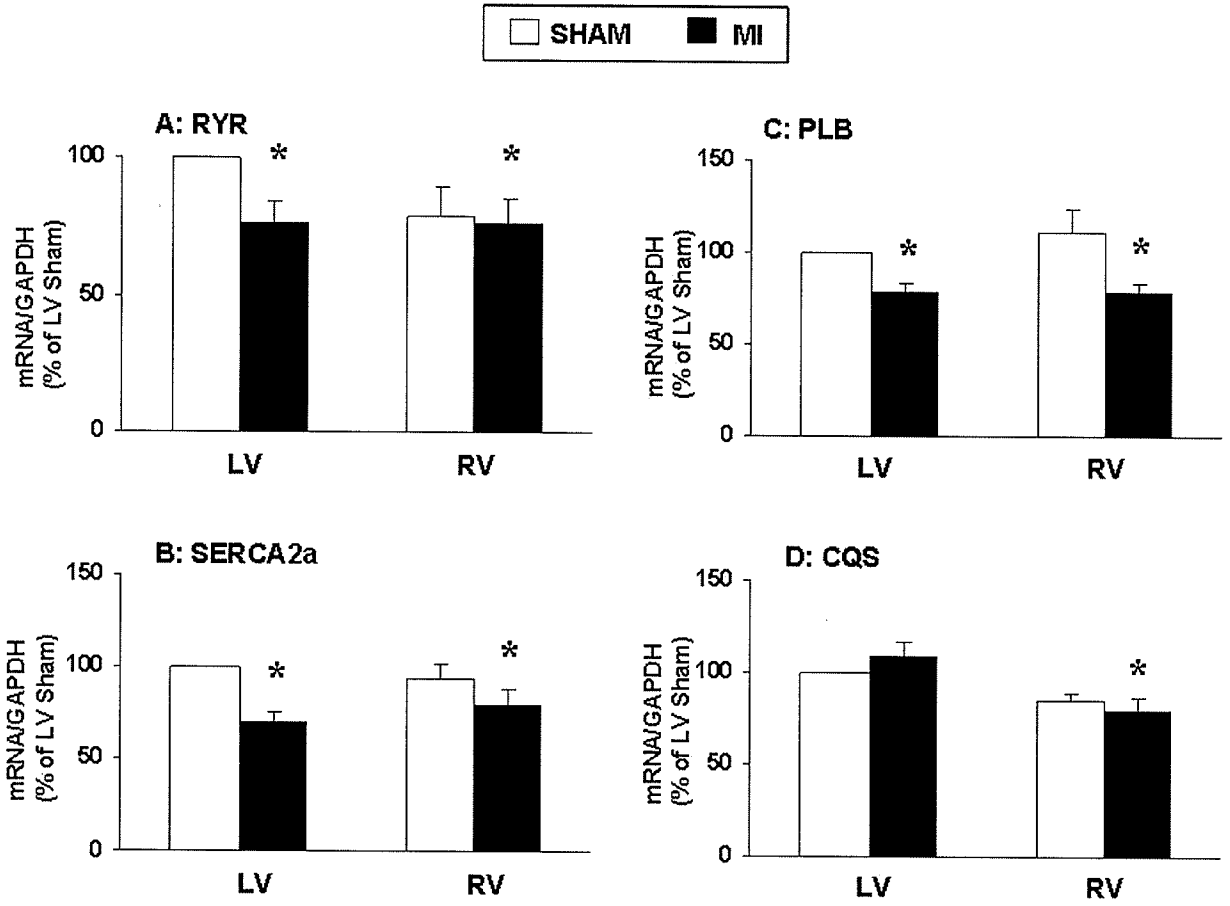

Figure 23. Comparison of mRNA abundance for cardiac ryanodine receptor (RYR)(A), sarco-endoplasmic reticulum Ca^{2+}-ATPase (SERCA2a)(B), phospholamban (PLB)(C) and calsequestrin (CQS)(D), in the viable tissue of both left and right ventricles from sham and infarcted (MI) rats. The values were normalized with respect to glyceraldehydes-3-phosphate dehydrogenase (GAPDH) mRNA levels and were expressed as a percentage of values for left ventricle in sham. Values are means ± SE of 6 animals for each group. * $P < 0.05$ *vs* Sham LV.

changes post MI as seen in the LV, including a decrease of gene expression in RYR, SERCA2a and PLB. The reduction of SERCA2a in RV post MI was not significant ($P > 0.05$) compared to RV Sham, but it was significant ($P < 0.05$) compared to LV gene expression in the sham group. Also a depression in mRNA level for CQS was observed in RV following MI, when compared to LV Sham ($P < 0.05$).

In summary, the RV had higher mRNA expression of PMCA1 as well as lower expression of β-MHC and β-actin in the sham group, and the difference was significant ($P < 0.05$). The rest of the changes in cardiac gene expression in the LV and RV were similar. Following MI, the reduction in PLB and α-MHC gene expression as well as the increase in NCX and β-MHC occurred bi-ventricular. The decreases in Na^+-K^+-ATPase α_2 isoform, RYR, and SERCA2a, however, were only significant in the LV, but not in the RV. Also, the increases in the LV in PMCA1 and Na^+-K^+-ATPase α_3 isoform were replaced by decreases in RV, although not significant.

V. DISCUSSION

1. SL Na^+-K^+-ATPase Remodeling in Failing Rat Heart

In this study, both +d*P*/d*t* and –d*P*/d*t* were decreased whereas LVEDP was markedly increased indicating cardiac dysfunction in the infarcted animals. These hearts were hypertrophied as the heart wt/body wt ratio was increased and the animals showed signs of lung congestion as the lung wet wt/dry wt ratio was also increased. In addition, heart dysfunction due to MI was found to be associated with depressed SL Na^+-K^+-ATPase activity and changes of Na^+-K^+-ATPase isoforms. An increase in SL Na^+-K^+-ATPase α_3 isoform protein and gene expression as well as a decrease in Na^+-K^+-ATPase α_2, β_2, and β_3 isoform protein and gene expression were also evident in hearts following MI. These results, showing depressed cardiac function and SL Na^+-K^+-ATPase activity as well as changes in SL Na^+-K^+-ATPase isoforms protein and gene expression, are in agreement with our results reported previously in this experimental model [39,40,74]. With respect to changes in Na^+-K^+-ATPase α_3 isoform, it is pointed out that there are different studies available for the distribution and activation, including retinoic acid induced increased Na^+-K^+-ATPase α_3 isoform and associated cardiac hypertrophy [290] and ouabain-induced depression in the gene expression of Na^+-K^+-ATPase α_3 isoform [291,292]. However, sufficient information about Na^+-K^+-ATPase α_3 isoform in the failing heart following MI is not available. The observed alterations in the relative values for protein contents of Na^+-K^+-ATPase isoforms are seen to result in changes in the composition as well as molecular structure of Na^+-K^+-ATPase and reduced SL Na^+-K^+-ATPase activity, thereby representing the process of SL Na^+-K^+-ATPase remodeling

during the development of heart failure. On the other hand, the function of Na^+-K^+-ATPase β_2 and β_3 isoform as well as the mechanism of the depression in Na^+-K^+-ATPase β_2 and β_3 isoforms in the failing heart following MI are not clear. Although we did not measure changes in any components of RAS, it can assumed that the observed changes in Na^+-K^+-ATPase isoforms are related to the activation of RAS because enalapril and losartan therapy modulated their reduction at protein level in failing heart. Since increase in α_3 isoform has been regarded as re-induction of a fetal program in heart failure models [269], it is reasonable to conclude that this process of SL remodeling in the failing heart may occur at the level of gene expression. Our data showed that mRNA levels for Na^+-K^+-ATPase α_2, β_2, and β_3 isoform were decreased and those for Na^+-K^+-ATPase α_3 isoform were increased. Since such a remodeling has also been shown to occur in the SR [35,40], myofibrils [39], and PKC isozymes [41] in CHF due to MI, it is likely that remodeling of these subcellular components may play a role in determining the strength of the contraction and relaxation of cardiomyocytes as well as in the adaption of the heart to the stress due to CHF. In view of the critical role of SL Na^+-K^+-ATPase isoforms in determining the action potential and Ca^{2+} transportation across the cardiomyocyte membrane that is associated with the depressed the cardiac contractility, it is likely that the depressed SL Na^+-K^+-ATPase activity in the failing heart may be due to the observed alterations of SL Na^+-K^+-ATPase isoforms. Due to the development of isoform-specific monoclonal antibodies to Na^+-K^+-ATPase isoforms [293], it is possible for us to examine the individual isoforms in the failing heart. Although the total protein density of SL Na^+-K^+-ATPase was not tested, it appears that there occurs a "shift" in SL Na^+-K^+-ATPase α isoforms from α_2 (high affinity to Na^+) to α_3 (low affinity to Na^+) in this model, and this

may explain the reduced SL Na^+-K^+-ATPase activity. This shift is exactly the reversal of postnatal changes of Na^+-K^+-ATPase isoforms from α_3 to α_2 observed in rats [294]. Such a change in the protein contents of Na^+-K^+-ATPase seems specific because the protein contents of both Na^+-K^+-ATPase α_1 and β_1 isoforms in the failing hearts were unchanged. There are reports showing no changes in Na^+-K^+-ATPase α_1 and β_1 isoforms in different experimental models of heart failure [272,273,290,292]. Since we did not determine the absolute values of the Na^+-K^+-ATPase isoforms in the failing heart by employing ELISA, some caution should be exercised while interpreting the observed changes in Na^+-K^+-ATPase isoforms in terms of quantitative alterations in Na^+-K^+-ATPase isoforms protein contents. In addition, although there is evidence that all human Na^+-K^+-ATPase α subunit isoforms have a similar affinity for cardiac glycosides [295], the activity of different isoforms in rat is different [63]. The development of cardiac hypertrophy as well as the observed alterations of contractile dysfunction may not be fully explained by the impairment of Na^+-K^+-ATPase. Nevertheless, due to the importance of Na^+-K^+-ATPase in heart function, it may at least contribute to the remodeling of heart following MI. Treatment of infarcted animals with enalapril was observed to partially prevent alterations in cardiac hypertrophy, lung congestion, heart function, SL Na^+-K^+-ATPase activity and alteration in Na^+-K^+-ATPase α_2, α_3, β_2, and β_3 isoform protein as well as gene expression. Since neither enalapril nor losartan affected the protein contents and mRNA levels for Na^+-K^+-ATPase α_1 and β_1 isoforms, it is evident that the observed effect of these drugs in Na^+-K^+-ATPase protein and gene expression is specific in nature. In view of the fact that the effects of both enalapril and losartan were simulated by combined therapy of enalapril and losartan, it appears that the beneficial actions of both enalapril and losartan on cardiac

function and SL Na^+-K^+-ATPase remodeling are due to the blockade of RAS in animals with heart failure. Both enalapril and losartan as well as other ACE inhibitors such as captopril, imidapril and trandolapril have also been shown to partially prevent cardiac remodeling in the failing hearts [37,39-41,61,296]. Thus, it is evident that the blockade of RAS may play a critical role in preventing cardiac and subcellular remodeling in infarcted animals. Such effects of the RAS blockade may not be due to reduction in the afterload because we did not observe any change in the MAP upon treatments with ACE inhibitors or losartan. Since ACE inhibitors are also known to prevent the breakdown of bradykinin [297,298], it can be argued that the beneficial effects of enalapril are mediated through the actions of bradykinin. Although we have not carried out any experiments to rule out this possibility, this mechanism in the experimental model used may not be of any major significance. This view is based on our observation that the combination therapy with both enalapril and losartan did not produce an additive effect on heart dysfunction, myofibrillar remodeling [299] or SL Na^+-K^+-ATPase alterations.

2. SL Ca^{2+}-regulatory Proteins Expression in Failing Rat Heart

In this study, we have observed that cardiac dysfunction in the infarcted animals was associated with an increase in protein content for SL NCX. It should be mentioned that the changes in NCX protein content are based on the densitometer analysis of the 116/112 kDa bands in Western blots whereas a 70-kDa protein band, which is likely to be proteolyic fragment [90], was not included in our measurement. Furthermore, it should be noted that mRNA levels for SL NCX were also significantly increased in the viable LV at 8 weeks post MI. These results are in agreement with the report of end-stage human heart

failure due to coronary artery disease in which NCX has been reported to be increased significanly with respect to both mRNA level and protein contents [58]. However, there are some controversial reports about the changes of NCX following MI. In view of the depressed SR function, as evident from the decreased RYR and SERCA2a in the infarcted rats [40], it is reasonable to assume that the elevated levels of NCX in SL may serve as a compensatory mechanism to accommodate the increased diastolic $[Ca^{2+}]_i$ due to the reduced Ca^{2+}-uptake in the SR. It has been suggested earlier that the changes of NCX and SERCA2a in the failing heart may compensate for each other [45,300]. However, on the basis of information in this study, it is difficult to conclude depression in SERCA2a induces the elevation of NCX. Although arrhythmias have been reported to be associated with the elevated NCX [45,301], it was not observed in our study.

It was interesting to observe the increased SL Ca^{2+}-pump protein content and corresponding mRNA level in the failing heart following MI. In view of the small amount of PMCA1 in sham control heart and less than 60% increase in proteins contents, the physiological significance of increased PMCA1 in failing heart is not of any major consequence [99]. Increased PMCA1 may compensate the reduced SERCA2a function to attenuate the increased diastolic $[Ca^{2+}]_i$ in the infarcted heart. However, our previous data in the infarcted rat showed that SL Ca^{2+}-pump activity was not reduced [96]. Therefore, the post-translation regulation of Ca^{2+}-pump by calmodulin [302] and acidic phospholipids [303] may play an important role in determining the SL Ca^{2+}-pump activity in the failing heart. On the other hand, the depressed SL Ca^{2+}-channel activity in CHF due to MI may be a consequence of alterations in SL Ca^{2+}-channel subunits. In this regard, it was observed that protein content for α_1-subunit was decreased whereas that for β-subunit

was increased without any change in α_2-subunit in the infarcted heart. However, due to insufficient knowledge about the structure and function of Ca^{2+}-channel, the exact interpretation of the results in terms of SL Ca^{2+}-channel activity is difficult. Nonetheless, it appears that the reduced L-type current during heart failure may be due to the remodeling of the Ca^{2+}-channel components. Particularly, there was a reduction in α_1 subunit, which is considered to contain the cation-conducting pore and the binding sites for channel blockers. These results are consistent with the observation in human failing heart showing reduced Ca^{2+}-channel mRNA expression [304].

The increased protein content for NCX and PMCA1 and a decrease in α_1-subunit for SL Ca^{2+}-channel in the failing heart may be associated with depressd LV function. The changes in SL were attenuated after treatment with enalapril and losartan. The benefical effects of blockade of RAS were observed at both protein contents and the corresponding mRNA levels for NCX and PMCA1. The increases in NCX and PMCA1 in failing heart are explained on the basis of elevated gene expression of these two proteins. There was no difference between enalapril and losartan treatment on these two proteins, indicating that the SL Ca^{2+}-regulatory protein gene may predominately be under AT_1R influence apart from AT_2R. Moreover, the Ca^{2+}-channel subunits are altered when AT_1R is activated. In accordance with our previous work, blockade of RAS has shown beneficial effects on both SL and SR Ca^{2+}-regulatory proteins. Although it is difficult to conclude which component of the SL membrane is more important, it is clear that cardiac remodeling of the SL is a result of RAS activation in failing heart post MI.

3. Changes in Left and Right Ventricular Gene Expression in Heart Failure

Although MI induced rat model of CHF [305] is hampered by high mortality and marked variability in infarct size and cardiac dysfunction, it is regarded as a useful model for studying the progression of cardiac dysfunction as well as for evaluating different therapeutic approaches. During the past decades, several modifications have been implied for improvements in this model; these include different species of animals such as Lewis inbred rat [306], mice [307]and dogs [308-313] as well as improvements of surgical methods [226,314]. Although both RV and LV are important for the proper functioning of the heart, in view of relatively less information available for the RV in comparison to the LV especially post MI, it should be noted that the development of cardiac hypertrophy of both LV and RV in infarcted rats was confirmed by different parameters such as increased heart wt (including LV viable tissue, scar and RV) and increased RV wt. *In vivo* hemodynamic data provided the evidence of impaired LV systolic and dystolic function. The increased lung wet wt/dry wt ratio was the proof for the presence of LV heart failure. In this model, LV was at a stage of moderate to severe heart failure while RV was under hypertrophy without signs of heart failure [261,277,315]. Since no liver congestion was evident, it is confirmed that the RV was not in the failing stage. It should, however, be mentioned that some investigators have reported that both left and right ventricular end-diastolic pressures were significantly increased and the depression of RV systolic pressure that was observed from 1 day to 6 weeks after coronary artery ligation was explained as acute and chronic biventricular failure [29].

This study has revealed that the observed differential changes in gene expression

in RV and LV are consistent with earlier reports showing differences in SR, Ca^{2+}-transport, β-adrenoreceptor linked signal transduction and contractile proteins [261,277,315,316]. The results reported in this study indicate that SERCA2 was depressed significantly in LV while there was no significant change in RV. SERCA2a plays a major role in the ECC and is responsible for transporting Ca^{2+} into the lumen of SR. The post-transcriptional regulation of SERCA2 is important since elevated mRNA level can lead to the increase of SERCA2a protein contents as well as its activity [317]. In LV from the failing human heart, the protein level of SERCA2a protein and mRNA levels were significantly reduced but there was a difference between the *endo-* and *epi-*myocardium [95]. PLB, the post-translation regulator of SERCA2a, was significantly reduced in both the LV and the RV in this project, while it is reported to be reduced in the LV in human heart failure [95]. This is consistent with the view that reduction in PLB may indicate the cardiac remodeling of the failing heart with respect to the post-translational modification of SERCA2a. This will partially release the inhibition upon SERCA2a activity under conditions of increased diastolic $[Ca^{2+}]_i$ in the failing heart. However, with the development of heart failure and long term increased expression of NCX, the SERCA2a undergoes the depression and results in the development of cardiac remodeling. When this compensatory mechanism reaches its limits, it results in the reduction of SERCA2a function.

The NCX gene expression in heart failure was significantly elevated in LV, which shows depression in SERCA2a. However, such a relationship was not observed for the RV because the elevated NCX gene expression in RV occurred without any change in SERCA2a in RV. It is possible that cardiac remodeling in NCX occurs before that in

SERCA2a in RV. This contradicts the view that the increased NCX compensates for the reduction in SERCA2a during heart failure, or that the reduced SERCA2a is compensatory response to increased NCX. Further experiments regarding time-course changes in both RV and LV during the development of CHF are needed to make any conclusions in this regard. However, it should be noted that mRNA levels for PMCA1 in the RV are higher than those in the LV and these are slightly reduced rather than markedly increased in the infarcted animals. Such changes in PMCA1 mRNA level may be due to greater stress in the LV in comparison to the RV. Nonetheless, these results provide additional evidence regarding differential changes in gene expression in RV and LV.

It can be argued that attenuation of depression in LV and RV gene expressions for α-MHC and PLB proteins in the infarcted heart are the consequence of improvement in heart function upon treatments with enalapril and losartan. However, this may not be the case because attenuation of depressions in LV gene expression for Na^+-K^+-ATPase α_2 isoform, RYR and SERCA2a were not associated with any effect on the RV. Furthermore, the increased mRNA levels for NCX and β-MHC proteins in both RV and LV in the infarcted animals were decreased upon treatment with enalapril and losartan. Although the increased mRNA levels for Na^+-K^+-ATP α_3 isoform and PMCA1 in the LV were normalized upon treatment with these agents, no changes in the RV were seen with or without drug treatment. Such differential effects of both enalapril and losartan in LV and RV may, therefore, be neither due to the direct effect of these agents on the genetic machinery nor are these the results of improved cardiac performance. Since enalapril has been seen to reduce the formation of Ang II where losartan would antagonize the effect of

Ang II, the observed differential effects of these agents are most probably due to the blockade of RAS. Such differential changes in LV and RV gene expression in the infarcted hearts with or without drug treatment may be due to the differential changes in cardiac RAS in both ventricles rather than changes in the circulating RAS. This view is supported by the fact that differential changes in RV and LV SNS activations have been shown to occur in the infarcted myocardium [318]. Although compartmentalization of Ang II formation in the heart has been observed [179], the exact status of RAS in both LV and RV remains to be demonstrated. Nonetheless, the effects of both enalapril and losartan on changes in cardiac performance and gene expression in the infarcted heart appears to be due to the blockade of RAS because combination therapy with these agents did not show any additive effects in the infarcted animals.

VI. SUMMARY AND CONCLUSIONS

This study was undertaken to test the hypothesis if the beneficial effects of RAS blockade by enalapril and/or losartan on cardiac performance are associated with attenuation of subcellular remodeling in protein and gene expression levels for SL Na^+-K^+-ATPase, NCX, Ca^{2+}-pump, and Ca^{2+}-channel. It was also the objective of this study to investigate if there occurs a differential remodeling for SL and SR Ca^{2+}-transport proteins as well as contractile components at mRNA level in both LV and RV due to CHF. On the basis of the results obtained in this study, the following conclusions can be made:

1. Cardiac hypertrophy and heart failure in the LV are accompanied by RV hypertrophy at 8 weeks post MI in rats.
2. Decreased SL Na^+-K^+-ATPase is due to changes in Na^+-K^+-ATPase isoforms, which are associated with alterations in corresponding gene expression following MI.
3. Remodeling in SL Ca^{2+}-regulatory proteins is associated with elevations in NCX and PMCA1 at both protein and mRNA levels as well as the alterations of Ca^{2+}-channel subunits.
4. In control animals, RV has a similar pattern of gene expression for cardiac SL and SR Ca^{2+}-regulatory proteins and contractile components as that in the LV, except for the higher level of PMCA1 and lower level for the β-MHC and β-actin.
5. The differential gene expression in the LV and RV is evident for SL, SR and myofibrillar components following MI.
6. Activation of RAS in infarcted animals causes cardiac hypertrophy and heart failure as these changes are attenuated by treatment with enalapril, an ACE

inhibitor, or losartan, an AT_1R antagonist.

7. Treatment of infarcted animals with enalapril or losartan significantly modifies the cardiac remodeling with respect to gene expression for the SL, SR and myofibrillar components as this is associated with attenuation of corresponding protein contents.
8. The beneficial effect of enalapril and losartan on cardiac and subcellular remodeling is not additive indicating that the actions of these agents are mediated by the blockade of RAS.

Thus, the RAS activation following MI contributes to the cardiac remodeling in failing heart, particularly the alterations of cardiac gene expression and corresponding protein contents. The blockade of the RAS prevents cardiac remodeling at the gene expression and protein level. This is associated with an improvement in heart function post MI.

REFERENCES

[1] McMurray JJ, Stewart S. Epidemiology, aetiology, and prognosis of heart failure. *Heart* 2000; **83:** 596-602.

[2] Goldstein S. Heart failure therapy at the turn of the century. *Heart Fail Rev* 2001; **6:** 7-14.

[3] MacIntyre K, Capewell S, Stewart S, Chalmers JW, Boyd J, Finlayson A, Redpath A, Pell JP, McMurray JJ. Evidence of improving prognosis in heart failure: trends in case fatality in 66 547 patients hospitalized between 1986 and 1995. *Circulation* 2000; **102:** 1126-1131.

[4] Siniorakis E, Arvanitakis S, Voyatzopoulos G, Hatziandreou P, Plataris G, Alexandris A, Bonoris P. Hemodynamic classification in acute myocardial infarction. *Chest* 2000; **117:** 1286-1290.

[5] Davis RC, Hobbs FD, Lip GY. ABC of heart failure. History and epidemiology. *BMJ* 2000; **320:** 39-42.

[6] Milavetz JJ, Giebel DW, Christian TF, Schwartz RS, Holmes DR, Jr., Gibbons RJ. Time to therapy and salvage in myocardial infarction. *J Am Coll Cardiol* 1998; **31:** 1246-1251.

[7] Brodie BR, Stuckey TD, Wall TC, Kissling G, Hansen CJ, Muncy DB, Weintraub RA, Kelly TA. Importance of time to reperfusion for 30-day and late survival and recovery of left ventricular function after primary angioplasty for acute myocardial infarction. *J Am Coll Cardiol* 1998; **32:** 1312-1319.

[8] Tomaselli GF, Marban E. Electrophysiological remodeling in hypertrophy and heart failure. *Cardiovasc Res* 1999; **42:** 270-283.

[9] Pfeffer MA, Braunwald E. Ventricular remodeling after myocardial infarction. Experimental observations and clinical implications. *Circulation* 1990; **81:** 1161-1172.

[10] Rumberger JA. Ventricular dilatation and remodeling after myocardial infarction. *Mayo Clin Proc* 1994; **69:** 664-674.

[11] Pfeffer JM, Pfeffer MA, Fletcher PJ, Braunwald E. Progressive ventricular remodeling in rat with myocardial infarction. *Am J Physiol Heart Circ Physiol* 1991; **260:** H1406-H1414.

[12] Deedwania PC. Early intervention in patients with heart failure and left ventricular dysfunction. *Med Clin North Am* 1995; **79:** 1191-1203.

[13] Anand IS, Liu D, Chugh SS, Prahash AJ, Gupta S, John R, Popescu F, Chandrashekhar Y. Isolated myocyte contractile function is normal in postinfarct remodeled rat heart with systolic dysfunction. *Circulation* 1997; **96:** 3974-3984.

[14] Roberts CS, Maclean D, Maroko P, Kloner RA. Early and late remodeling of the left ventricle after acute myocardial infarction. *Am J Cardiol* 1984; **54:** 407-410.

[15] Pfeffer JM, Fischer TA, Pfeffer MA. Angiotensin-converting enzyme inhibition and ventricular remodeling after myocardial infarction. *Annu Rev Physiol* 1995; **57:** 805-826.

[16] Nelissen-Vrancken HJ, Debets JJ, Snoeckx LH, Daemen MJ, Smits JF. Time-related normalization of maximal coronary flow in isolated perfused hearts of rats with myocardial infarction. *Circulation* 1996; **93:** 349-355.

[17] Pfeffer JM. Progressive ventricular dilation in experimental myocardial infarction and its attenuation by angiotensin-converting enzyme inhibition. *Am J Cardiol* 1991; **68:** 17D-25D.

[18] Sun Y, Weber KT. Angiotensin II receptor binding following myocardial infarction in the rat. *Cardiovasc Res* 1994; **28:** 1623-1628.

[19] Schieffer B, Wirger A, Meybrunn M, Seitz S, Holtz J, Riede UN, Drexler H. Comparative effects of chronic angiotensin-converting enzyme inhibition and angiotensin II type 1 receptor blockade on cardiac remodeling after myocardial infarction in the rat. *Circulation* 1994; **89:** 2273-2282.

[20] Schieffer B, Wollert KC, Berchtold M, Saal K, Schieffer E, Hornig B, Riede UN, Drexler H. Development and prevention of skeletal muscle structural alterations after experimental myocardial infarction. *Am J Physiol Heart Circ Physiol* 1995; **269:** H1507-H1513.

[21] Thai HM, Van HT, Gaballa MA, Goldman S, Raya TE. Effects of AT1 receptor blockade after myocardial infarct on myocardial fibrosis, stiffness, and contractility. *Am J Physiol Heart Circ Physiol* 1999; **276:** H873-H880.

[22] Van Kerckhoven R, Kalkman EA, Saxena PR, Schoemaker RG. Altered cardiac collagen and associated changes in diastolic function of infarcted rat hearts. *Cardiovasc Res* 2000; **46:** 316-323.

[23] Pelouch V, Dixon IM, Sethi R, Dhalla NS. Alteration of collagenous protein profile in congestive heart failure secondary to myocardial infarction. *Mol Cell Biochem* 1993; **129:** 121-131.

[24] Marijianowski MM, Teeling P, Becker AE. Remodeling after myocardial infarction in humans is not associated with interstitial fibrosis of noninfarcted myocardium. *J Am Coll Cardiol* 1997; **30:** 76-82.

[25] Anversa P, Beghi C, Kikkawa Y, Olivetti G. Myocardial infarction in rats. Infarct size, myocyte hypertrophy, and capillary growth. *Circ Res* 1986; **58:** 26-37.

[26] Tajima M, Weinberg EO, Bartunek J, Jin H, Yang R, Paoni NF, Lorell BH. Treatment with growth hormone enhances contractile reserve and intracellular calcium transients in myocytes from rats with postinfarction heart failure. *Circulation* 1999; **99:** 127-134.

[27] Capasso JM, Li P, Anversa P. Cytosolic calcium transients in myocytes isolated from rats with ischemic heart failure. *Am J Physiol Heart Circ Physiol* 1993; **265:** H1953-H1964.

[28] Cheung JY, Musch TI, Misawa H, Semanchick A, Elensky M, Yelamarty RV, Moore RL. Impaired cardiac function in rats with healed myocardial infarction: cellular vs. myocardial mechanisms. *Am J Physiol Cell Physiol* 1994; **266:** C29-C36.

[29] Yue P, Long CS, Austin R, Chang KC, Simpson PC, Massie BM. Post-infarction heart failure in the rat is associated with distinct alterations in cardiac myocyte molecular phenotype. *J Mol Cell Cardiol* 1998; **30:** 1615-1630.

[30] Maisch B. Ventricular remodeling. *Cardiology* 1996; **87 Suppl 1:** 2-10.

[31] Kurrelmeyer K, Kalra D, Bozkurt B, Wang F, Dibbs Z, Seta Y, Baumgarten G, Engle D, Sivasubramanian N, Mann DL. Cardiac remodeling as a consequence and cause of progressive heart failure. *Clin Cardiol* 1998; **21:** I14-I19.

[32] Pfeffer JM, Pfeffer MA, Fletcher PJ, Braunwald E. Ventricular performance in rats with myocardial infarction and failure. *Am J Med* 1984; **76:** 99-103.

[33] DeFelice A, Frering R, Horan P. Time course of hemodynamic changes in rats with healed severe myocardial infarction. *Am J Physiol Heart Circ Physiol* 1989; **257:** H289-H296.

[34] Afzal N, Dhalla NS. Sarcoplasmic reticular Ca^{2+} pump ATPase activity in congestive heart failure due to myocardial infarction. *Can J Cardiol* 1996; **12:** 1065-1073.

[35] Yamaguchi F, Sanbe A, Takeo S. Cardiac sarcoplasmic reticular function in rats with chronic heart failure following myocardial infarction. *J Mol Cell Cardiol* 1997; **29:** 753-763.

[36] Holt E, Tonnessen T, Lunde PK, Semb SO, Wasserstrom JA, Sejersted OM, Christensen G. Mechanisms of cardiomyocyte dysfunction in heart failure following myocardial infarction in rats. *J Mol Cell Cardiol* 1998; **30:** 1581-1593.

[37] Yamaguchi F, Sanbe A, Takeo S. Effects of long-term treatment with trandolapril on sarcoplasmic reticulum function of cardiac muscle in rats with chronic heart failure following myocardial infarction. *Br J Pharmacol* 1998; **123:** 326-334.

[38] Litwin SE, Bridge JH. Enhanced Na^{+}-Ca^{2+} exchange in the infarcted heart. Implications for excitation for excitation-contraction coupling. *Circ Res* 1997; **81:** 1083-1093.

[39] Wang J, Liu X, Ren B, Rupp H, Takeda N, Dhalla NS. Modification of myosin gene expression by imidapril in failing heart due to myocardial infarction. *J Mol Cell Cardiol* 2002; **34:** 847-857.

[40] Guo X, Chapman D, Dhalla NS. Partial prevention of changes in SR gene expression in congestive heart failure due to myocardial infarction by enalapril or losartan. *Mol Cell Biochem* 2003; **254:** 163-172.

[41] Wang J, Liu X, Sentex E, Takeda N, Dhalla NS. Increased expression of protein kinase C isoforms in heart failure due to myocardial infarction. *Am J Physiol Heart Circ Physiol* 2003; **284:** H2277-H2287.

[42] Lindpaintner K, Lu W, Neidermajer N, Schieffer B, Just H, Ganten D, Drexler H. Selective activation of cardiac angiotensinogen gene expression in post-infarction ventricular remodeling in the rat. *J Mol Cell Cardiol* 1993; **25:** 133-143.

[43] Iijima K, Geshi E, Nomizo A, Arata Y, Katagiri T. Alterations in sarcoplasmic reticulum and angiotensin II type 1 receptor gene expression after myocardial infarction in rats. *Jpn Circ J* 1998; **62:** 449-454.

[44] Packer M. Neurohormonal interactions and adaptations in congestive heart failure. *Circulation* 1988; **77:** 721-730.

[45] Hasenfuss G, Pieske B. Calcium cycling in congestive heart failure. *J Mol Cell Cardiol* 2002; **34:** 951-969.

[46] Sakai S, Miyauchi T, Yamaguchi I. Long-term endothelin receptor antagonist administration improves alterations in expression of various cardiac genes in failing myocardium of rats with heart failure. *Circulation* 2000; **101:** 2849-2853.

[47] Hanatani A, Yoshiyama M, Takeuchi K, Kim S, Nakayama K, Omura T, Iwao H, Yoshikawa J. Angiotensin II type 1-receptor antagonist candesartan cilexitil prevents left ventricular dysfunction in myocardial infarcted rats. *Jpn J Pharmacol* 1998; **78:** 45-54.

[48] Dhalla NS, Pierce GN, Panagia V, Singal PK, Beamish RE. Calcium movements in relation to heart function. *Basic Res Cardiol* 1982; **77:** 117-139.

[49] Dhalla NS, Afzal N, Beamish RE, Naimark B, Takeda N, Nagano M. Pathophysiology of cardiac dysfunction in congestive heart failure. *Can J Cardiol* 1993; **9:** 873-887.

[50] Dhalla NS, Wang X, Beamish RE. Intracellular calcium handling in normal and failing hearts. *Exp Clin Cardiol* 1996; **1:** 7-20.

[51] Morgan HE, Baker KM. Cardiac hypertrophy. Mechanical, neural, and endocrine dependence. *Circulation* 1991; **83:** 13-25.

[52] Barry WH, Bridge JH. Intracellular calcium homeostasis in cardiac myocytes. *Circulation* 1993; **87:** 1806-1815.

[53] Zhang XQ, Moore RL, Tenhave T, Cheung JY. [Ca^{2+}]i transients in hypertensive and postinfarction myocytes. *Am J Physiol Cell Physiol* 1995; **269:** C632-C640.

[54] Li P, Park C, Micheletti R, Li B, Cheng W, Sonnenblick EH, Anversa P, Bianchi G. Myocyte performance during evolution of myocardial infarction in rats: effects of propionyl-L-carnitine. *Am J Physiol Heart Circ Physiol* 1995; **268:** H1702-H1713.

[55] Limas CJ, Olivari MT, Goldenberg IF, Levine TB, Benditt DG, Simon A. Calcium uptake by cardiac sarcoplasmic reticulum in human dilated cardiomyopathy. *Cardiovasc Res* 1987; **21:** 601-605.

[56] Gwathmey JK, Copelas L, MacKinnon R, Schoen FJ, Feldman MD, Grossman W, Morgan JP. Abnormal intracellular calcium handling in myocardium from patients with end-stage heart failure. *Circ Res* 1987; **61:** 70-76.

[57] Morgan JP, Erny RE, Allen PD, Grossman W, Gwathmey JK. Abnormal intracellular calcium handling, a major cause of systolic and diastolic dysfunction in ventricular myocardium from patients with heart failure. *Circulation* 1990; **81:** III21-III32.

[58] Studer R, Reinecke H, Bilger J, Eschenhagen T, Bohm M, Hasenfuss G, Just H, Holtz J, Drexler H. Gene expression of the cardiac Na^{+}-Ca^{2+} exchanger in end-stage human heart failure. *Circ Res* 1994; **75:** 443-453.

[59] Schillinger W, Schneider H, Minami K, Ferrari R, Hasenfuss G. Importance of sympathetic activation for the expression of Na^{+}-Ca^{2+} exchanger in end-stage failing human myocardium. *Eur Heart J* 2002; **23:** 1118-1124.

[60] Hasenfuss G, Schillinger W, Lehnart SE, Preuss M, Pieske B, Maier LS, Prestle J, Minami K, Just H. Relationship between Na^{+}-Ca^{2+}-exchanger protein levels and diastolic function of failing human myocardium. *Circulation* 1999; **99:** 641-648.

[61] Shao Q, Ren B, Zarain-Herzberg A, Ganguly PK, Dhalla NS. Captopril treatment improves the sarcoplasmic reticular Ca^{2+} transport in heart failure due to myocardial infarction. *J Mol Cell Cardiol* 1999; **31:** 1663-1672.

[62] Zarain-Herzberg A, Afzal N, Elimban V, Dhalla NS. Decreased expression of cardiac sarcoplasmic reticulum Ca(2+)-pump ATPase in congestive heart failure due to myocardial infarction. *Mol Cell Biochem* 1996; **163-164:** 285-290.

[63] Mobasheri A, Avila J, Cozar-Castellano I, Brownleader MD, Trevan M, Francis MJ, Lamb JF, Martin-Vasallo P. Na^+, K^+-ATPase isozyme diversity; comparative biochemistry and physiological implications of novel functional interactions. *Biosci Rep* 2000; **20:** 51-91.

[64] Jorgensen PL. Aspects of gene structure and functional regulation of the isozymes of Na,K-ATPase. *Cell Mol Biol (Noisy -le-grand)* 2001; **47:** 231-238.

[65] Brotherus JR, Jacobsen L, Jorgensen PL. Soluble and enzymatically stable (Na+ + K+)-ATPase from mammalian kidney consisting predominantly of protomer alpha beta-units. Preparation, assay and reconstitution of active Na+, K+ transport. *Biochim Biophys Acta* 1983; **731:** 290-303.

[66] Petrecca K, Atanasiu R, Grinstein S, Orlowski J, Shrier A. Subcellular localization of the Na^+/H^+ exchanger NHE1 in rat myocardium. *Am J Physiol Heart Circ Physiol* 1999; **276:** H709-H717.

[67] James PF, Grupp IL, Grupp G, Woo AL, Askew GR, Croyle ML, Walsh RA, Lingrel JB. Identification of a specific role for the Na,K-ATPase alpha 2 isoform as a regulator of calcium in the heart. *Mol Cell* 1999; **3:** 555-563.

[68] Jewell EA, Lingrel JB. Comparison of the substrate dependence properties of the rat Na,K-ATPase alpha 1, alpha 2, and alpha 3 isoforms expressed in HeLa cells. *J Biol Chem* 1991; **266:** 16925-16930.

[69] Shamraj OI, Lingrel JB. A putative fourth Na^+,K^+-ATPase alpha-subunit gene is expressed in testis. *Proc Natl Acad Sci U S A* 1994; **91:** 12952-12956.

[70] Pierre S, Paganelli F, Sennoune S, Roche R, Schwinger RH, Mesana T, Maixe JM. RT-PCR detection of the Na,K-ATPase beta3-isoform in human heart. *Cell Mol Biol (Noisy -le-grand)* 2001; **47:** 261-264.

[71] Seppet EK, Kolar F, Dixon IM, Hata T, Dhalla NS. Regulation of cardiac sarcolemmal Ca^{2+} channels and Ca^{2+} transporters by thyroid hormone. *Mol Cell Biochem* 1993; **129:** 145-159.

[72] Kato K, Shao Q, Elimban V, Lukas A, Dhalla NS. Mechanism of depression in cardiac sarcolemmal Na^+-K^+-ATPase by hypochlorous acid. *Am J Physiol Cell Physiol* 1998; **275:** C826-C831.

[73] Shao Q, Matsubara T, Bhatt SK, Dhalla NS. Inhibition of cardiac sarcolemma Na^+-K^+ ATPase by oxyradical generating systems. *Mol Cell Biochem* 1995; **147:** 139-144.

[74] Dixon IM, Hata T, Dhalla NS. Sarcolemmal Na^+-K^+-ATPase activity in congestive heart failure due to myocardial infarction. *Am J Physiol Cell Physiol* 1992; **262:** C664-C671.

[75] Sethi R, Dhalla KS, Ganguly PK, Ferrari R, Dhalla NS. Beneficial effects of propionyl L-carnitine on sarcolemmal changes in congestive heart failure due to myocardial infarction. *Cardiovasc Res* 1999; **42:** 607-615.

[76] Satoh H, Ginsburg KS, Qing K, Terada H, Hayashi H, Bers DM. KB-R7943 block of Ca^{2+} influx via Na^+/Ca^{2+} exchange does not alter twitches or glycoside inotropy but prevents Ca^{2+} overload in rat ventricular myocytes. *Circulation* 2000; **101:** 1441-1446.

[77] Bers DM, Perez-Reyes E. Ca channels in cardiac myocytes: structure and function in Ca influx and intracellular Ca release. *Cardiovasc Res* 1999; **42:** 339-360.

[78] Bangalore R, Mehrke G, Gingrich K, Hofmann F, Kass RS. Influence of L-type Ca channel alpha 2/delta-subunit on ionic and gating current in transiently transfected HEK 293 cells. *Am J Physiol Heart Circ Physiol* 1996; **270:** H1521-H1528.

[79] Serikov VB, Petrashevskaya NN, Canning AM, Schwartz A. Reduction of $[Ca^{2+}]i$ restores uncoupled beta-adrenergic signaling in isolated perfused transgenic mouse hearts. *Circ Res* 2001; **88:** 9-11.

[80] Ruth P, Rohrkasten A, Biel M, Bosse E, Regulla S, Meyer HE, Flockerzi V, Hofmann F. Primary structure of the beta subunit of the DHP-sensitive calcium channel from skeletal muscle. *Science* 1989; **245:** 1115-1118.

[81] Jay SD, Ellis SB, McCue AF, Williams ME, Vedvick TS, Harpold MM, Campbell KP. Primary structure of the gamma subunit of the DHP-sensitive calcium channel from skeletal muscle. *Science* 1990; **248:** 490-492.

[82] Wang Y, Wagner MB, Joyner RW, Kumar R. cGMP-dependent protein kinase mediates stimulation of L-type calcium current by cGMP in rabbit atrial cells. *Cardiovasc Res* 2000; **48:** 310-322.

[83] Qin D, Zhang ZH, Caref EB, Boutjdir M, Jain P, el Sherif N. Cellular and ionic basis of arrhythmias in postinfarction remodeled ventricular myocardium. *Circ Res* 1996; **79:** 461-473.

[84] Zhang XQ, Moore RL, Tillotson DL, Cheung JY. Calcium currents in postinfarction rat cardiac myocytes. *Am J Physiol Cell Physiol* 1995; **269:** C1464-C1473.

[85] Zhang XQ, Tillotson DL, Moore RL, Zelis R, Cheung JY. Na^+/Ca^{2+} exchange currents and SR Ca^{2+} contents in postinfarction myocytes. *Am J Physiol Cell Physiol* 1996; **271:** C1800-C1807.

[86] Gomez AM, Valdivia HH, Cheng H, Lederer MR, Santana LF, Cannell MB, McCune SA, Altschuld RA, Lederer WJ. Defective excitation-contraction coupling in experimental cardiac hypertrophy and heart failure. *Science* 1997; **276:** 800-806.

[87] Dixon IM, Lee SL, Dhalla NS. Nitrendipine binding in congestive heart failure due to myocardial infarction. *Circ Res* 1990; **66:** 782-788.

[88] Ming Z, Nordin C, Siri F, Aronson RS. Reduced calcium current density in single myocytes isolated from hypertrophied failing guinea pig hearts. *J Mol Cell Cardiol* 1994; **26:** 1133-1143.

[89] Sandmann S, Claas R, Cleutjens JP, Daemen MJ, Unger T. Calcium channel blockade limits cardiac remodeling and improves cardiac function in myocardial infarction-induced heart failure in rats. *J Cardiovasc Pharmacol* 2001; **37:** 64-77.

[90] Nicoll DA, Longoni S, Philipson KD. Molecular cloning and functional expression of the cardiac sarcolemmal Na^+-Ca^{2+} exchanger. *Science* 1990; **250:** 562-565.

[91] Porzig H, Li Z, Nicoll DA, Philipson KD. Mapping of the cardiac sodium-calcium exchanger with monoclonal antibodies. *Am J Physiol Cell Physiol* 1993; **265:** C748-C756.

[92] Philipson KD, Longoni S, Ward R. Purification of the cardiac Na^+-Ca^{2+} exchange protein. *Biochim Biophys Acta* 1988; **945:** 298-306.

[93] Magee WP, Deshmukh G, DeNinno MP, Sutt JC, Chapman JG, Tracey WR. Differing cardioprotective efficacy of the Na^+-Ca^{2+} exchanger inhibitors, SEA0400 and KB-R7943. *Am J Physiol Heart Circ Physiol* 2002;

[94] Schotten U, Koenigs B, Rueppel M, Schoendube F, Boknik P, Schmitz W, Hanrath P. Reduced myocardial sarcoplasmic reticulum Ca^{2+}-ATPase protein expression in compensated primary and secondary human cardiac hypertrophy. *J Mol Cell Cardiol* 1999; **31:** 1483-1494.

[95] Prestle J, Dieterich S, Preuss M, Bieligk U, Hasenfuss G. Heterogeneous transmural gene expression of calcium-handling proteins and natriuretic peptides in the failing human heart. *Cardiovasc Res* 1999; **43:** 323-331.

[96] Dixon IM, Hata T, Dhalla NS. Sarcolemmal calcium transport in congestive heart failure due to myocardial infarction in rats. *Am J Physiol Heart Circ Physiol* 1992; **262:** H1387-H1394.

[97] Dipla K, Mattiello JA, Margulies KB, Jeevanandam V, Houser SR. The sarcoplasmic reticulum and the Na^+/Ca^{2+} exchanger both contribute to the Ca^{2+} transient of failing human ventricular myocytes. *Circ Res* 1999; **84:** 435-444.

[98] Stauffer TP, Guerini D, Carafoli E. Tissue distribution of the four gene products of the plasma membrane Ca^{2+} pump. A study using specific antibodies. *J Biol Chem* 1995; **270:** 12184-12190.

[99] Hammes A, Oberdorf-Maass S, Rother T, Nething K, Gollnick F, Linz KW, Meyer R, Hu K, Han H, Gaudron P, Ertl G, Hoffmann S, Ganten U, Vetter R, Schuh K, Benkwitz C, Zimmer HG, Neyses L. Overexpression of the sarcolemmal calcium pump in the myocardium of transgenic rats. *Circ Res* 1998; **83:** 877-888.

[100] Golfman LS, Takeda N, Dhalla NS. Cardiac membrane Ca^{2+}-transport in alloxan-induced diabetes in rats. *Diabetes Res Clin Pract* 1996; **31 Suppl:** S73-S77.

[101] Matsubara T, Dhalla NS. Relationship between mechanical dysfunction and depression of sarcolemmal Ca^{2+}-pump activity in hearts perfused with oxygen free radicals. *Mol Cell Biochem* 1996; **160-161:** 179-185.

[102] Meissner G. Ryanodine activation and inhibition of the Ca^{2+} release channel of sarcoplasmic reticulum. *J Biol Chem* 1986; **261:** 6300-6306.

[103] Rousseau E, Smith JS, Meissner G. Ryanodine modifies conductance and gating behavior of single Ca^{2+} release channel. *Am J Physiol Cell Physiol* 1987; **253:** C364-C368.

[104] Anderson K, Lai FA, Liu QY, Rousseau E, Erickson HP, Meissner G. Structural and functional characterization of the purified cardiac ryanodine receptor-Ca^{2+} release channel complex. *J Biol Chem* 1989; **264:** 1329-1335.

[105] Otsu K, Willard HF, Khanna VK, Zorzato F, Green NM, MacLennan DH. Molecular cloning of cDNA encoding the Ca^{2+} release channel (ryanodine receptor) of rabbit cardiac muscle sarcoplasmic reticulum. *J Biol Chem* 1990; **265:** 13472-13483.

[106] Lai FA, Erickson HP, Rousseau E, Liu QY, Meissner G. Purification and reconstitution of the calcium release channel from skeletal muscle. *Nature* 1988; **331:** 315-319.

[107] Fabiato A. Simulated calcium current can both cause calcium loading in and trigger calcium release from the sarcoplasmic reticulum of a skinned canine cardiac Purkinje cell. *J Gen Physiol* 1985; **85:** 291-320.

[108] Arai M, Alpert NR, MacLennan DH, Barton P, Periasamy M. Alterations in sarcoplasmic reticulum gene expression in human heart failure. A possible mechanism for alterations in systolic and diastolic properties of the failing myocardium. *Circ Res* 1993; **72:** 463-469.

[109] Meyer M, Schillinger W, Pieske B, Holubarsch C, Heilmann C, Posival H, Kuwajima G, Mikoshiba K, Just H, Hasenfuss G, . Alterations of sarcoplasmic reticulum proteins in failing human dilated cardiomyopathy. *Circulation* 1995; **92:** 778-784.

[110] Hisamatsu Y, Ohkusa T, Kihara Y, Inoko M, Ueyama T, Yano M, Sasayama S, Matsuzaki M. Early changes in the functions of cardiac sarcoplasmic reticulum in volume-overloaded cardiac hypertrophy in rats. *J Mol Cell Cardiol* 1997; **29:** 1097-1109.

[111] Ohkusa T, Hisamatsu Y, Yano M, Kobayashi S, Tatsuno H, Saiki Y, Kohno M, Matsuzaki M. Altered cardiac mechanism and sarcoplasmic reticulum function in pressure overload-induced cardiac hypertrophy in rats. *J Mol Cell Cardiol* 1997; **29:** 45-54.

[112] Sapp JL, Howlett SE. Density of ryanodine receptors is increased in sarcoplasmic reticulum from prehypertrophic cardiomyopathic hamster heart. *J Mol Cell Cardiol* 1994; **26:** 325-334.

[113] Jorgensen AO, Shen AC, Daly P, MacLennan DH. Localization of Ca^{2+} + Mg^{2+}-ATPase of the sarcoplasmic reticulum in adult rat papillary muscle. *J Cell Biol* 1982; **93:** 883-892.

[114] Zarain-Herzberg A, MacLennan DH, Periasamy M. Characterization of rabbit cardiac sarco(endo)plasmic reticulum Ca^{2+}-ATPase gene. *J Biol Chem* 1990; **265:** 4670-4677.

[115] Wu KD, Lee WS, Wey J, Bungard D, Lytton J. Localization and quantification of endoplasmic reticulum Ca^{2+} -ATPase isoform transcripts. *Am J Physiol Cell Physiol* 1995; **269:** C775-C784.

[116] Cantilina T, Sagara Y, Inesi G, Jones LR. Comparative studies of cardiac and skeletal sarcoplasmic reticulum ATPases. Effect of a phospholamban antibody on enzyme activation by Ca^{2+}. *J Biol Chem* 1993; **268:** 17018-17025.

[117] Periasamy M, Reed TD, Liu LH, Ji Y, Loukianov E, Paul RJ, Nieman ML, Riddle T, Duffy JJ, Doetschman T, Lorenz JN, Shull GE. Impaired cardiac performance in heterozygous mice with a null mutation in the sarco(endo)plasmic reticulum Ca^{2+}-ATPase isoform 2 (SERCA2) gene. *J Biol Chem* 1999; **274:** 2556-2562.

[118] Burk SE, Lytton J, MacLennan DH, Shull GE. cDNA cloning, functional expression, and mRNA tissue distribution of a third organellar Ca^{2+} pump. *J Biol Chem* 1989; **264:** 18561-18568.

[119] Kiss E, Ball NA, Kranias EG, Walsh RA. Differential changes in cardiac phospholamban and sarcoplasmic reticular Ca^{2+}-ATPase protein levels. Effects on Ca^{2+} transport and mechanics in compensated pressure-overload hypertrophy and congestive heart failure. *Circ Res* 1995; **77:** 759-764.

[120] Feldman AM, Weinberg EO, Ray PE, Lorell BH. Selective changes in cardiac gene expression during compensated hypertrophy and the transition to cardiac decompensation in rats with chronic aortic banding. *Circ Res* 1993; **73:** 184-192.

[121] Bluhm WF, Meyer M, Sayen MR, Swanson EA, Dillmann WH. Overexpression of sarcoplasmic reticulum Ca^{2+}-ATPase improves cardiac contractile function in hypothyroid mice. *Cardiovasc Res* 1999; **43:** 382-388.

[122] Baker DL, Hashimoto K, Grupp IL, Ji Y, Reed T, Loukianov E, Grupp G, Bhagwhat A, Hoit B, Walsh R, Marban E, Periasamy M. Targeted overexpression of the sarcoplasmic reticulum Ca^{2+}-ATPase increases cardiac contractility in transgenic mouse hearts. *Circ Res* 1998; **83:** 1205-1214.

[123] Miyamoto MI, del Monte F, Schmidt U, DiSalvo TS, Kang ZB, Matsui T, Guerrero JL, Gwathmey JK, Rosenzweig A, Hajjar RJ. Adenoviral gene transfer of SERCA2a improves left-ventricular function in aortic-banded rats in transition to heart failure. *Proc Natl Acad Sci U S A* 2000; **97:** 793-798.

[124] Loukianov E, Ji Y, Grupp IL, Kirkpatrick DL, Baker DL, Loukianova T, Grupp G, Lytton J, Walsh RA, Periasamy M. Enhanced myocardial contractility and increased Ca^{2+} transport fucntion in transgenic hearts expressing the fast-twitch skeletal msucle sarcoplasmic reticulum Ca^{2+}-ATPase. *Circ Res* 1998; **83:** 889-897.

[125] Lalli MJ, Yong J, Prasad V, Hashimoto K, Plank D, Babu GJ, Kirkpatrick D, Walsh RA, Sussman M, Yatani A, Marban E, Periasamy M. Sarcoplasmic reticulum Ca^{2+} atpase (SERCA) 1a structurally substitutes for SERCA2a in the cardiac sarcoplasmic reticulum and increases cardiac Ca^{2+} handling capacity. *Circ Res* 2001; **89:** 160-167.

[126] Hasenfuss G, Reinecke H, Studer R, Meyer M, Pieske B, Holtz J, Holubarsch C, Posival H, Just H, Drexler H. Relation between myocardial function and expression of sarcoplasmic reticulum Ca^{2+}-ATPase in failing and nonfailing human myocardium. *Circ Res* 1994; **75:** 434-442.

[127] Schmidt U, del Monte F, Miyamoto MI, Matsui T, Gwathmey JK, Rosenzweig A, Hajjar RJ. Restoration of diastolic function in senescent rat hearts through adenoviral gene transfer of sarcoplasmic reticulum Ca^{2+}-ATPase. *Circulation* 2000; **101:** 790-796.

[128] Movsesian MA, Karimi M, Green K, Jones LR. Ca^{2+}-transporting ATPase, phospholamban, and calsequestrin levels in nonfailing and failing human myocardium. *Circulation* 1994; **90:** 653-657.

[129] Linck B, Boknik P, Eschenhagen T, Muller FU, Neumann J, Nose M, Jones LR, Schmitz W, Scholz H. Messenger RNA expression and immunological quantification of phospholamban and SR-Ca^{2+}-ATPase in failing and nonfailing human hearts. *Cardiovasc Res* 1996; **31:** 625-632.

[130] Schwinger RH, Bohm M, Schmidt U, Karczewski P, Bavendiek U, Flesch M, Krause EG, Erdmann E. Unchanged protein levels of SERCA II and phospholamban but reduced Ca^{2+} uptake and Ca^{2+}-ATPase activity of cardiac sarcoplasmic reticulum from dilated cardiomyopathy patients compared with patients with nonfailing hearts. *Circulation* 1995; **92:** 3220-3228.

[131] Davia K, Davies CH, Harding SE. Effects of inhibition of sarcoplasmic reticulum calcium uptake on contraction in myocytes isolated from failing human ventricle. *Cardiovasc Res* 1997; **33:** 88-97.

[132] Mercadier JJ, Lompre AM, Duc P, Boheler KR, Fraysse JB, Wisnewsky C, Allen PD, Komajda M, Schwartz K. Altered sarcoplasmic reticulum Ca^{2+}-ATPase gene expression in the human ventricle during end-stage heart failure. *J Clin Invest* 1990; **85:** 305-309.

[133] Denvir MA, MacFarlane NG, Cobbe SM, Miller DJ. Sarcoplasmic reticulum Ca^{2+} loading in rabbits 8 and 15 weeks after coronary artery ligation. *Pflugers Arch* 1998; **436:** 436-442.

[134] del M, Harding SE, Schmidt U, Matsui T, Kang ZB, Dec GW, Gwathmey JK, Rosenzweig A, Hajjar RJ. Restoration of contractile function in isolated cardiomyocytes from failing human hearts by gene transfer of SERCA2a. *Circulation* 1999; **100:** 2308-2311.

[135] Jones LR, Besch HR, Jr., Watanabe AM. Regulation of the calcium pump of cardiac sarcoplasmic reticulum. Interactive roles of potassium and ATP on the phosphoprotein intermediate of the (K^+,Ca^{2+})-ATPase. *J Biol Chem* 1978; **253:** 1643-1653.

[136] Verboomen H, Wuytack F, De Smedt H, Himpens B, Casteels R. Functional difference between SERCA2a and SERCA2b Ca^{2+} pumps and their modulation by phospholamban. *Biochem J* 1992; **286 (Pt 2):** 591-595.

[137] Tada M, Kirchberger MA, Katz AM. Phosphorylation of a 22,000-dalton component of the cardiac sarcoplasmic reticulum by adenosine 3':5'-monophosphate-dependent protein kinase. *J Biol Chem* 1975; **250:** 2640-2647.

[138] Kirchberger MA, Antonetz T. Calmodulin-mediated regulation of calcium transport and (Ca^{2+} + Mg^{2+})-activated ATPase activity in isolated cardiac sarcoplasmic reticulum. *J Biol Chem* 1982; **257:** 5685-5691.

[139] Brittsan AG, Carr AN, Schmidt AG, Kranias EG. Maximal inhibition of SERCA2 Ca^{2+} affinity by phospholamban in transgenic hearts overexpressing a non-phosphorylatable form of phospholamban. *J Biol Chem* 2000; **275:** 12129-12135.

[140] He H, Meyer M, Martin JL, McDonough PM, Ho P, Lou X, Lew WY, Hilal-Dandan R, Dillmann WH. Effects of mutant and antisense RNA of

phospholamban on SR Ca^{2+}-ATPase activity and cardiac myocyte contractility. *Circulation* 1999; **100:** 974-980.

[141] Feldman AM, Ray PE, Silan CM, Mercer JA, Minobe W, Bristow MR. Selective gene expression in failing human heart. Quantification of steady-state levels of messenger RNA in endomyocardial biopsies using the polymerase chain reaction. *Circulation* 1991; **83:** 1866-1872.

[142] Schmidt U, Hajjar RJ, Kim CS, Lebeche D, Doye AA, Gwathmey JK. Human heart failure: cAMP stimulation of SR Ca^{2+}-ATPase activity and phosphorylation level of phospholamban. *Am J Physiol Heart Circ Physiol* 1999; **277:** H474-H480.

[143] Huang B, Wang S, Qin D, Boutjdir M, el Sherif N. Diminished basal phosphorylation level of phospholamban in the postinfarction remodeled rat ventricle: role of beta-adrenergic pathway, G(i) protein, phosphodiesterase, and phosphatases. *Circ Res* 1999; **85:** 848-855.

[144] Eizema K, Fechner H, Bezstarosti K, Schneider-Rasp S, van der LA, Wang H, Schultheiss HP, Poller WC, Lamers JM. Adenovirus-based phospholamban antisense expression as a novel approach to improve cardiac contractile dysfunction: comparison of a constitutive viral versus an endothelin-1-responsive cardiac promoter. *Circulation* 2000; **101:** 2193-2199.

[145] Hajjar RJ, Schmidt U, Matsui T, Guerrero JL, Lee KH, Gwathmey JK, Dec GW, Semigran MJ, Rosenzweig A. Modulation of ventricular function through gene transfer in vivo. *Proc Natl Acad Sci U S A* 1998; **95:** 5251-5256.

[146] Metzger JM, Wahr PA, Michele DE, Albayya F, Westfall MV. Effects of myosin heavy chain isoform switching on Ca^{2+}-activated tension development in single adult cardiac myocytes. *Circ Res* 1999; **84:** 1310-1317.

[147] Welikson RE, Buck SH, Patel JR, Moss RL, Vikstrom KL, Factor SM, Miyata S, Weinberger HD, Leinwand LA. Cardiac myosin heavy chains lacking the light chain binding domain cause hypertrophic cardiomyopathy in mice. *Am J Physiol Heart Circ Physiol* 1999; **276:** H2148-H2158.

[148] Depre C, Young ME, Ying J, Ahuja HS, Han Q, Garza N, Davies PJ, Taegtmeyer H. Streptozotocin-induced changes in cardiac gene expression in the absence of severe contractile dysfunction. *J Mol Cell Cardiol* 2000; **32:** 985-996.

[149] Tardiff JC, Hewett TE, Factor SM, Vikstrom KL, Robbins J, Leinwand LA. Expression of the beta (slow)-isoform of MHC in the adult mouse heart causes dominant-negative functional effects. *Am J Physiol Heart Circ Physiol* 2000; **278:** H412-H419.

[150] Muangmingsuk S, Ingram P, Gupta MP, Arcilla RA, Gupta M. Dexamethasone induced cardiac hypertrophy in newborn rats is accompanied by changes in

myosin heavy chain phenotype and gene transcription. *Mol Cell Biochem* 2000; **209:** 165-173.

[151] Holt JC, Caulfield JB, Norton P, Chantler PD, Slayter HS, Margossian SS. Human cardiac myosin light chains: sequence comparisons between myosin LC1 and LC2 from normal and idiopathic dilated cardiomyopathic hearts. *Mol Cell Biochem* 1995; **145:** 89-96.

[152] Liu X, Shao Q, Dhalla NS. Myosin light chain phosphorylation in cardiac hypertrophy and failure due to myocardial infarction. *J Mol Cell Cardiol* 1995; **27:** 2613-2621.

[153] Akiyama K, Akopian G, Jinadasa P, Gluckman TL, Terhakopian A, Massey B, Bing RJ. Myocardial infarction and regulatory myosin light chain. *J Mol Cell Cardiol* 1997; **29:** 2641-2652.

[154] Liu X, Takeda N, Dhalla NS. Myosin light-chain phosphorylation in diabetic cardiomyopathy in rats. *Metabolism* 1997; **46:** 71-75.

[155] Griendling KK, Murphy TJ, Alexander RW. Molecular biology of the renin-angiotensin system. *Circulation* 1993; **87:** 1816-1828.

[156] Dzau VJ, Burt DW, Pratt RE. Molecular biology of the renin-angiotensin system. *Am J Physiol Renal Physiol* 1988; **255:** F563-F573.

[157] Donoghue M, Hsieh F, Baronas E, Godbout K, Gosselin M, Stagliano N, Donovan M, Woolf B, Robison K, Jeyaseelan R, Breitbart RE, Acton S. A novel angiotensin-converting enzyme-related carboxypeptidase (ACE2) converts angiotensin I to angiotensin 1-9. *Circ Res* 2000; **87:** E1-E9.

[158] Furuta H, Guo DF, Inagami T. Molecular cloning and sequencing of the gene encoding human angiotensin II type 1 receptor. *Biochem Biophys Res Commun* 1992; **183:** 8-13.

[159] Timmermans PB, Smith RD. Angiotensin II receptor subtypes: selective antagonists and functional correlates. *Eur Heart J* 1994; **15 Suppl D:** 79-87.

[160] Sechi LA, Griffin CA, Grady EF, Kalinyak JE, Schambelan M. Characterization of angiotensin II receptor subtypes in rat heart. *Circ Res* 1992; **71:** 1482-1489.

[161] Hansen JL, Servant G, Baranski TJ, Fujita T, Iiri T, Sheikh SP. Functional reconstitution of the angiotensin II type 2 receptor and G(i) activation. *Circ Res* 2000; **87:** 753-759.

[162] Yonemochi H, Yasunaga S, Teshima Y, Iwao T, Akiyoshi K, Nakagawa M, Saikawa T, Ito M. Mechanism of beta-adrenergic receptor upregulation induced by ACE inhibition in cultured neonatal rat cardiac myocytes: roles of bradykinin and protein kinase C. *Circulation* 1998; **97:** 2268-2273.

[163] Malendowicz SL, Ennezat PV, Testa M, Murray L, Sonnenblick EH, Evans T, LeJemtel TH. Angiotensin II receptor subtypes in the skeletal muscle vasculature of patients with severe congestive heart failure. *Circulation* 2000; **102:** 2210-2213.

[164] Anthonio RL, van Veldhuisen DJ, van Gilst WH. Left ventricular dilatation after myocardial infarction: ACE inhibitors, beta-blockers, or both? *J Cardiovasc Pharmacol* 1998; **32 Suppl 1:** S1-S8.

[165] Yamada H, Fabris B, Allen AM, Jackson B, Johnston CI, Mendelsohn AO. Localization of angiotensin converting enzyme in rat heart. *Circ Res* 1991; **68:** 141-149.

[166] Urata H, Kinoshita A, Misono KS, Bumpus FM, Husain A. Identification of a highly specific chymase as the major angiotensin II-forming enzyme in the human heart. *J Biol Chem* 1990; **265:** 22348-22357.

[167] Urata H, Boehm KD, Philip A, Kinoshita A, Gabrovsek J, Bumpus FM, Husain A. Cellular localization and regional distribution of an angiotensin II-forming chymase in the heart. *J Clin Invest* 1993; **91:** 1269-1281.

[168] Wolkowicz PE, Urthaler F, Forrest C, Shen H, Durand J, Wei CC, Oparil S, Dell'Italia LJ. 2-Tetradecylglycidic acid, an inhibitor of carnitine palmitoyltransferase-1, induces myocardial hypertrophy via the AT1 receptor. *J Mol Cell Cardiol* 1999; **31:** 1405-1412.

[169] Morgan JP, Perreault CL, Morgan KG. The cellular basis of contraction and relaxation in cardiac and vascular smooth muscle. *Am Heart J* 1991; **121:** 961-968.

[170] Shao, Q, Panagia, V., Beamish, R. E., and Dhalla, N. S. Role of renin-angiotensin system in cardiac hypertrophy and failure. In: *Angiotensin II Receptor blockade: Physiological and clinical Implications,* 1st ed. Dhalla, N. S., Zahradka, P, Dixon, I. M., and Beamish, R. E. (ed). Boston: Kluwer Academic Publishers, 1998 pp. 283-310.

[171] Shao Q, Saward L, Zahradka P, Dhalla NS. Ca^{2}+ mobilization in adult rat cardiomyocytes by angiotensin type 1 and 2 receptors. *Biochem Pharmacol* 1998; **55:** 1413-1418.

[172] Bartunek J, Weinberg EO, Tajima M, Rohrbach S, Lorell BH. Angiotensin II type 2 receptor blockade amplifies the early signals of cardiac growth response to angiotensin II in hypertrophied hearts. *Circulation* 1999; **99:** 22-25.

[173] Sadoshima J, Xu Y, Slayter HS, Izumo S. Autocrine release of angiotensin II mediates stretch-induced hypertrophy of cardiac myocytes in vitro. *Cell* 1993; **75:** 977-984.

[174] Sigurdsson A, Held P, Swedberg K. S. *Am Heart J* 1993; **126:** 1068-1076.

[175] Wollert KC, Drexler H. The renin-angiotensin system and experimental heart failure. *Cardiovasc Res* 1999; **43:** 838-849.

[176] Reid IA, Morris BJ, Ganong WF. The renin-angiotensin system. *Annu Rev Physiol* 1978; **40:** 377-410.

[177] von Lutterotti N, Catanzaro DF, Sealey JE, Laragh JH. Renin is not synthesized by cardiac and extrarenal vascular tissues. A review of experimental evidence. *Circulation* 1994; **89:** 458-470.

[178] van Kats JP, Danser AH, van Meegen JR, Sassen LM, Verdouw PD, Schalekamp MA. Angiotensin production by the heart: a quantitative study in pigs with the use of radiolabeled angiotensin infusions. *Circulation* 1998; **98:** 73-81.

[179] Dell'Italia LJ, Meng QC, Balcells E, Wei CC, Palmer R, Hageman GR, Durand J, Hankes GH, Oparil S. Compartmentalization of angiotensin II generation in the dog heart. Evidence for independent mechanisms in intravascular and interstitial spaces. *J Clin Invest* 1997; **100:** 253-258.

[180] Leenen FH, Skarda V, Yuan B, White R. Changes in cardiac ANG II postmyocardial infarction in rats: effects of nephrectomy and ACE inhibitors. *Am J Physiol Heart Circ Physiol* 1999; **276:** H317-H325.

[181] Hokimoto S, Yasue H, Fujimoto K, Sakata R, Miyamoto E. Increased angiotensin converting enzyme activity in left ventricular aneurysm of patients after myocardial infarction. *Cardiovasc Res* 1995; **29:** 664-669.

[182] van Kats JP, Duncker DJ, Haitsma DB, Schuijt MP, Niebuur R, Stubenitsky R, Boomsma F, Schalekamp MA, Verdouw PD, Danser AH. Angiotensin-converting enzyme inhibition and angiotensin II type 1 receptor blockade prevent cardiac remodeling in pigs after myocardial infarction: role of tissue angiotensin II. *Circulation* 2000; **102:** 1556-1563.

[183] Francis GS, McDonald KM, Cohn JN. Neurohumoral activation in preclinical heart failure. Remodeling and the potential for intervention. *Circulation* 1993; **87:** IV90-IV96.

[184] Kohzuki M, Kanazawa M, Yoshida K, Kamimoto M, Wu XM, Jiang ZL, Yasujima M, Abe K, Johnston CI, Sato T. Cardiac angiotensin converting enzyme and endothelin receptor in rats with chronic myocardial infarction. *Jpn Circ J* 1996; **60:** 972-980.

[185] Schunkert H, Jackson B, Tang SS, Schoen FJ, Smits JF, Apstein CS, Lorell BH. Distribution and functional significance of cardiac angiotensin converting enzyme in hypertrophied rat hearts. *Circulation* 1993; **87:** 1328-1339.

[186] Duncan AM, Burrell LM, Kladis A, Campbell DJ. Angiotensin and bradykinin peptides in rats with myocardial infarction. *J Card Fail* 1997; **3:** 41-52.

[187] Nio Y, Matsubara H, Murasawa S, Kanasaki M, Inada M. Regulation of gene transcription of angiotensin II receptor subtypes in myocardial infarction. *J Clin Invest* 1995; **95:** 46-54.

[188] Meggs LG, Coupet J, Huang H, Cheng W, Li P, Capasso JM, Homcy CJ, Anversa P. Regulation of angiotensin II receptors on ventricular myocytes after myocardial infarction in rats. *Circ Res* 1993; **72:** 1149-1162.

[189] Zhu YC, Zhu YZ, Gohlke P, Stauss HM, Unger T. Effects of angiotensin-converting enzyme inhibition and angiotensin II AT1 receptor antagonism on cardiac parameters in left ventricular hypertrophy. *Am J Cardiol* 1997; **80:** 110A-117A.

[190] Nelson KM, Yeager BF. What is the role of angiotensin-converting enzyme inhibitors in congestive heart failure and after myocardial infarction? *Ann Pharmacother* 1996; **30:** 986-993.

[191] The SOLVD Investigattors. Effect of enalapril on mortality and the development of heart failure in asymptomatic patients with reduced left ventricular ejection fractions. *N Engl J Med* 1992; **327:** 685-691.

[192] The CONSENSUS Trial Study Group. Effects of enalapril on mortality in severe congestive heart failure. Results of the Cooperative North Scandinavian Enalapril Survival Study (CONSENSUS). *N Engl J Med* 1987; **316:** 1429-1435.

[193] Cohn JN, Johnson G, Ziesche S, Cobb F, Francis G, Tristani F, Smith R, Dunkman WB, Loeb H, Wong M, . A comparison of enalapril with hydralazine-isosorbide dinitrate in the treatment of chronic congestive heart failure. *N Engl J Med* 1991; **325:** 303-310.

[194] The SOLVD Investigators. Effect of enalapril on survival in patients with reduced left ventricular ejection fractions and congestive heart failure. *N Engl J Med* 1991; **325:** 293-302.

[195] Cody RJ. ACE inhibitors: myocardial infarction and congestive heart failure. *Am Fam Physician* 1995; **52:** 1801-1806.

[196] Sanbe A, Tanonaka K, Kobayasi R, Takeo S. Effects of long-term therapy with ACE inhibitors, captopril, enalapril and trandolapril, on myocardial energy metabolism in rats with heart failure following myocardial infarction. *J Mol Cell Cardiol* 1995; **27:** 2209-2222.

[197] Mulder P, Devaux B, Richard V, Henry JP, Wimart MC, Thibout E, Mace B, Thuillez C. Early versus delayed angiotensin-converting enzyme inhibition in experimental chronic heart failure. Effects on survival, hemodynamics, and cardiovascular remodeling. *Circulation* 1997; **95:** 1314-1319.

[198] Taylor K, Patten RD, Smith JJ, Aronovitz MJ, Wight J, Salomon RN, Konstam MA. Divergent effects of angiotensin-converting enzyme inhibition and angiotensin II-receptor antagonism on myocardial cellular proliferation and collagen deposition after myocardial infarction in rats. *J Cardiovasc Pharmacol* 1998; **31:** 654-660.

[199] Raya TE, Fonken SJ, Lee RW, Daugherty S, Goldman S, Wong PC, Timmermans PB, Morkin E. Hemodynamic effects of direct angiotensin II blockade compared to converting enzyme inhibition in rat model of heart failure. *Am J Hypertens* 1991; **4:** 334S-340S.

[200] Nabel EG, Topol EJ, Galeana A, Ellis SG, Bàtes ER, Werns SW, Walton JA, Muller DW, Schwaiger M, Pitt B. A randomized placebo-controlled trial of combined early intravenous captopril and recombinant tissue-type plasminogen activator therapy in acute myocardial infarction. *J Am Coll Cardiol* 1991; **17:** 467-473.

[201] Oldroyd KG, Pye MP, Ray SG, Christie J, Ford I, Cobbe SM, Dargie HJ. Effects of early captopril administration on infarct expansion, left ventricular remodeling and exercise capacity after acute myocardial infarction. *Am J Cardiol* 1991; **68:** 713-718.

[202] Pinto YM, van Wijngaarden J, van Gilst WH, de Graeff PA, Wesseling H. The effects of short- and long- term treatment with an ACE-inhibitor in rats with myocardial infarction. *Basic Res Cardiol* 1991; **86 Suppl 1:** 165-172.

[203] Swedberg K, Held P, Kjekshus J, Rasmussen K, Ryden L, Wedel H. Effects of the early administration of enalapril on mortality in patients with acute myocardial infarction. Results of the Cooperative New Scandinavian Enalapril Survival Study II (CONSENSUS II). *N Engl J Med* 1992; **327:** 678-684.

[204] Coirault C, Langeron O, Lambert F, Blanc FX, Lerebours G, Claude N, Riou B, Chemla D, Lecarpentier Y. Impaired skeletal muscle performance in the early stage of cardiac pressure overload in rabbits: beneficial effects of angiotensin-converting enzyme inhibition. *J Pharmacol Exp Ther* 1999; **291:** 70-75.

[205] Dominiak P, Blochl A. Does converting enzyme inhibition change the neuronal and extraneuronal uptake of catecholamines? *Basic Res Cardiol* 1991; **86 Suppl 3:** 149-156.

[206] Spinale FG, de Gasparo M, Whitebread S, Hebbar L, Clair MJ, Melton DM, Krombach RS, Mukherjee R, Iannini JP, SJ O. Modulation of the renin-angiotensin pathway through enzyme inhibition and specific receptor blockade in pacing-induced heart failure: I. Effects on left ventricular performance and neurohormonal systems. *Circulation* 1997; **96:** 2385-2396.

[207] van den Heuvel AF, van Gilst WH, van Veldhuisen DJ, de Vries RJ, Dunselman PH, Kingma JH. Long-term anti-ischemic effects of angiotensin-converting

enzyme inhibition in patients after myocardial infarction. The Captopril and Thrombolysis Study (CATS) Investigators. *J Am Coll Cardiol* 1997; **30:** 400-405.

[208] Westlin W, Mullane K. Does captopril attenuate reperfusion-induced myocardial dysfunction by scavenging free radicals? *Circulation* 1988; **77:** I30-I39.

[209] Pfeffer MA, Pfeffer JM, Steinberg C, Finn P. Survival after an experimental myocardial infarction: beneficial effects of long-term therapy with captopril. *Circulation* 1985; **72:** 406-412.

[210] Pfeffer MA, Braunwald E, Moye LA, Basta L, Brown EJ, Jr., Cuddy TE, Davis BR, Geltman EM, Goldman S, Flaker GC, . Effect of captopril on mortality and morbidity in patients with left ventricular dysfunction after myocardial infarction. Results of the survival and ventricular enlargement trial. The SAVE Investigators. *N Engl J Med* 1992; **327:** 669-677.

[211] ISIS-4 (Fourth International Study of Infarct Survival) Collaborative Group. ISIS-4: a randomised factorial trial assessing early oral captopril, oral mononitrate, and intravenous magnesium sulphate in 58,050 patients with suspected acute myocardial infarction. *Lancet* 1995; **345:** 669-685.

[212] van Gilst WH, Kingma JH, Peels KH, Dambrink JH, St John SM. Which patient benefits from early angiotensin-converting enzyme inhibition after myocardial infarction? Results of one-year serial echocardiographic follow-up from the Captopril and Thrombolysis Study (CATS). *J Am Coll Cardiol* 1996; **28:** 114-121.

[213] Borghi C, Marino P, Zardini P, Magnani B, Collatina S, Ambrosioni E. Post acute myocardial infarction: the Fosinopril in Acute Myocardial Infarction Study (FAMIS). *Am J Hypertens* 1997; **10:** 247S-254S.

[214] Gruppo Italiano per lo Studio della Sopravvivenza nell'Infarto Miocardico. Six-month effects of early treatment with lisinopril and transdermal glyceryl trinitrate singly and together withdrawn six weeks after acute myocardial infarction: the GISSI-3 trial. *J Am Coll Cardiol* 1996; **27:** 337-344.

[215] The Acute Infarction Ramipril Efficacy (AIRE) Study Investigators. Effect of ramipril on mortality and morbidity of survivors of acute myocardial infarction with clinical evidence of heart failure. *Lancet* 1993; **342:** 821-828.

[216] Yusuf S, Sleight P, Pogue J, Bosch J, Davies R, Dagenais G. Effects of an angiotensin-converting-enzyme inhibitor, ramipril, on cardiovascular events in high-risk patients. The Heart Outcomes Prevention Evaluation Study Investigators. *N Engl J Med* 2000; **342:** 145-153.

[217] Kober L, Torp-Pedersen C, Carlsen JE, Bagger H, Eliasen P, Lyngborg K, Videbaek J, Cole DS, Auclert L, Pauly NC. A clinical trial of the angiotensin-converting-enzyme inhibitor trandolapril in patients with left ventricular

dysfunction after myocardial infarction. Trandolapril Cardiac Evaluation (TRACE) Study Group. *N Engl J Med* 1995; **333:** 1670-1676.

[218] Ambrosioni E, Borghi C, Magnani B. The effect of the angiotensin-converting-enzyme inhibitor zofenopril on mortality and morbidity after anterior myocardial infarction. The Survival of Myocardial Infarction Long-Term Evaluation (SMILE) Study Investigators. *N Engl J Med* 1995; **332:** 80-85.

[219] Schoemaker RG, Debets JJ, Struyker-Boudier HA, Smits JF. Delayed but not immediate captopril therapy improves cardiac function in conscious rats, following myocardial infarction. *J Mol Cell Cardiol* 1991; **23:** 187-197.

[220] Milavetz JJ, Raya TE, Johnson CS, Morkin E, Goldman S. Survival after myocardial infarction in rats: captopril versus losartan. *J Am Coll Cardiol* 1996; **27:** 714-719.

[221] Jain P, Korlipara G, Mallavarapu C, Sikand V, Lillis O, Cohn PF. Effects of captopril therapy after late reperfusion on left ventricular remodeling after experimental myocardial infarction. *Am Heart J* 1994; **127:** 756-763.

[222] McDonald KM, Chu C, Francis GS, Carlyle W, Judd DL, Hauer K, Hartman M, Cohn JN. Effect of delayed intervention with ACE-inhibitor therapy on myocyte hypertrophy and growth of the cardiac interstitium in the rat model of myocardial infarction. *J Mol Cell Cardiol* 1997; **29:** 3203-3210.

[223] Hugel S, Horn M, de Groot M, Remkes H, Dienesch C, Hu K, Ertl G, Neubauer S. Effects of ACE inhibition and beta-receptor blockade on energy metabolism in rats postmyocardial infarction. *Am J Physiol Heart Circ Physiol* 1999; **277:** H2167-H2175.

[224] Alhaddad IA, Sahgal P, Mir R, Brown EJ, Jr. Early angiotensin converting enzyme inhibitor therapy enhances the benefits of late coronary artery reperfusion on infarct expansion. *Coron Artery Dis* 2000; **11:** 183-189.

[225] Waltman TJ, Harris TJ, Cesario D, Ziegler M, Maisel AS. Effects of enalapril on T and B cell function in rats after myocardial infarction. *J Card Fail* 1995; **1:** 293-302.

[226] Youn TJ, Kim HS, Oh BH. Ventricular remodeling and transforming growth factor-beta 1 mRNA expression after nontransmural myocardial infarction in rats: effects of angiotensin converting enzyme inhibition and angiotensin II type 1 receptor blockade. *Basic Res Cardiol* 1999; **94:** 246-253.

[227] Milanez MC, Gomes MG, Vassallo DV, Mill JG. Effects of captopril on interstitial collagen in the myocardium after infarction in rats. *J Card Fail* 1997; **3:** 189-197.

[228] Ali SM, Brown EJ, Jr., Nallapati SR, Alhaddad IA. Early angiotensin converting enzyme inhibitor therapy after experimental myocardial infarction prevents left ventricular dilation by reducing infarct expansion: a possible mechanism of clinical benefits. *Coron Artery Dis* 1998; **9:** 815-821.

[229] Wagner KD, Theres H, Born A, Strube S, Wunderlich N, Pfitzer G, Baumann G, Gunther J. Contractile function of papillary muscle from rats with different infarct size after beta-adrenergic blockade and ACE-inhibition. *J Mol Cell Cardiol* 1997; **29:** 2941-2951.

[230] Tappia PS, Liu SY, Shatadal S, Takeda N, Dhalla NS, Panagia V. Changes in sarcolemmal PLC isoenzymes in postinfarct congestive heart failure: partial correction by imidapril. *Am J Physiol Heart Circ Physiol* 1999; **277:** H40-H49.

[231] Hu K, Gaudron P, Anders HJ, Weidemann F, Turschner O, Nahrendorf M, Ertl G. Chronic effects of early started angiotensin converting enzyme inhibition and angiotensin AT1-receptor subtype blockade in rats with myocardial infarction: role of bradykinin. *Cardiovasc Res* 1998; **39:** 401-412.

[232] Cody RJ. Comparing angiotensin-converting enzyme inhibitor trial results in patients with acute myocardial infarction. *Arch Intern Med* 1994; **154:** 2029-2036.

[233] ISIS-4 collaborative group. Fourth International Study of Infarct Survival: protocol for a large simple study of the effects of oral mononitrate, of oral captopril, and of intravenous magnesium. *Am J Cardiol* 1991; **68:** 87D-100D.

[234] Shao Q, Takeda N, Temsah N, Dhalla KS, Dhalla NS. Prevention of hemodynamic changes due to myocardial infarction by early treatment with imidapril. *Cardiovasc Pathobiol* 1996; **1:** 180-186.

[235] Ren B, Lukas A, Shao Q, Guo M, Takeda N, Aitken RM, Dhalla NS. Electrocardiographic Changes and Mortality Due to Myocardial Infarction in Rats With or Without Imidapril Treatment. *J Cardiovasc Pharmacol Ther* 1998; **3:** 11-22.

[236] Pitt B. Importance of angiotensin-converting enzyme inhibitors in myocardial infarction and congestive heart failure: implications for clinical practice. *Cardiology* 1995; **86 Suppl 1:** 41-45.

[237] Chiu AT, McCall DE, Price WA, Wong PC, Carini DJ, Duncia JV, Wexler RR, Yoo SE, Johnson AL, Timmermans PB. Nonpeptide angiotensin II receptor antagonists. VII. Cellular and biochemical pharmacology of DuP 753, an orally active antihypertensive agent. *J Pharmacol Exp Ther* 1990; **252:** 711-718.

[238] Siragy H. Angiotensin II receptor blockers: review of the binding characteristics. *Am J Cardiol* 1999; **84:** 3S-8S.

[239] Sweet CS, Rucinska EJ. Losartan in heart failure: preclinical experiences and initial clinical outcomes. *Eur Heart J* 1994; **15 Suppl D:** 139-144.

[240] Smits JF, van Krimpen C, Schoemaker RG, Cleutjens JP, Daemen MJ. Angiotensin II receptor blockade after myocardial infarction in rats: effects on hemodynamics, myocardial DNA synthesis, and interstitial collagen content. *J Cardiovasc Pharmacol* 1992; **20:** 772-778.

[241] Regitz-Zagrosek V, Neuss M, Fleck E. Effects of angiotensin receptor antagonists in heart failure: clinical and experimental aspects. *Eur Heart J* 1995; **16 Suppl N:** 86-91.

[242] Hamroff G, Katz SD, Mancini D, Blaufarb I, Bijou R, Patel R, Jondeau G, Olivari MT, Thomas S, Le Jemtel TH. Addition of angiotensin II receptor blockade to maximal angiotensin-converting enzyme inhibition improves exercise capacity in patients with severe congestive heart failure. *Circulation* 1999; **99:** 990-992.

[243] Dickstein K, Kjekshus J. Effects of losartan and captopril on mortality and morbidity in high-risk patients after acute myocardial infarction: the OPTIMAAL randomised trial. Optimal Trial in Myocardial Infarction with Angiotensin II Antagonist Losartan. *Lancet* 2002; **360:** 752-760.

[244] Pitt B, Segal R, Martinez FA, Meurers G, Cowley AJ, Thomas I, Deedwania PC, Ney DE, Snavely DB, Chang PI. Randomised trial of losartan versus captopril in patients over 65 with heart failure (Evaluation of Losartan in the Elderly Study, ELITE). *Lancet* 1997; **349:** 747-752.

[245] Dickstein K, Chang P, Willenheimer R, Haunso S, Remes J, Hall C, Kjekshus J. Comparison of the effects of losartan and enalapril on clinical status and exercise performance in patients with moderate or severe chronic heart failure. *J Am Coll Cardiol* 1995; **26:** 438-445.

[246] Warner JG, Jr., Metzger DC, Kitzman DW, Wesley DJ, Little WC. Losartan improves exercise tolerance in patients with diastolic dysfunction and a hypertensive response to exercise. *J Am Coll Cardiol* 1999; **33:** 1567-1572.

[247] Tsutamoto T, Wada A, Maeda K, Mabuchi N, Hayashi M, Tsutsui T, Ohnishi M, Sawaki M, Fujii M, Matsumoto T, Kinoshita M. Angiotensin II type 1 receptor antagonist decreases plasma levels of tumor necrosis factor alpha, interleukin-6 and soluble adhesion molecules in patients with chronic heart failure. *J Am Coll Cardiol* 2000; **35:** 714-721.

[248] Mitrovic V, Willenbrock R, Miric M, Seferovic P, Spinar J, Dabrowski M, Kiowski W, Marks DS, Alegria E, Dukat A, Lenz K, Arens HA. Acute and 3-month treatment effects of candesartan cilexetil on hemodynamics, neurohormones, and clinical symptoms in patients with congestive heart failure. *Am Heart J* 2003; **145:** E14.

[249] Murdoch DR, McDonagh TA, Farmer R, Morton JJ, McMurray JJ, Dargie HJ. ADEPT: Addition of the AT1 receptor antagonist eprosartan to ACE inhibitor therapy in chronic heart failure trial: hemodynamic and neurohormonal effects. *Am Heart J* 2001; **141:** 800-807.

[250] Jain M, Liao R, Ngoy S, Whittaker P, Apstein CS, Eberli FR. Angiotensin II receptor blockade attenuates the deleterious effects of exercise training on post-MI ventricular remodelling in rats. *Cardiovasc Res* 2000; **46:** 66-72.

[251] Hao J, Wang B, Jones SC, Jassal DS, Dixon IM. Interaction between angiotensin II and Smad proteins in fibroblasts in failing heart and in vitro. *Am J Physiol Heart Circ Physiol* 2000; **279:** H3020-H3030.

[252] Ambrose J, Pribnow DG, Giraud GD, Perkins KD, Muldoon L, Greenberg BH. Angiotensin type 1 receptor antagonism with irbesartan inhibits ventricular hypertrophy and improves diastolic function in the remodeling post-myocardial infarction ventricle. *J Cardiovasc Pharmacol* 1999; **33:** 433-439.

[253] Spinale FG, Mukherjee R, Iannini JP, Whitebread S, Hebbar L, Clair MJ, Melton DM, Cox MH, Thomas PB, de Gasparo M. Modulation of the renin-angiotensin pathway through enzyme inhibition and specific receptor blockade in pacing-induced heart failure: II. Effects on myocyte contractile processes. *Circulation* 1997; **96:** 2397-2406.

[254] Sudhir K, MacGregor JS, Gupta M, Barbant SD, Redberg R, Yock PG, Chatterjee K. Effect of selective angiotensin II receptor antagonism and angiotensin converting enzyme inhibition on the coronary vasculature in vivo. Intravascular two-dimensional and Doppler ultrasound studies. *Circulation* 1993; **87:** 931-938.

[255] Meffert S, Stoll M, Steckelings UM, Bottari SP, Unger T. The angiotensin II AT2 receptor inhibits proliferation and promotes differentiation in PC12W cells. *Mol Cell Endocrinol* 1996; **122:** 59-67.

[256] Stoll M, Steckelings UM, Paul M, Bottari SP, Metzger R, Unger T. The angiotensin AT2-receptor mediates inhibition of cell proliferation in coronary endothelial cells. *J Clin Invest* 1995; **95:** 651-657.

[257] Siragy HM, Carey RM. The subtype-2 (AT2) angiotensin receptor regulates renal cyclic guanosine 3', 5'-monophosphate and AT1 receptor-mediated prostaglandin E2 production in conscious rats. *J Clin Invest* 1996; **97:** 1978-1982.

[258] Dickstein K, Kjekshus J. Comparison of the effects of losartan and captopril on mortality in patients after acute myocardial infarction: the OPTIMAAL trial design. Optimal Therapy in Myocardial Infarction with the Angiotensin II Antagonist Losartan. *Am J Cardiol* 1999; **83:** 477-481.

[259] Unger T. Neurohormonal modulation in cardiovascular disease. *Am Heart J* 2000; **139:** S2-S8.

[260] Kim S, Yoshiyama M, Izumi Y, Kawano H, Kimoto M, Zhan Y, Iwao H. Effects of combination of ACE inhibitor and angiotensin receptor blocker on cardiac remodeling, cardiac function, and survival in rat heart failure. *Circulation* 2001; **103:** 148-154.

[261] Afzal N, Dhalla NS. Differential changes in left and right ventricular SR calcium transport in congestive heart failure. *Am J Physiol Heart Circ Physiol* 1992; **262:** H868-H874.

[262] Geenen DL, Malhotra A, Scheuer J. Regional variation in rat cardiac myosin isoenzymes and ATPase activity after infarction. *Am J Physiol Heart Circ Physiol* 1989; **256:** H745-H750.

[263] Dhalla, N. S., Shao, Q, and Panagia, V. Remodeling of cardiac membranes during the development of congetive heart failure. In: *Heart Failure Reviews,* 2 ed. Boston: Kluwer Academic Publishers, 1998 pp. 261-272.

[264] Dixon IM, Ju H, Jassal DS, Peterson DJ. Effect of ramipril and losartan on collagen expression in right and left heart after myocardial infarction. *Mol Cell Biochem* 1996; **165:** 31-45.

[265] Sharma SK, Chapman D, Temsah R, Netticadan T, Brasil DP, Dhalla NS. Prevention of Vascular Apoptosis in Myocardial Infarction by Losartan. *J Cardiovasc Pharmacol Ther* 1999; **4:** 77-84.

[266] Sakai T, Li RK, Weisel RD, Mickle DA, Kim EJ, Tomita S, Jia ZQ, Yau TM. Autologous heart cell transplantation improves cardiac function after myocardial injury. *Ann Thorac Surg* 1999; **68:** 2074-2080.

[267] Li RK, Jia ZQ, Weisel RD, Merante F, Mickle DA. Smooth muscle cell transplantation into myocardial scar tissue improves heart function. *J Mol Cell Cardiol* 1999; **31:** 513-522.

[268] Li RK, Mickle DA, Weisel RD, Mohabeer MK, Zhang J, Rao V, Li G, Merante F, Jia ZQ. Natural history of fetal rat cardiomyocytes transplanted into adult rat myocardial scar tissue. *Circulation* 1997; **96:** II-179-II-187.

[269] Swynghedauw B. Molecular mechanisms of myocardial remodeling. *Physiol Rev* 1999; **79:** 215-262.

[270] Dhalla NS, Ziegelhoffer A, Harrow JA. Regulatory role of membrane systems in heart function. *Can J Physiol Pharmacol* 1977; **55:** 1211-1234.

[271] Urayama O, Shutt H, Sweadner KJ. Identification of three isozyme proteins of the catalytic subunit of the Na,K-ATPase in rat brain. *J Biol Chem* 1989; **264:** 8271-8280.

[272] Charlemagne D, Orlowski J, Oliviero P, Rannou F, Sainte BC, Swynghedauw B, Lane LK. Alteration of Na,K-ATPase subunit mRNA and protein levels in hypertrophied rat heart. *J Biol Chem* 1994; **269:** 1541-1547.

[273] Elmoselhi AB, Lukas A, Ostadal P, Dhalla NS. Preconditioning attenuates ischemia-reperfusion-induced remodeling of Na^+-K^+-ATPase in hearts. *Am J Physiol Heart Circ Physiol* 2003; **285:** H1055-H1063.

[274] Shamraj OI, Grupp IL, Grupp G, Melvin D, Gradoux N, Kremers W, Lingrel JB, De Pover A. Characterisation of Na/K-ATPase, its isoforms, and the inotropic response to ouabain in isolated failing human hearts. *Cardiovasc Res* 1993; **27:** 2229-2237.

[275] Pfeffer JM, Pfeffer MA, Braunwald E. Hemodynamic benefits and prolonged survival with long-term captopril therapy in rats with myocardial infarction and heart failure. *Circulation* 1987; **75:** I149-I155.

[276] Khaper N, Singal PK. Modulation of oxidative stress by a selective inhibition of angiotensin II type 1 receptors in MI rats. *J Am Coll Cardiol* 2001; **37:** 1461-1466.

[277] Sethi R, Dhalla KS, Beamish RE, Dhalla NS. Differential changes in left and right ventricular adenylyl cyclase activities in congestive heart failure. *Am J Physiol Heart Circ Physiol* 1997; **272:** H884-H893.

[278] Sharpe N. Ventricular remodeling following myocardial infarction. *Am J Cardiol* 1992; **70:** 20C-26C.

[279] Wagner, G. Myocardial infarction. In: *Marriott's practical electrocardiography,* 9th ed. Pine, J. (ed). Baltimore: Williams & Wilkins, 1994 pp. 154-171.

[280] Wagner GS, Freye CJ, Palmeri ST, Roark SF, Stack NC, Ideker RE, Harrell FE, Jr., Selvester RH. Evaluation of a QRS scoring system for estimating myocardial infarct size. I. Specificity and observer agreement. *Circulation* 1982; **65:** 342-347.

[281] Hindman NB, Schocken DD, Widmann M, Anderson WD, White RD, Leggett S, Ideker RE, Hinohara T, Selvester RH, Wagner GS. Evaluation of a QRS scoring system for estimating myocardial infarct size. V. Specificity and method of application of the complete system. *Am J Cardiol* 1985; **55:** 1485-1490.

[282] Dellborg M, Herlitz J, Risenfors M, Swedberg K. Electrocardiographic assessment of infarct size: comparison between QRS scoring of 12-lead electrocardiography and dynamic vectorcardiography. *Int J Cardiol* 1993; **40:** 167-172.

[283] Pitts BJ. Stoichiometry of sodium-calcium exchange in cardiac sarcolemmal vesicles. Coupling to the sodium pump. *J Biol Chem* 1979; **254:** 6232-6235.

[284] TAUSSKY HH, SHORR E. A microcolorimetric method for the determination of inorganic phosphorus. *J Biol Chem* 1953; **202:** 675-685.

[285] Chomczynski P, Sacchi N. Single-step method of RNA isolation by acid guanidinium thiocyanate-phenol-chloroform extraction. *Anal Biochem* 1987; **162:** 156-159.

[286] Tso JY, Sun XH, Kao TH, Reece KS, Wu R. Isolation and characterization of rat and human glyceraldehyde-3-phosphate dehydrogenase cDNAs: genomic complexity and molecular evolution of the gene. *Nucleic Acids Res* 1985; **13:** 2485-2502.

[287] Asemu G, Tappia PS, Dhalla NS. Identification of the changes in phospholipase C isozymes in ischemic-reperfused rat heart. *Arch Biochem Biophys* 2003; **411:** 174-182.

[288] Mamic TM, Holman NA, Roberts-Thomson SJ, Monteith GR. PMCA1 mRNA expression in rat aortic myocytes: a real-time RT-PCR study. *Biochem Biophys Res Commun* 2000; **276:** 1024-1027.

[289] Stauffer TP, Guerini D, Celio MR, Carafoli E. Immunolocalization of the plasma membrane Ca2+ pump isoforms in the rat brain. *Brain Res* 1997; **748:** 21-29.

[290] Chin S, He H, Gick G. Selective induction of Na,K-ATPase alpha3 subunit mRNA abundance in cardiac myocytes by retinoic acid. *J Mol Cell Cardiol* 1998; **30:** 2403-2410.

[291] Xie Z, Kometiani P, Liu J, Li J, Shapiro JI, Askari A. Intracellular reactive oxygen species mediate the linkage of Na^+/K^+-ATPase to hypertrophy and its marker genes in cardiac myocytes. *J Biol Chem* 1999; **274:** 19323-19328.

[292] Huang L, Kometiani P, Xie Z. Differential regulation of Na/K-ATPase alpha-subunit isoform gene expressions in cardiac myocytes by ouabain and other hypertrophic stimuli. *J Mol Cell Cardiol* 1997; **29:** 3157-3167.

[293] Arystarkhova E, Sweadner KJ. Isoform-specific monoclonal antibodies to Na,K-ATPase alpha subunits. Evidence for a tissue-specific post-translational modification of the alpha subunit. *J Biol Chem* 1996; **271:** 23407-23417.

[294] Lucchesi PA, Sweadner KJ. Postnatal changes in Na,K-ATPase isoform expression in rat cardiac ventricle. Conservation of biphasic ouabain affinity. *J Biol Chem* 1991; **266:** 9327-9331.

[295] Wang J, Velotta JB, McDonough AA, Farley RA. All human Na^+-K^+-ATPase alpha-subunit isoforms have a similar affinity for cardiac glycosides. *Am J Physiol Cell Physiol* 2001; **281:** C1336-C1343.

[296] Watanabe M, Kawaguchi H, Onozuka H, Mikami T, Urasawa K, Okamoto H, Watanabe S, Abe K, Kitabatake A. Chronic effects of enalapril and amlodipine on cardiac remodeling in cardiomyopathic hamster hearts. *J Cardiovasc Pharmacol* 1998; **32:** 248-259.

[297] Linz W, Scholkens BA. A specific B2-bradykinin receptor antagonist HOE 140 abolishes the antihypertrophic effect of ramipril. *Br J Pharmacol* 1992; **105:** 771-772.

[298] Gohlke P, Linz W, Scholkens BA, Kuwer I, Bartenbach S, Schnell A, Unger T. Angiotensin-converting enzyme inhibition improves cardiac function. Role of bradykinin. *Hypertension* 1994; **23:** 411-418.

[299] Wang J, Guo X, Dhalla NS. Modification of myosin protein and gene expression in failing hearts due to myocardial infarction by enalapril or losartan. *Biochim Biophys Acta* 2004 (in press);

[300] Pieske B, Maier LS, Bers DM, Hasenfuss G. Ca^{2+} handling and sarcoplasmic reticulum Ca^{2+} content in isolated failing and nonfailing human myocardium. *Circ Res* 1999; **85:** 38-46.

[301] Wu Y, Roden DM, Anderson ME. Calmodulin kinase inhibition prevents development of the arrhythmogenic transient inward current. *Circ Res* 1999; **84:** 906-912.

[302] Carafoli E. The plasma membrane calcium pump. Structure, function, regulation. *Biochim Biophys Acta* 1992; **1101:** 266-267.

[303] Suju M, Davila M, Poleo G, Docampo R, Benaim G. Phosphatidylethanol stimulates the plasma-membrane calcium pump from human erythrocytes. *Biochem J* 1996; **317 (Pt 3):** 933-938.

[304] Takahashi T, Allen PD, Lacro RV, Marks AR, Dennis AR, Schoen FJ, Grossman W, Marsh JD, Izumo S. Expression of dihydropyridine receptor (Ca^{2+} channel) and calsequestrin genes in the myocardium of patients with end-stage heart failure. *J Clin Invest* 1992; **90:** 927-935.

[305] Kumar R, Hood WB, Jr., Abelmann WH. Hemodynamic spectrum of left ventricular failure in experimental myocardial infarction. *Am Heart J* 1971; **82:** 713-714.

[306] Liu YH, Yang XP, Nass O, Sabbah HN, Peterson E, Carretero OA. Chronic heart failure induced by coronary artery ligation in Lewis inbred rats. *Am J Physiol Heart Circ Physiol* 1997; **272:** H722-H727.

[307] Lutgens E, Daemen MJ, de Muinck ED, Debets J, Leenders P, Smits JF. Chronic myocardial infarction in the mouse: cardiac structural and functional changes. *Cardiovasc Res* 1999; **41:** 586-593.

[308] Jugdutt BI, Schwarz-Michorowski BL, Khan MI. Effect of long-term captopril therapy on left ventricular remodeling and function during healing of canine myocardial infarction. *J Am Coll Cardiol* 1992; **19:** 713-721.

[309] Jugdutt BI. Effects of amlodipine versus enalapril on left ventricular remodelling after reperfused anterior myocardial canine infarction. *Can J Cardiol* 1997; **13:** 945-954.

[310] Kambayashi M, Miura T, Oh BH, Murata K, Rockman HA, Parra G, Ross J, Jr. Myocardial cell hypertrophy after myocardial infarction with reperfusion in dogs. *Circulation* 1992; **86:** 1935-1944.

[311] Horrigan MC, MacIsaac AI, Nicolini FA, Vince DG, Lee P, Ellis SG, Topol EJ. Reduction in myocardial infarct size by basic fibroblast growth factor after temporary coronary occlusion in a canine model. *Circulation* 1996; **94:** 1927-1933.

[312] de Lorgeril M, Ovize M, Delaye J, Renaud S. Importance of the flow perfusion deficit in the response to captopril in experimental myocardial infarction. *J Cardiovasc Pharmacol* 1992; **19:** 324-329.

[313] Richard V, Murry CE, Reimer KA. Healing of myocardial infarcts in dogs. Effects of late reperfusion. *Circulation* 1995; **92:** 1891-1901.

[314] Ye J, Yang L, Sethi R, Copps J, Ramjiawan B, Summers R, Deslauriers R. A new technique of coronary artery ligation: experimental myocardial infarction in rats in vivo with reduced mortality. *Mol Cell Biochem* 1997; **176:** 227-233.

[315] Sethi R, Elimban V, Chapman D, Dixon IM, Dhalla NS. Differential alterations in left and right ventricular G-proteins in congestive heart failure due to myocardial infarction. *J Mol Cell Cardiol* 1998; **30:** 2153-2163.

[316] Green HJ, Duscha BD, Sullivan MJ, Keteyian SJ, Kraus WE. Normal skeletal muscle Na^{+}-K^{+} pump concentration in patients with chronic heart failure. *Muscle Nerve* 2001; **24:** 69-76.

[317] Ribadeau-Dumas A, Brady M, Boateng SY, Schwartz K, Boheler KR. Sarco(endo)plasmic reticulum Ca^{2+}-ATPase (SERCA2) gene products are regulated post-transcriptionally during rat cardiac development. *Cardiovasc Res* 1999; **43:** 426-436.

[318] Ganguly PK, Dhalla KS, Shao Q, Beamish RE, Dhalla NS. Differential changes in sympathetic activity in left and right ventricles in congestive heart failure after myocardial infarction. *Am Heart J* 1997; **133:** 340-345.